PARABOLIZATION AND STRUCTURAL INTEGRITY OF SIDE BULB APPLIED PLATFORM SUPPLY VESSEL HULL FORM

by

Ozgur DELI

BASc., Yıldız Technical University, 2002

A THESIS SUBMITTED IN PARTIAL FULFILMENT OF
THE REQUIREMENTS FOR THE DEGREE OF

MASTER OF APPLIED SCIENCE

in

The Faculty of Graduate and Postdoctoral Studies
(Mechanical Engineering)

THE UNIVERSITY OF BRITISH COLUMBIA

(VANCOUVER)

August 2014

Abstract

The parabolization work is a hull-optimization method for minimizing total resistance of ship by using numerical and experimental methods. Ship total hydrodynamic resistance is a sum of frictional resistance, form resistance and wave resistance. The form resistance is a fraction of frictional resistance while the wave resistance dominates as speed increases. It becomes clear to turn toward minimizing wave resistance for hull-form optimization studies regarding increased speeds.

In 2002, Calisal et al. reported a 10% decrease in effective horse power at Fn = 0.275 for a coaster tanker. The objective was to attain a beneficial wave-resistance reduction over a moderate to relatively high operating speed range. The parabolization work was done by a computer software that expends the form at waterline and replaces the conventional parallel middle-body section with parabolic side bulbs.

This study was made for a oil platform supply vessel (PSV)and studies an improved , new hull form. The form is a new “retrofit” , for the present parent hull form, increasing the vessel’s beam up to 5% and its displacement accordingly. In this thesis new scantling was calculated for the parabolized hull. The structural analysis and design for the parent and “retrofit” hull forms were done, using the rules and guidelines of the American Bureau of Shipping (ABS).

The final part of the thesis provides a cost payback analysis of the parabolized PSV. A fuel savings of 280,000 liters/year provides $235,000.00 per year saving based on a 5.88% drop in resistance . The investment for the construction of an amidships bulb is estimated at $161,000. The payback period for the construction of an amidships bulb is estimated to be nine to seventeen months, with different ship type factors. In addition resistance reduction saves 753,900 kg of CO2 and 134,100 kg of NOx .

The parabolization cost analysis is seen in three parts. First, the investment cost of the side bulb. Second, the savings in fuel cost representing the savings in the running

cost and the change in the investment cost of propulsion machinery of the vessel and thirdly, the environmental savings by low CO2 and NOx emission.

Preface

The research about waterline parabolization is an ongoing subject at the UBC Naval Lab. for long time. There were some collaboration between UBC and ITU about this parabolization study. For previous studies numerical computations were generally done at UBC and the experimental tank tests at ITU. Numerous studies have been done and papers published on this topic. The following references (Calisal et al. 2002; Vyselaar 2006; McRoberts and Klaptocz 2007; Çalisal, Gören et al. 2009; Gould, Çalisal et al. 2010) could outline a summary of the past work.

Trawson argos and optimizer softwares are used for the necessary calculations for parabolization. Both software packages rely on a potential flow code named Trawson that was developed by Gören and Atlar (1998). The code was developed to calculate the potential flow around a hull using Dawson's algorithm for the wave resistance of displacement type hullforms. James McRoberts developed the code required for the argos and the optimizer at UBC naval lab. In chapter 2 the previous work and literature survey on parabolization is discussed. This thesis used Trawson software packages presented in chapter 3 for the calculation of the wave and total resistance of the parent and the parabolized hulls. The author created the 3D hull model and the necessary meshing, and run the argos software. The support received from James McRoberts for the running of the optimizer software to create amidship bulb is acknowledged.

In Chapter 4 to 6 the structural scantling design for the parabolized hull using the rules and regulations of the American Bureau of Shipping (ABS) is explained. The design loads applied to the ship structure and the boundary conditions for the FEA are obtained from the ABS rules. In chapter 7 all calculations and results of FEA are presented. Structural FEA analysis is done with the software ANSYS. In Chapter 8 the cost analysis done for amidship bulb construction. The construction cost of the amidship bulb structure and the return of this investment by fuel savings is done using PODAC Cost Model Parametric Module. (Ennis, Dougherty et al. 1997). The author made all of the design and calculations for the structural scantling, FEA and cost analysis.

Table of Contents

List of Tables

List of Figures

LIST OF SYMBOLS, NOMENCLATURES AND ABBREVIATIONS

Δ *(or W)*	*Displacement*
∇ *(or V)*	*Displaced volume*
θ	*Wave propagating or radiating direction*
λ	*Wave length*
γ	*Integration variable used in Michell's integral*
ρ	*Water density*
ζ $(\text{or } \eta, \text{z, Z})$	*Wave heights*
ATTC	*American Towing Tank Conference*
B	*Beam*
C_A	*Model-ship correlation allowance (applicable only to full scale, typically 0.0004)*
C_B	*Block coefficient*
C_F	*Frictional resistance coefficient*
C_P	*Prismatic coefficient*
C_R	*Residuary resistance coefficient*
C_T	*Total resistance coefficient*
C_V	*Viscous resistance coefficient*
C_W	*Wave resistance coefficient*
EHP	*Effective horsepower*
$f(x,y)$	*Half breadth or offsets of hull*
$f_x(x,y)$	*Slope of hull*
Fn_h (*or* $F_{n,h}$)	*Froude number (depth based)*
Fn_L (*or* $F_{n,L}$)	*Froude number (length based)*
FEA	*Finite Element Analysis*
FW (*or fw*)	*Fresh water*

g	*Gravitational acceleration*
h	*Water depth*
I	*Second moment of area*
ITTC	*International Towing Tank Conference*
L_{OA}	*Length overall*
L_{PP}	*Length between perpendiculars*
L_{WL}	*Length of load waterline*
NALAB	*Offshore Engineering & Naval Architecture Laboratory at University of British Columbia*
R_F	*Frictional resistance*
Rn (*or* R_n)	*Reynolds number (length based)*
R_R	*Residuary resistance*
R_T	*Total resistance*
R_V	*Viscous resistance*
R_W	*Wave resistance*
S	*Wetted surface area of hull*
SNAME	*Society of Naval Architects & Marine Engineers*
SW (*or sw*)	*Sea water*
SWL (or swl)	*Still water level*
T	*Draft*
U	*Ship speed*
UBC	*University of British Columbia*

Acknowledments

Here, I would like to thank my supervisor Dr. Sander M. Calisal for accepting me as his graduate student under his studies for the past four years and sharing his knowledge in naval architecture and fluid dynamics. I met him quite late but I am very happy to know him and be a student of his at UBC.

I would also like to thank Dr. Farrokh Sassani as my co-supervisor during my study at UBC. I feel lucky to share his knowledge and to have his friendship and encouragement. I would also like to thank Jon Mikkelsen. He was the co-worker of Dr. Calisal at UBC for Naval Architecture and a good friend.

Furthermore, I am happy to share the office space of the Naval Lab with my colleagues, Dr. Mahmoud Alidadi and Kevin Gould. I have spent almost two years with these two colleagues at the Naval Lab. They are good friends

Special thanks to my colleague, James McRoberts. He is a great guy who developed the code of ARGOS for the hull-form optimization code for side-bulb application. He also helped me to create the side bulb on the Platform Supply Vessel. I also would like to thank Dan McGreer who is a naval architect at STX Marine Vancouver branch. He gave me the hull form of the platform supply vessel which I have used on my thesis.

I would also like to thank my colleague, Cem Doganci, who is a good friend of mine and gave me some aid about structural scantling of hull form. Levent Kaydihan also helped me with Finite Element Analysis of ship structure.

Finally special thanks to Mrs. Carol A. Ferris for checking my thesis before printing and editing for English structure and grammer. She helped me to bring this thesis into final shape.

Dedication

To my lovely daughter and my parents

1.1 INTRODUCTION

The aim of marine designers for self propelled marine structures to design more efficient vessels that meet the owner requirements. When efficiency is the main concern of a marine design, the main improvement comes up with lowering the ship's total resistance. The low resistance means, more efficient propulsion, low running cost and low carbon emission for saving environment, which is getting more important recently. This was always the main concern for all designers for every vessel.

There are many ways to improve a ship's resistance at the design stage. The traditional mindset that displacement hull vessels, operating at moderate to higher speeds, are to be built with a less beamy body, with a low block coefficient, in order to reduce resistance. However, the resistance of the hull form can be lovered down with some other improvements on the hull lines and main characteristics of the vessel. This research is based on reducing the hull resistance of a ship by using a waterline parabolization which is an optimization method to decrease the wave resistance of displacement hullforms through the addition of a bulb at amidships of the hull.

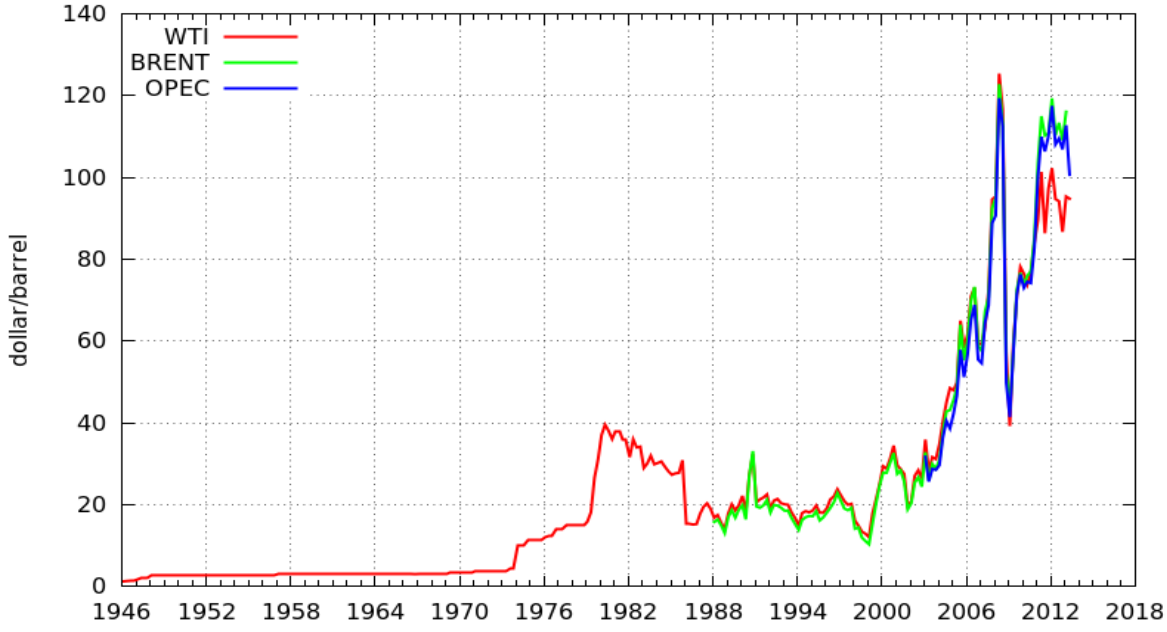

Figure 1: Nominal oil prices in dollar/barrel since January, 1946
(Short Report on Oil Price History, Revision 1.0, Giulio Bottazzi)

Additionally a designer has to consider the constructional cost of a vessel, as well as its running cost. While we are designing a side bulb at the amidships of the vessel, we have to consider also constructional integrity with a simple structure to build the vessel without increasing its cost. In this research, the structure of the vessel was examined and structurally analysed with an FEA method to control structural stiffness. The structural members are integrated to the new hull lines after the sidebulb was created.

The financial analysis of amidship bulb has done at the final part of the thesis. The financial part is showing the first investment of structural construction and return of this investment by fuel savings at running cost by total resistance reduction.

This research is not a parabolization, structural FEA or cost analysis of amiship bulb construction but a synthesis of them all.

1.1 Research Motivation

Some types of vessels have to have a displacement type hull form. The vessels that could have parabolization, are ferries, fishing boats, work boats and patrol vessels commonly operate in US & Canada. Platform supply vessel (often abbreviated as PSV) is a ship specially designed to supply offshore oil platforms. These ships range from 20 to 100 meters in length and accomplish a variety of tasks. The primary function for most of these vessels is the transportation of goods and personnel, to and from offshore oil platforms and other offshore structures. Platform supply vessel is one type of work boat and mainly operates at the Gulf of Mexico.

A primary function of a platform supply vessel is to transport supplies to the oil platform and return other cargoes to shore. Cargo tanks of the vessel for drilling mud, pulverized cement, diesel fuel, potable and non-potable water, and chemicals used in the drilling process, comprise the bulk of the cargo spaces, as well as constructional materials and tools for repair and maintenance. Fuel, water, and some chemicals are almost always required by oil platforms actively operating offshore. Certain other chemicals must be

returned to shore for proper recycling or disposal, however, crude oil product from the rig is usually not a supply vessel cargo.

Common and specialty tools are carried on the large decks of these vessels. Most carry a combination of deck cargoes and bulk cargo in tanks below deck. Many ships are constructed (or re-fitted) to accomplish a particular job. Some of these vessels are equipped with a firefighting capability and fire monitors for fighting platform fires. Some vessels are equipped with oil containment and recovery equipment to assist in the cleanup of a spill at sea. Other vessels are equipped with tools, chemicals and personnel to "work-over" existing oil wells for the purpose of increasing the wells' production.

Figure 2: Platform Supply Vessel moored to offshore platform.

The offshore industry is gearing up for major expansion in the near future. Growing global energy demand will necessitate exploration into deeper and new basins northerly locations. Increased application of new technological advances, such as drilling in ultra-

deep water (10,000ft+) has stimulated more sophisticated designs for mobile rigs and the offshore support vessels that service them.

Offshore oil production is forecast to increase by 55% from current production levels to reach over 36m bbls/d by 2025. Offshore gas production is also forecast to increase during this period, by 22% to over 1,000 bcm/yr. The forecast increase in offshore production will stimulate the demand for mobile rigs and the offshore support vessel fleets. Overall forecasts highlight that the mobile rig fleet will increase by 41% compared to the current fleet during the study period (2013 to 2025) to approximately 1,100 active rigs. To service the increase in the number of rigs the Anchor Handling Tug/Supply (AHT/S) fleet is forecast to grow by 41% to 3,900 vessels, whilst the Platform/Supply Vessel (P/SV) fleet is forecast to increase by approximately 40% over 3,200 vessels by the end of the study period.

These are some of the findings by the UK-based maritime research and consultancy company “Ocean Shipping Consultants”. (David Bull, Senior Consultant, Ocean Shipping Consultants, May 2013)

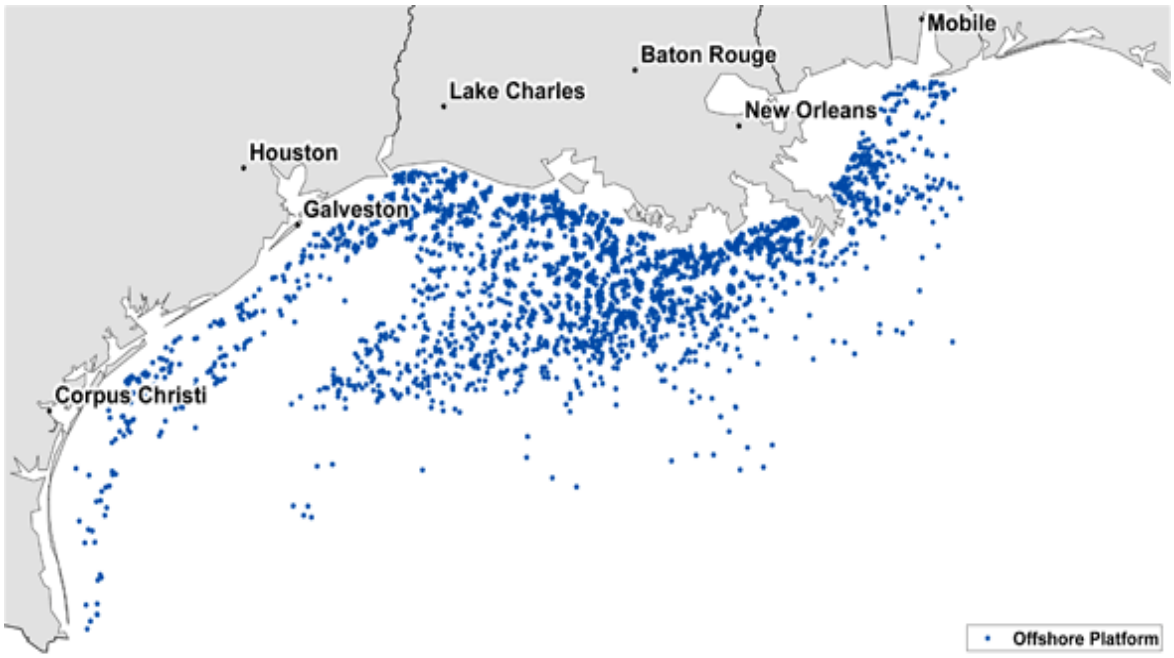

Figure 3: Offshore platform at Mexican gulf.
(Image courtesy of the American Petroleum Institute, 2014)

Platform Supply Vessel Fleet Development in near future will grow by developing offshore oil drilling. The current world offshore platform supply vessel (P/SV) fleet equates to over 2,350 vessels. The development of the P/SV sector will develop in line with offshore production patterns. P/SV demand will be boosted in the future with the trend towards more remote and harsher environments.

For the Base Case, annual new building levels are forecast at approximately 100 per year – this is around the yearly average of deliveries since 2000. The number of vessels scrapped each year is forecast to be approximately 30 units.

The P/SV fleet is forecast to increase at a rate of approximately 3.0% per annum. Overall, the fleet is forecast to increase by 13% to approximately 2,600 vessels by 2015, followed by a further increase of 13% to over 2,900 vessels by 2020 and then a further 10% to over 3,200 vessels by the end of the study period. Overall, the P/SV fleet is forecast to increase by 40% over current fleet levels.

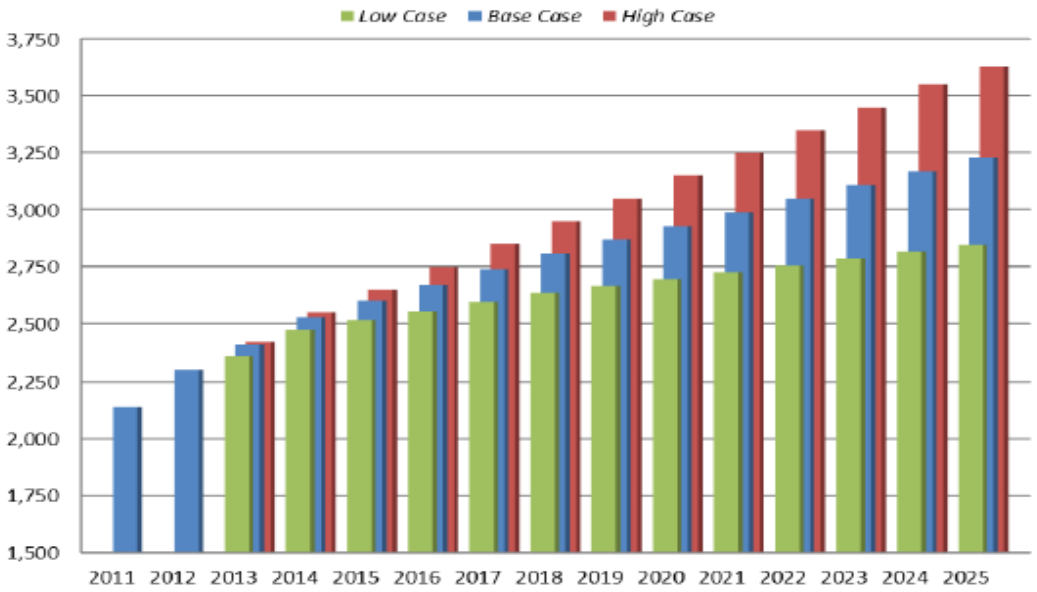

Figure 4: P/SV Fleet Development to 2025, by Case
(Ocean Shipping Consultant, David Bull,2014)

With the information mentioned above, one can save an amount of fuel by reducing the running cost of commercial (PSV) vessels and saving world resources as well as protecting nature for more greener world.

2. LITERATURE OVERVIEW & PREVIOUS WORK

UBC and ITU worked on amidships bulbs and waterline parabolization research. Most of the development have been done after year 2000. There have been two software packages named **ARGOS Trawson** and **ARGOS Optimization** have been developed by a graduate student, James McRoberts at UBC. The optimisation of PSV has been done by two separate softwares which will be discussed in the next chapter. Both software packages rely on a potential flow code named **Trawson** that was developed by Gören and Atlar (1998) to solve the wave resistance of a displacement hullforms. **Trawson** is a panel method code based on Dawson's method (Dawson 1977) and is discussed further in this section. Next, previous work is about side bulb creation which we call parabolization and results to resistance reduce of PSV. The following chapter is structural scantling of a vessel with ABS rules. The same chapter also contains FEA modeling and solution of parent hull and parabolized hull structures. It also presents the results of both parent and parabolized hull structures with their comparison. The final chapter is about for ship construction cost estimation.

2.1 Parabolization and Wave Resistance Reduction.

While trying to improve ship stability of an oceanographic vessel by some modification on the hull form with the additional volume on sides, Calisal et al. (2002) found that the modified hull with the increased beam had a reduced resistance. Then they performed research with a coaster tanker to drop down the resistance while increasing the beam. This research was performed experimentally and numerically. The beam increment at amidship was derived at the waterline to replace the wall-sided parallel middle body on conventional hull with parabolic-shaped side bulb to modify the wave characteristics of the hull. The modified hull had beam that is significantly larger than the original. As a result the total resistance exhibited a reduction with sidebulb.

Similar application has been successfully integrated on the bulbous bow of typical newly built vessels for minimizing bow wave. This results to reducing pressure variation prevailing along the hull length. The dimension, shape and location are unique for each hull and it can be optimized at the design speed. The wave interactions caused by these wave makers like side and bulbous bulbs would lead to beneficial wave resistance reduction. Accordingly, the total resistance or the effective horsepower is practically reduced. The improvement is due to a modified pressure field around the hull that alters the near and far-field flow pattern thereby generates new wave systems to interact with the original wave systems from the bow, stern and shoulders.

Resistance reduction by sidebulb modified hull is a reasonable development and gains economical profit by reducing the running cost of vessel but initial costs due to construction and materials are also important consideration variables. It may be less desirable to have parabolic-shaped side bulbs as opposed to a wall-sided parallel middle body sections. But when overlooking the operation of such a ship throughout its design and running life, it is still an attractive option considering the savings on fuel consumptions, which may cover the additional costs. More research and investigation are needed for economic feasibility on the idea of having side bulbs.

2.1.1 Previous Work

Wall sided hulls with constrained beams have been used for the design of displacement hulls in last century. The theory behind was the increases in the beam of displacement type hulls to the increase in resistance (Kent 1919; Schneekluth 1987; Harvald 1992). Çalisal et al. (2002) found that beam increases in the midbody could have a beneficial impact on total resistance. They found that parabolic side bulb at amidship helps to reduce the wave resistance and total resistance of the vessel. That paper has a theoretical justification, based on Mitchell's integral, and an experimental validation on the wave-making characteristics of an oceanographic vessel. Tow-tank results indicated that a 20% increase to the beam, while keeping the draught and length constant and

increasing the displacement, resulted in 10 % reduction in the effective power at a Froude number of 0.275.

The increase on the beam with a side bulb means also increase in the wetted surface area that cause an increase at friction drag, but the reduction by wave resistance is greater than friction drag and as a sum it results a reduction at total resistance of the vessel. Tan and Sireli (2004) conducted a systematic empirical study of the effect on wave resistance of adding parabolic midship bulbs to a fishing hull (UBC Model 3). The parent hull was designed by Çalisal and McGreer (1993) for use in Canadian Pacific waters. They tested several different bulb locations and sizes for this research. A total resistance reduction of 10% was achieved through “retro-fit” amidships bulbs. Çalisal, Şirelli et al.(2009) performed a new research using a new hull with “constant displacement” that means parent hull and side bulb added hull have the same displacement by slightly modifying the parent hull lines to decrease the side bulb volume. As a result they found that, despite an increase in viscous resistance (including an increase in viscous pressure drag), a hull with a faired bulb with a maximum width of 11% the baseline beam and 5% decrease in transom width the design achieved a 15% decrease in EHP.

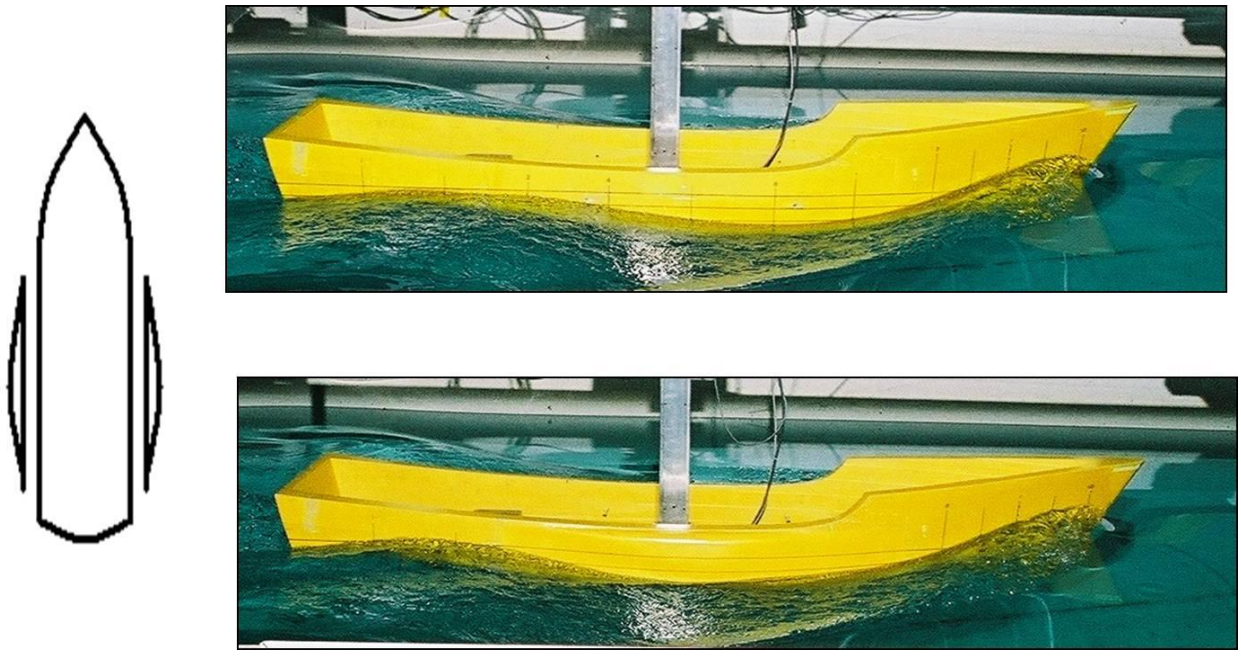

Figure 5: On the left side schematic parent hull and amidship bulb together, Top is parent hull and bottom is parabolized hull during test at towing tank of ITU.

Vyselaar (2006) and Klaptocz (2006) were the foundation of waterline parabolization and resulted in typical modified waterlines. They are “retro-fit” and “constant displacement”. Retro-fit means adding side bulb over a parent hull without having any modification. The constant displacement is subtracting the volume of sidebulb from parent hull to keep the displacement of the vessel same as parent hull. The differences can be seen Figure 6.

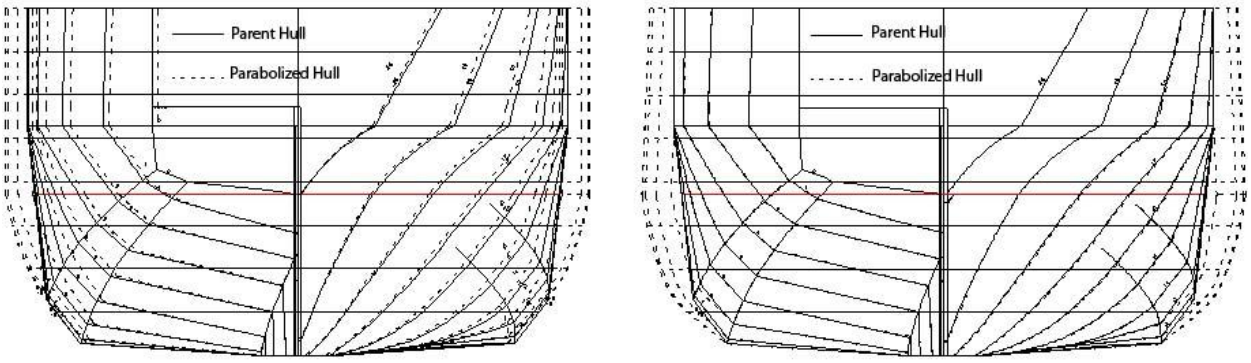

Figure 6: “constant displacement” and “retro-fit” Hull waterlines.

The potential flow code Trawson, was first used by Vyselaar (2006) for a research about NPL trimaran for different configurations of sidebulb forms. Vyselaar (2006) used the original Trawson code that was written in FORTRAN. The original code required an input hull form and free surface which needs to be defined by a series of points with mesh connectivity created by the user manually. To make this imput more user friendly Yavar Naddaf and James McRoberts in 2006 developed a pre-processor for Trawson, and eventually led to the ARGOS. Gauld (2011) made a research about UBC ferry hull which was parabolized by James McRoberts. This reseach also includes work on powering and seakeeping property of the vessel.

2.1.2 Total Resistance of Vessel and Wave resistance

The resistance of a ship at a given speed is the force required to tow the ship at that speed in still water, assuming no interference from the towing ship. If the hull has no

appendages, this is called the bare-hull resistance. The power necessary to overcome this resistance is called the towrope or effective power and is given by

$$P_E = R_T * V$$

where P_E= effective power in kWatt (kW)

R_T = total resistance in kNewton (kN)

V = speed in m / sec

This total resistance is made up of a number of different components, which are caused by a variety of factors and which interact with each the other in an extremely complicated way. In order to deal with this question more simply, it is usual to consider the total calm water resistance as being made up of four main components.

(a) The frictional resistance, due to the motion of the hull through a viscous fluid.
(b) The wave-making resistance, due to the energy that must be supplied continuously by the ship to the wave system created on the surface of the water.
(c) Eddy resistance, due to the energy carried away by eddies shed from the hull or appendages. Local eddying will occur behind appendages such as bossings, shafts and shaft struts, and from stern frames and rudders if these items are not properly streamlined and aligned with the flow. Also, if the after end of the ship is too blunt, the water may be unable to follow the curvature and will break away from the hull, again giving rise to eddies and separation resistance.
(d) Air resistance experienced by the above-water part of the main hull and the superstructures due to the motion of the ship through the air.

The resistances under *(b)* and *(c)* are commonly taken together under the name residuary resistance. Further analysis of the resistance has led to the identification of other sub-components, as discussed subsequently.

Wave Resistance; A displacement hull vessel sailing through the water at a steady speed generates waves on the surface of the water, even if the fluid through which the

ship is assumed to be ideal (i.e. inviscid and irrotational). The ship generates waves and consumes its power to create them. The aim of the parabolization is cancelling the waves by modification on the hull lines and reducing the wave resistance. Froude's hypothesis brings the wave resistance. It explains the total ship resistance, separated into two which are frictional resistance and residuary resistance. The frictional resistance is the drag due to tangential stresses arising from fluid viscosity. The residuary resistance is the sum of viscous resistance which is also known as drag and wave resistance.

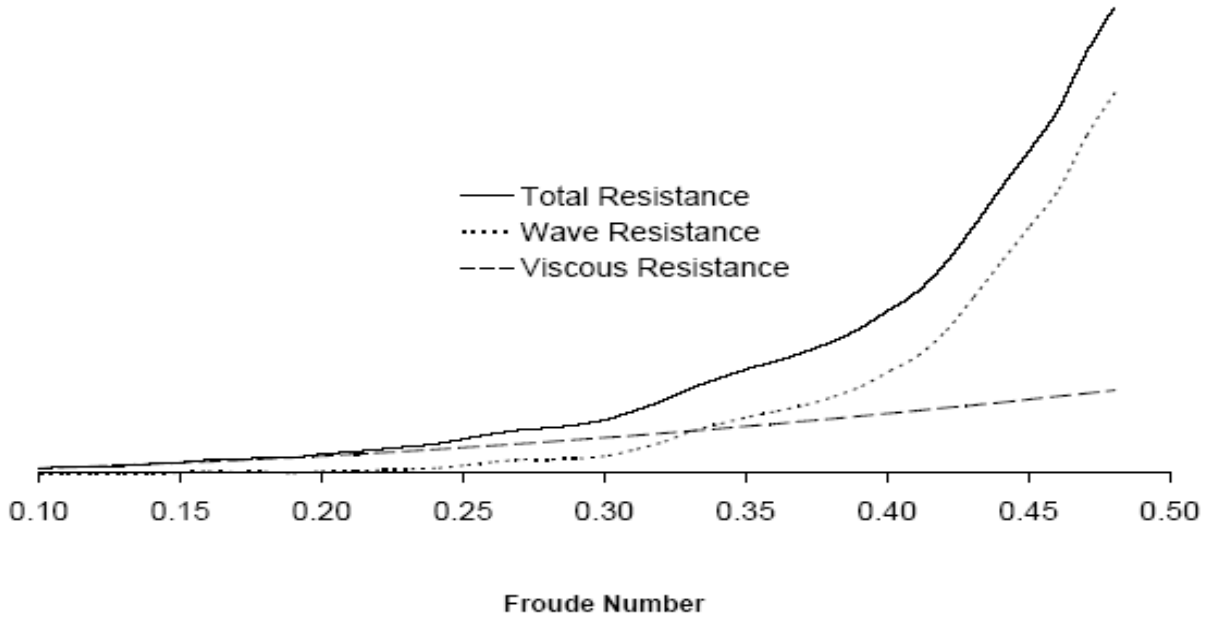

Figure 7: Main Components of Resistance for a Typical Canadian Fishing Hull
(A resistance study on a systematic series of low L/B vessels, Calisal, McGreer 1993)

Wave resistance is relates to the slope of hull lines and is very sensitive to the shape of hull lines. It becomes the main component of the total resistance at high Froude Number rather than the frictional resistance. This can be seen at resistance speed graph shown at figure 7 for a typical Canadian fishing a hull. The figure graph is created as a result of the research done at UBC to create a side bulb for Canadian Fishing boat. On this graph it can be easily seen that the wave resistance value is rapidly increasing with the increasing Froude Number. So reducing the wave resistance is more important in the design of displacement ships as the fuel costs rise and ships travel at ever higher speeds.

2.2 The Wave Resistance Problem

The Trawson potential flow code solves the wave resistance problem using a panel method based on Dawson's algorithm (Gören and Atlar 1998). Dawson's method was published in 1977 and many subsequent studies have improved on its application (Bertram 1990; Raven 1992; Sclavounos, Kring et al. 1997). The main advantages of this method include 3D discretization of the hullform and calculation of the near field wave profile, which are both important in the creation of an amidships bulb.

Dawson's algorithm uses a double body image of the hullform to create an undisturbed free surface that acts like a wall and can be used to construct the streamlines around the hull shape. A linearized approximation to the free surface boundary condition can then be applied in the following manner:

$$(\Phi_l^2 * \emptyset_l)_l + g * \varphi_z = 2 * \Phi_l^2 * \Phi_u \qquad 2\text{-}1$$

The Φ represents the double body velocity potential at low speeds and the subscript implies differentiation along the streamlines. The velocity vectors of the free surface panels are assumed to follow those of the imposed streamlines. The other implied boundary conditions are an irrotational flow and incompressible fluid, with a constant atmospheric pressure at each free surface panel and the velocity is tangential to the hull at its surface. The hullform is discretized into quadrilateral panels each with a Rankine source of constant strength using the method presented by Hess and Smith (1967). The velocity potential around the double body Φ is given as:

$$\varphi(x,y,z) = -\iint_s \sigma(\xi,\eta,\zeta)\, dS(\xi,\eta,\zeta)/r(x,y,z;\xi,\eta,\zeta) \qquad 2\text{-}2$$

In this case σ is the source strength, (ξ, η, ς) is the source location, and (x,y,z) is the location of each individual field point. To ensure that the waves do not propagate forward, a radiation condition of the perturbation is applied to the calculation of velocity potential by using a special four point differentiation scheme. Differentiating the potential

equation along the streamlines we obtain the components of the velocity (Aij, Bij , Cij) at the point i induced by a source located at point j for a ship speed U:

$$\left(\frac{\partial \phi}{\partial x}\right)_i = U + \sum_{j=1}^{N} \sigma_j A_{ij}$$
$$\left(\frac{\partial \phi}{\partial y}\right)_i = \sum_{j=1}^{N} \sigma_j B_{ij} \qquad 2-3$$
$$\left(\frac{\partial \phi}{\partial z}\right)_i = \sum_{j=1}^{N} \sigma_j C_{ij}$$

The resulting problem to calculate the source strengths is a matrix of E equations and E unknowns where the E is the total number of mesh elements used in the calculation. The matrix is solved by Guassian elimination and then the pressure on each hull panel P_H and the wave elevations at each free surface panel Z_{FS} are calculated as follows:

$$Z_{FSi} = \frac{1}{2g}(U^2 + \phi_l \phi_l - 2\phi_l \phi_l) \qquad 2\text{-}4$$

$$P_{Hi} = \frac{P}{2}(U^2 + \nabla\phi.\nabla\phi - 2\nabla\phi.\phi) \qquad 2\text{-}5$$

Finally the wave resistance is calculated by integrating the pressures, P_{Hi}, over all of the hull panels. In the formula below n_{Xi} is the x component of the normal vector for panel *i* and the A_i is the area of the panel *i*.

$$R_W = \sum_{i=1}^{N} P_{Hi} * n_{xi} * A_i \qquad 2\text{-}6$$

One concern is that Dawson's method cannot predict the absolute magnitude of the wave resistance very accurately. The linearization of the free surface boundary condition ignores higher order terms and is likely the cause for Dawson's method to produce negative resistance values at slow speeds (Raven 1992). Also, Dawson's method requires continuity of the normal vectors along the hull surface. This poses problems at the stern region of full formed vessels or ones with a transom stern. Cheng (1989) solved this issue by forcing the streamlines at the edge of the transom to

continue straight back to infinity. An inlet flow of fluid is created by an imaginary row of panels inside the stern of the hull across the entire transom and given a velocity pointed aft equal to that of the ship speed U. The density and definition of the free surface panels are also very important to the accuracy of wave resistance prediction using Dawson's method. Hally (1995) recommended a uniform mesh size with a density of many thousands of cells to predict wave resistance to within 3 percent of actual values. These issues contribute to an inaccurate prediction of the overall wave resistance of displacement hullforms using Dawson's method. However, for the purposes of ranking hullforms that have been modified only in the amidships region, Dawson's method is very accurate.

3. THE PSV AND PARABOLIZATION WORK

The aim of the parabolization work is to create an amidship bulb to modify wave pattern of the parent hull which will reduce the vessel's total resistance. This will be useful for operating such a vessel at lower powering requirements or with a longer operating range. This parabolization may work while the vessel is operating at moderate Froude Numbers. As a basic information waterline parabolization doesn't guarantee resistance benefits for all types of displacement hullforms; therefore, the candidate hull forms must be examined carefully with experience. Once a hullform is chosen, a series of software packages are normally used to develop an optimal amidships bulb with several iterations. Before modeling the vessel's hull form we have to predict the approximate area of the possible amidship bulb with attention. The guide for this important step will be based on the cross sectional area of the hull.

The computer software and theoretical calculations are helping to reduce designer's time spent for hull form design time and the number of loops in the design spiral. It also helps to make more accurate hull lines before towing tank testing. If you compare the time and cost of a computer model examination with towing tank test with a scaled physical model one can easily see the time and money designer saves.

3.1 The Platform Supply Vessel

The subject vessel is a Platform Supply Vessel designed to serve offshore oil platforms operating at Mexican Gulf region of USA. The main purpose of PSV are supply of material for extracting oil, maintenance equipment for platform and all other necessary items to keep the platform running during its operational life.

The parent hull lines for a PSV can be seen in figure 8. The PSV hull has curved bow and a transom aft with a wall sided body as seen at lines plan. The original hull that called parent hull is modified with a parabolic side bulb. This parabolization work is processed by the software packages Trawson Argos.

Principal Dimensions		
Loa	87.17m	286’
Lwl	83.66 m	274’-6”
Beam	18.30 m	60’
Depth	7.47 m	24’-6”
Design Draft	5.90 m	19’-4”
Total Kilowatts	7300 kW	
Main Propulsion	2x2650 kW	
Total Deadweight	4500 Tons	
Service Speed	13,61 Knots	
Classification	ABS	

Table 1: Principal Dimensions of PSV

The service speed of the vessel is 13.61 knots (7 m/s) and it is used as service speed of PSV for parabolization. The Froude Number for service speed of the vessel is 0.244.

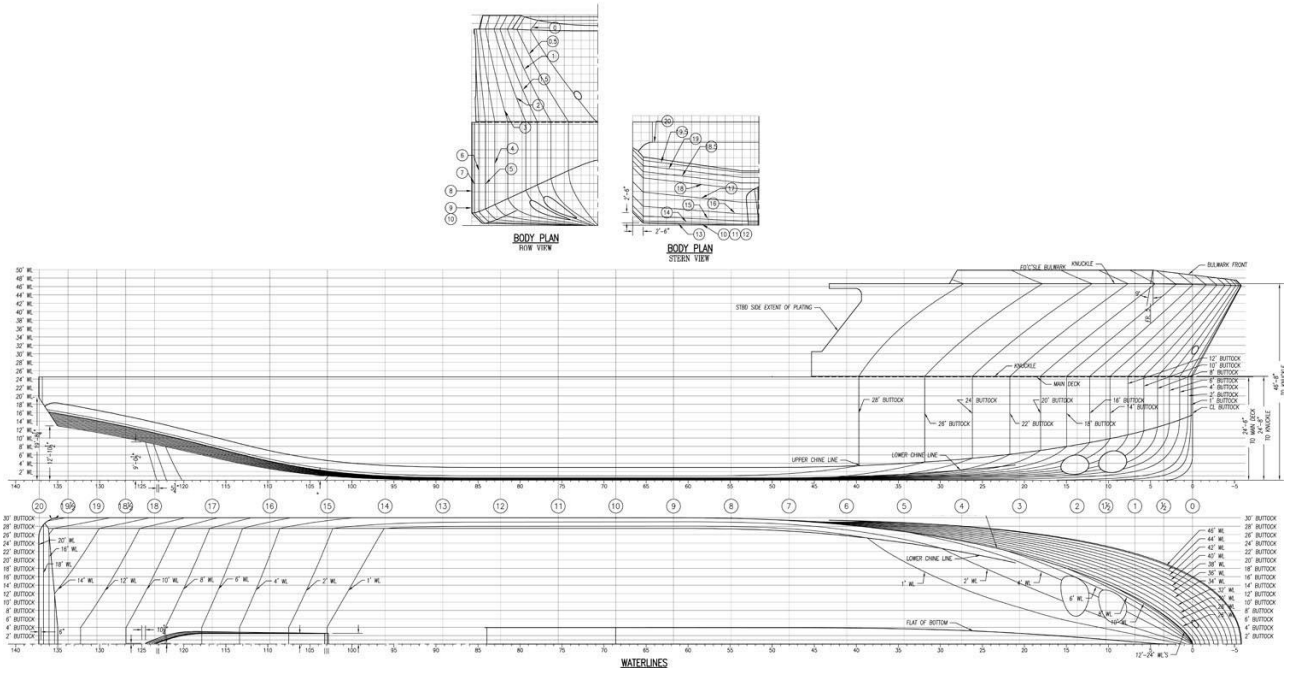

Figure 8: Lines Plan of Platform Supply Vessel
(Lines Plan & Body Plan, STX Canada Marine, 2011)

3.2 Argos Trawson Software: Wave Resistance Calculation

ARGOS Trawson and ARGOS Optimizer are the two moduls of ARGOS software package. Both programs are running based on a potential flow code. Trawson used for calculating wave resistance of displacement hullforms and Dawson's panel method used for writing the program codes. ARGOS Trawson has a user interface and is used to calculate wave resistance for given hullforms. ARGOS Optimizer uses a series of Matlab scripts and the base Trawson code to develop an amidships parabolic bulb shape of least wave resistance at a given speed.

The Platform supply vessel form is a displacement type hull with a considerable parallel mid-body hull lines. The service Froude Number which PSV operates is suitable for parabolization work. So the preliminary variables are looking appropriate for amidship bulb calculation. The first step in the parabolization design procedure is to generate a wave resistance curve and wave profiles of the parent hullform with the software called ARGOS Trawson. This program imports hull mesh data modeled at the Rhinoceros 3D modeling software which is the only preprocessor. Surface modeling of the hull at Rhinoceros is the very first step of the parabolization work

3.2.1. Rhino model of PSV

The hullform which ARGOS Trawson is used to determine a wave resistance curve must first be created in the Rhinoceros. The hull form will loft or create surface from frame sections and will be meshed using rectangular meshes. The mesh file is exported using a Wavefront file the extension of file must be (.obj). This .obj output file is the input file for the ARGOS Trawson. A series of parameters are defined within ARGOS Trawson, they are: the free surface size, shape and density as well as operational speeds, conditions and tolerances.

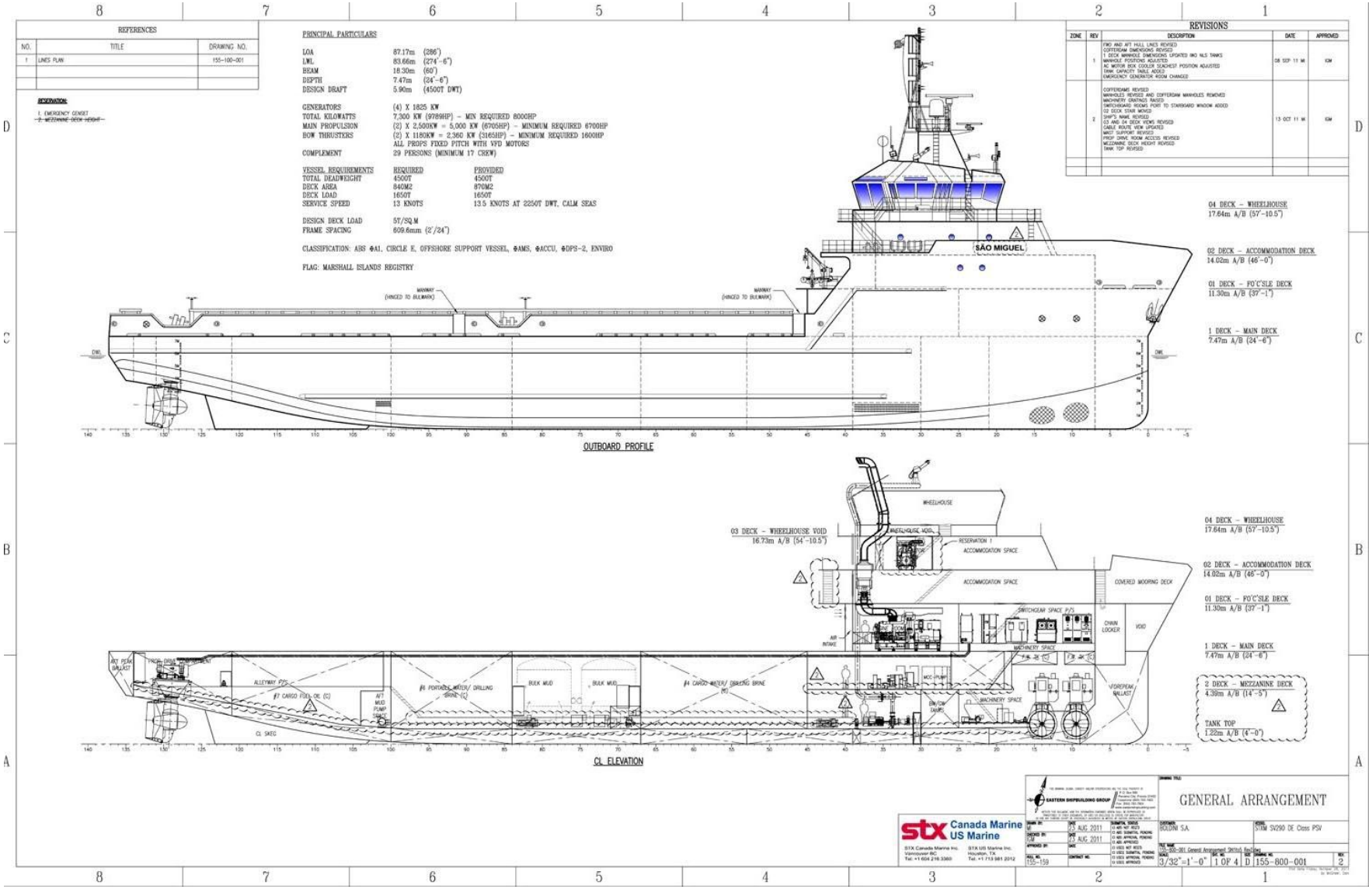

Figure 9: General Arrangement Plan of Platform Supply Vessel (STX Canada Marine, 2011)

SURFACE Creation

ARGOS Trawson uses a numerical model that can either created at Rhinoceros 3D by offset table or export from an existing 3D model. Rebuilding the geometry file within Rhinoceros is suggested, not to face with difficulties while creating the surface and mesh which will be used as the input file for ARGOS Trawson.

The hull and ship model of Platform supply vessel has already been done by STX marine office. So for this project I prefered to use the ready file for the hull mesh instead of building a new hull. The 3D model has been simplified and brought into required properties which are explained in following section. The Original model can be seen at figure 10.

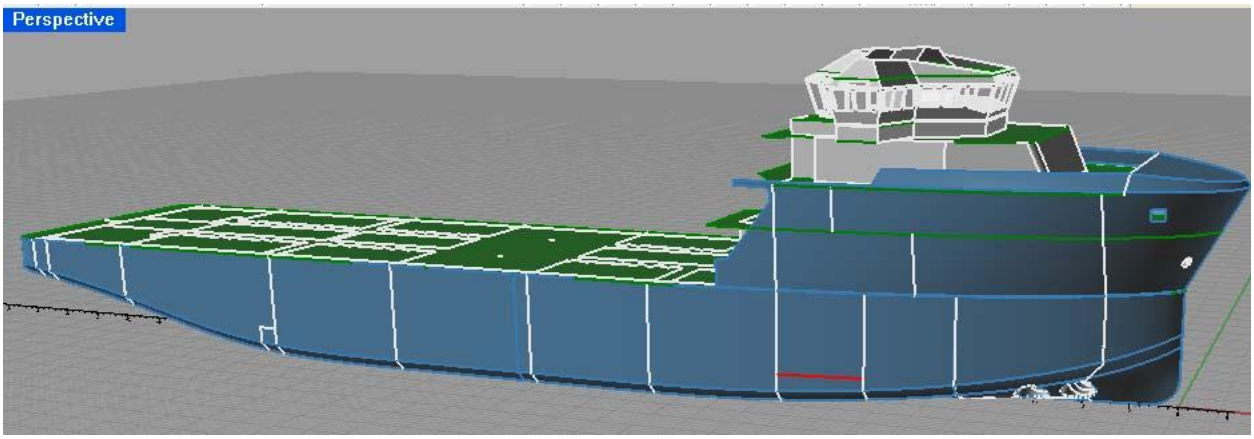

Figure 10: 3D mode of Platform Supply Vessel built at Rhinoceros 3D

All other parts than the hull form has been cleaned and document properties are defined as below.

Dimension Menu > Dimension Properties > Units

Model Units : meters
Absolute Tolerance : .0001 units
Relative Tolerance : .1 percent
Angle Tolerance : .5 degrees

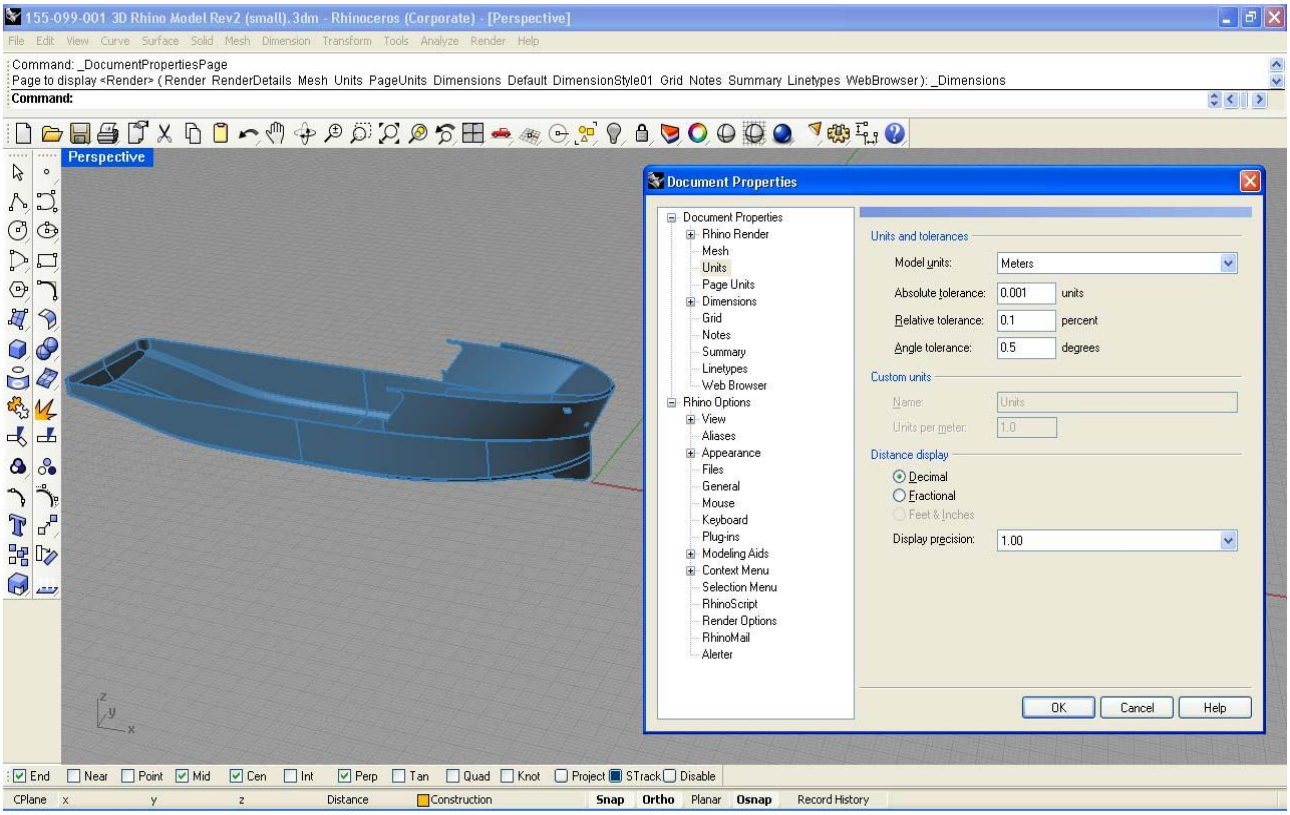

Figure 11: Document Properties interface at Rhinoceros 3D

The hull form surfaces was trimmed 5900 mm over Base Line (BL). This level is the DWL height for full draft of the vessel at operation speed. The coordinate has been modified regarding to input requirement of Argos Trawson. The details are explained like below.

- The base point and hull orientation. Z=0 at DWL, X=0 amidships with negative at bow. Y = keep only half beam of the hull, the starboard side will be kept and it stays at positive Y coordinate.
- The hull has trimmed by cutting plane at DWL and Z=0. Trawson only requires the underwater part of the hull on the starboard side.
- To make a simpler hull form all additional details other than the hull form body at model like skeg, propeller brackets are removed at aft side. The bow truster tunnels are closed at bow side of the model

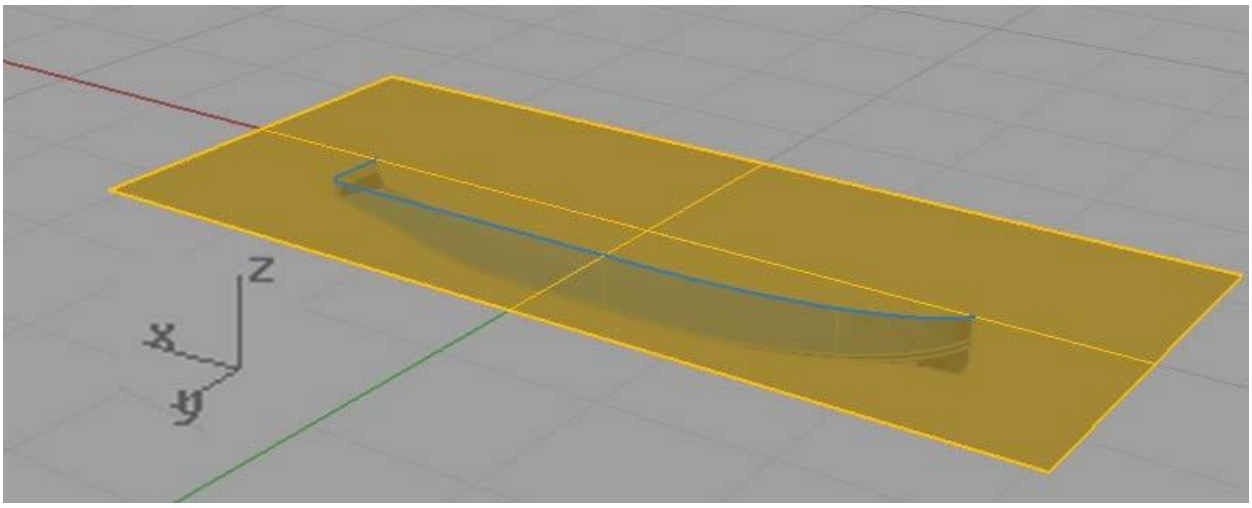

Figure 12: DWL level trim surface and new coordinate of hull

Before creating the mesh it is necessary to define the area of the side bulb. To predict the exact area where amidship bulb will be placed, we have to check the frame cross sectional area curve of the hull under examination. If we consider from bow to stern, the location of the sectional area curve where it turns into flat wall side is the begining and where flat wall side turns into form is the correct place. It can be easily seen at frame cross section of Platform Supply Vessel at figure 13.

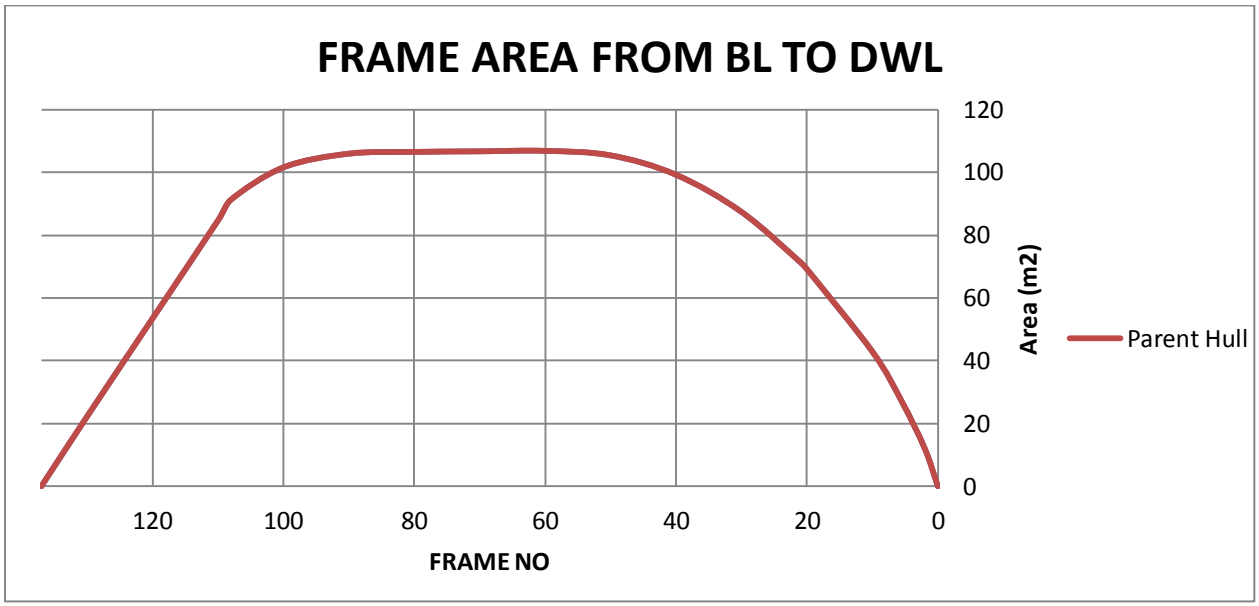

Figure 13: Frame area cross section curve of PSV from BL to DWL

So, regarding to figure above the parabolization area is defined between frame 20 to 110. For information about the vessel plan the frames numbers are increasing from the bow to the stern. The area separation is done from top of the bilge chine to the DWL between frame number 20 to 110. The area separated from hull lines can be easily seen in figure 14 down below.

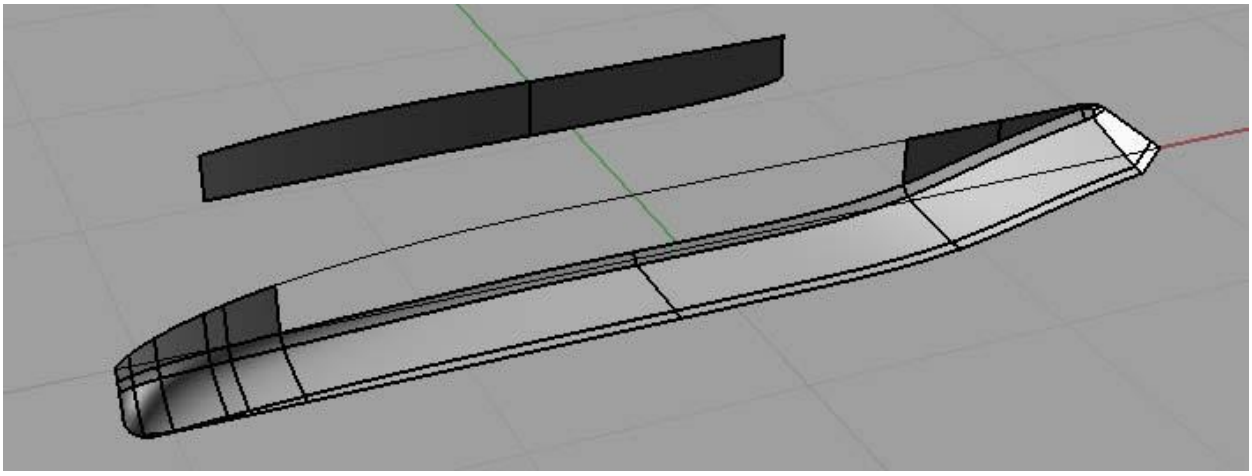

Figure 14: 3D surface model of PSV, the parabolization area separately seen from hull

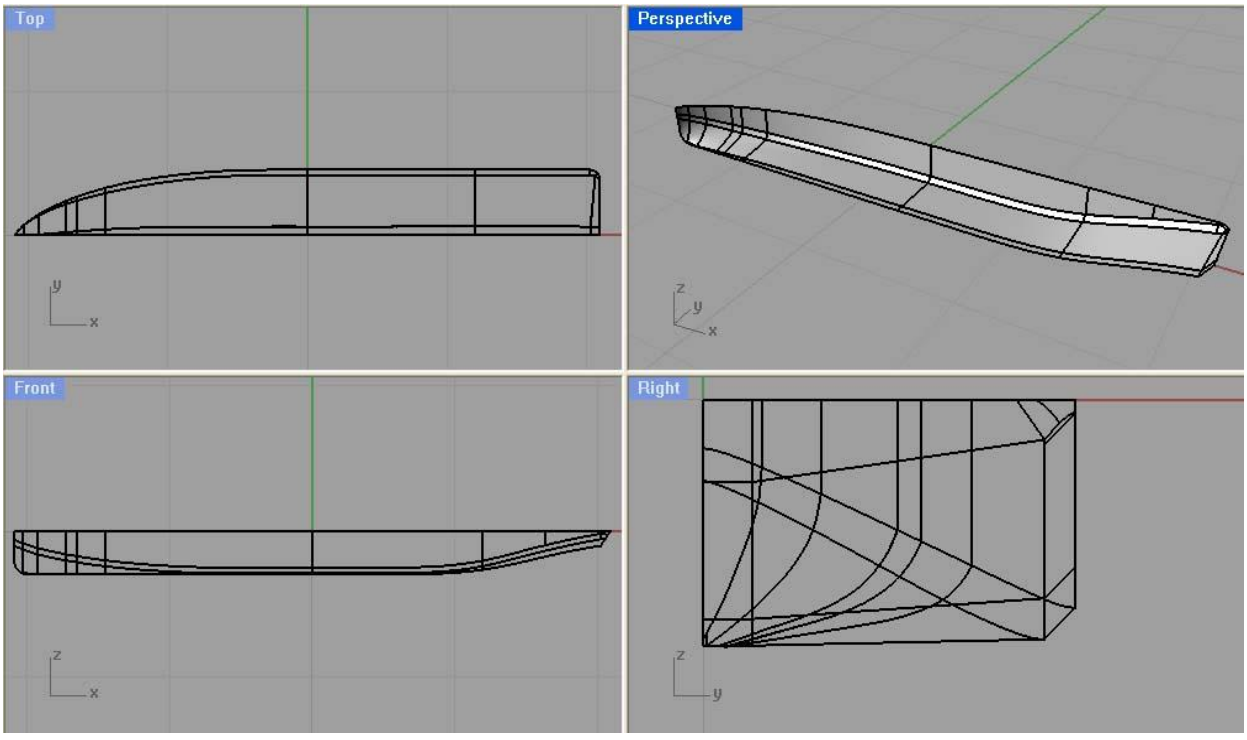

Figure 15: 3D surface model of PSV parent hull

MESH Creation

The hull form was created by using surface elements and now it is time to create the mesh out of it. The creation of surface can be done part by part regarding to mesh size. The other option is to divide the hull surfaces into pieces. Here I divide the hull surface regarding to fine and coarse mesh and parabolization area. The user of Trawson now start making mesh for each individual surface to represent the hullform as a series of meshes with flat rectangular elements. The bow and stern part of the ship normally must have finer mesh which means small size mesh elements are needed. The middle part which is out of full form area can have larger size mesh elements. Once all the surfaces are properly meshed they are exported to ARGOS Trawson as an .OBJ file.

The mesh creating work follows the work described below;

- Mesh > From NURBS Object
- Select the trimming surface independently
- Polygon Mesh Options dialog box should appear. Press the Detailed Controls button to open Polygon Mesh Detailed Options dialogue box to adjust the mesh.

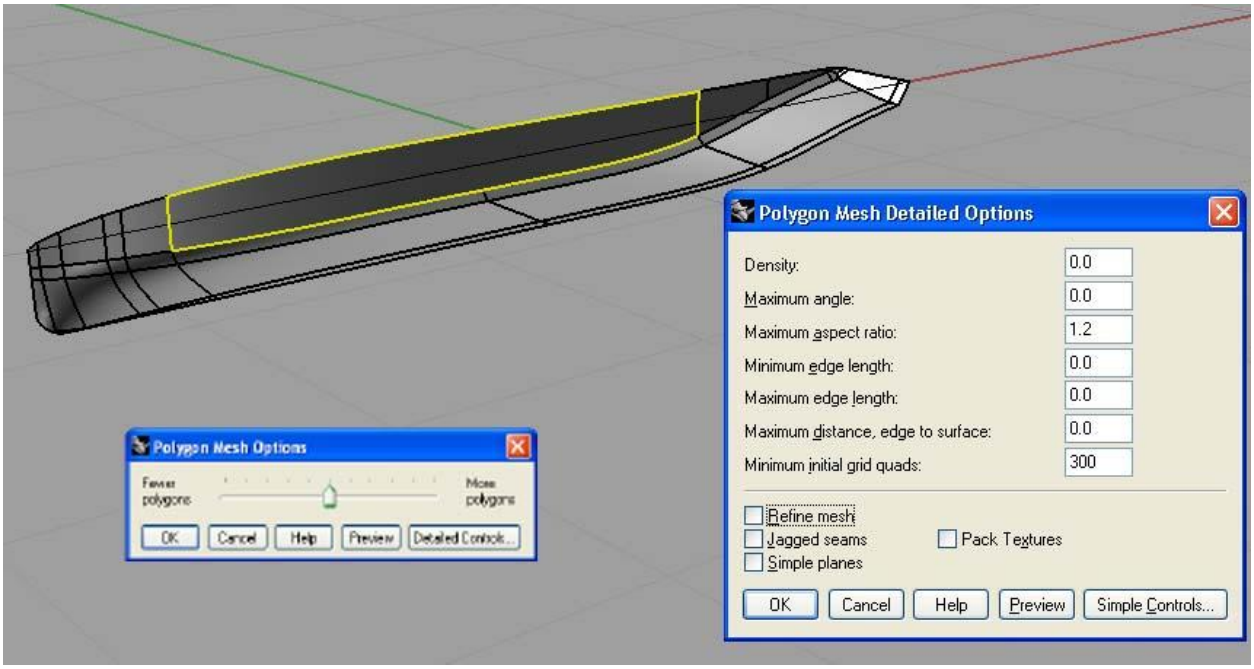

Figure 16: Mesh surface image selected surface appear with a yellow border line, Polygon mesh options and Polygon mesh detailed options dialog boxes

- The parameters should be filled as in figure 16
  - The aspect ratio determines how square the panels of the mesh will be. The closer the aspect ratio is to 1, it is better for the numerical work. The mesh elements need to be square to produce more robust and accurate results. Here I use aspect ratio 1.2.
  - Minimum initial grid quads setting is to define approximate number of mesh elements on surface.

    ARGOS Trawson is limited by the total mesh elements on the hull and the free surface. As the programmer informs the maximum number of elements is 6000. ARGOS Trawson will crash in case more elements are input in the program. It is recommended to have between 1500 and 2000. In my model there are 1588 elements which is acceptable
- And press OK button to create mesh over our hull surface part.

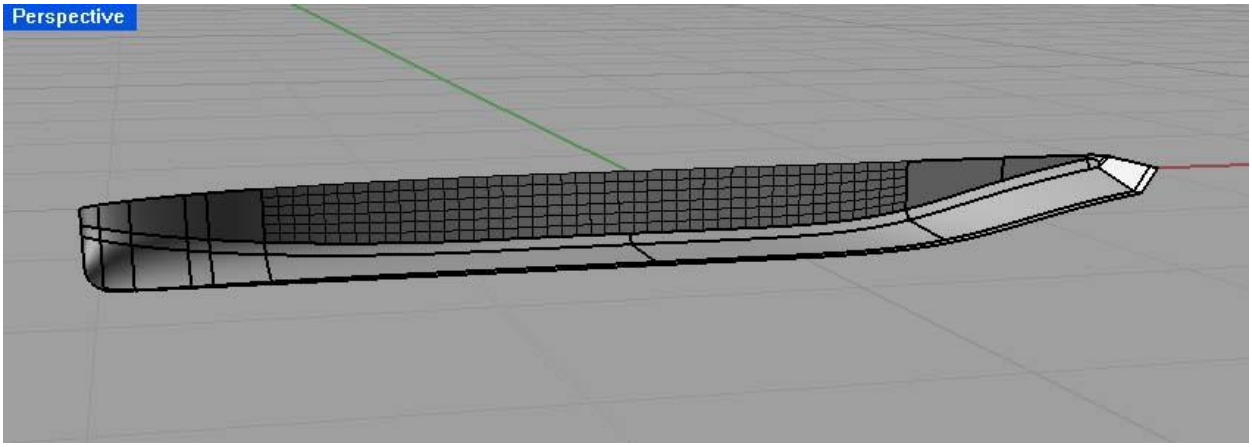

Figure 17: Mesh elements image of parabolization area on hull surface

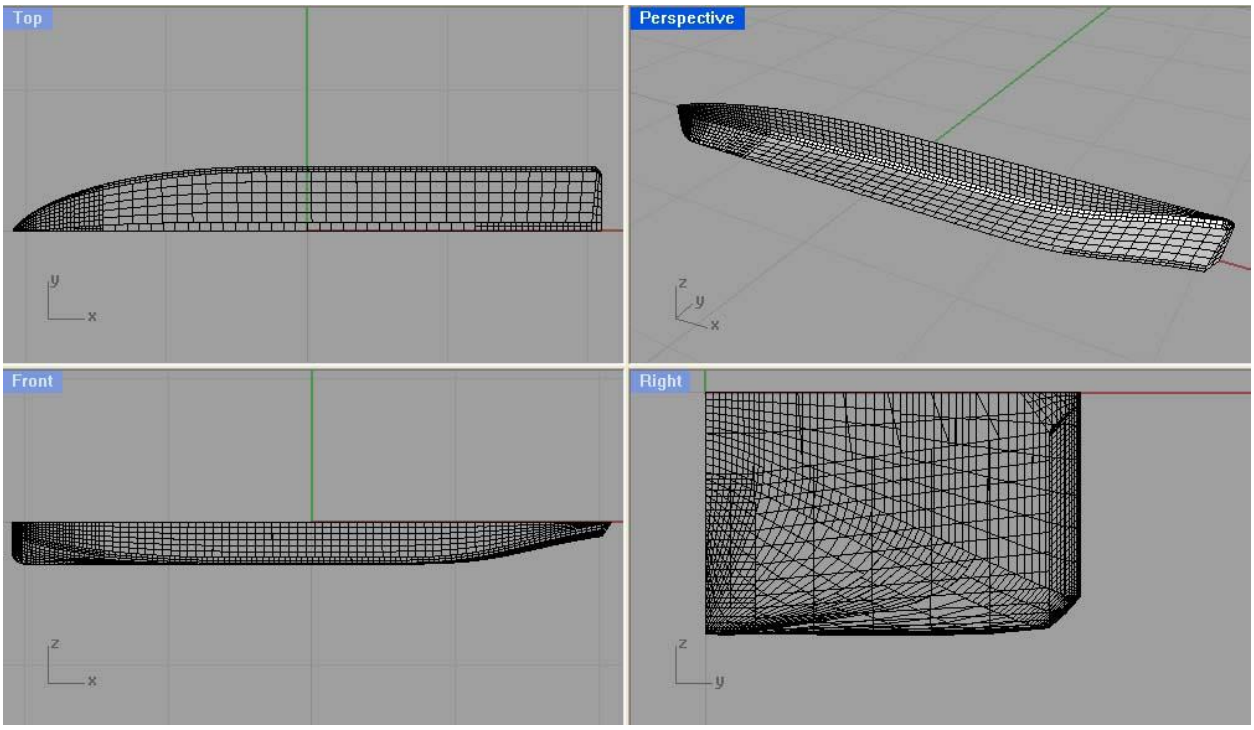

Figure 18: 3D mesh model of PSV

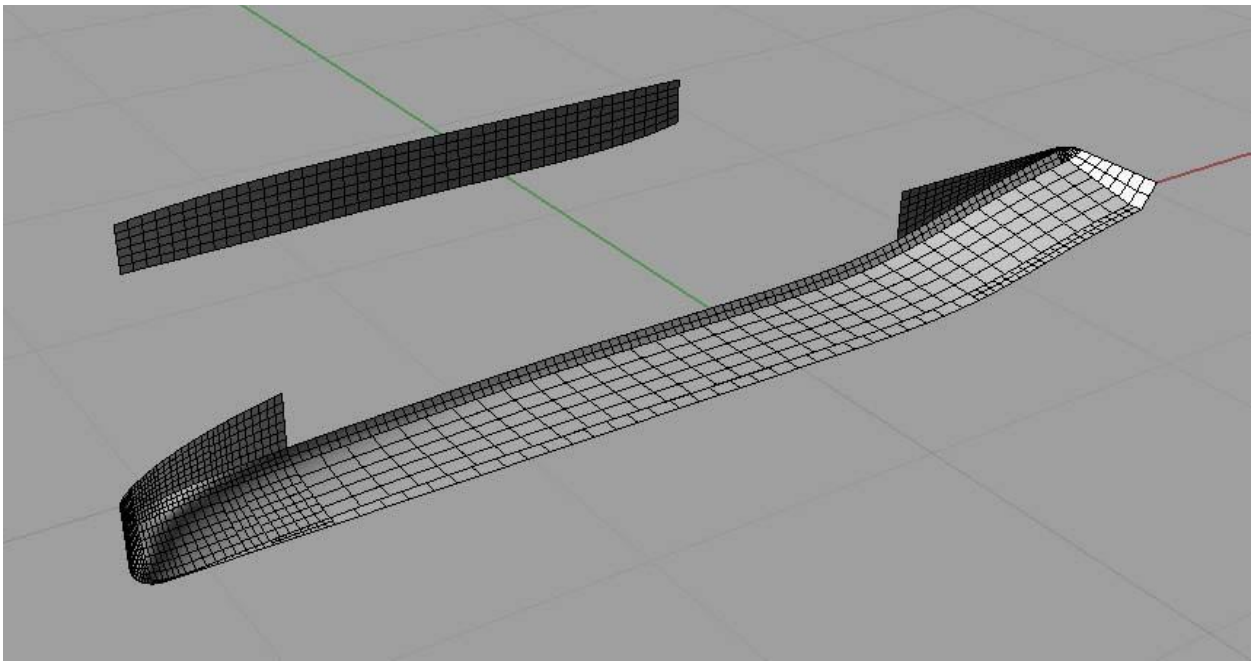

Figure 19: 3D Hull with Side bulb modification application area Mesh

The normals to the mesh elements must be pointed out of the hull, at meshed surfaces. **ARGOS Trawson** can only analize the surface mesh this way, if the surface normals looks thru inside of the hull then the software produces nonsense. The arrows appear on the hull surface indicate the mesh orientation. The orientation is correct if the arrows point out of the hull, If not their direction have to be chanced. The orientation arrows can be seen in Figure 20

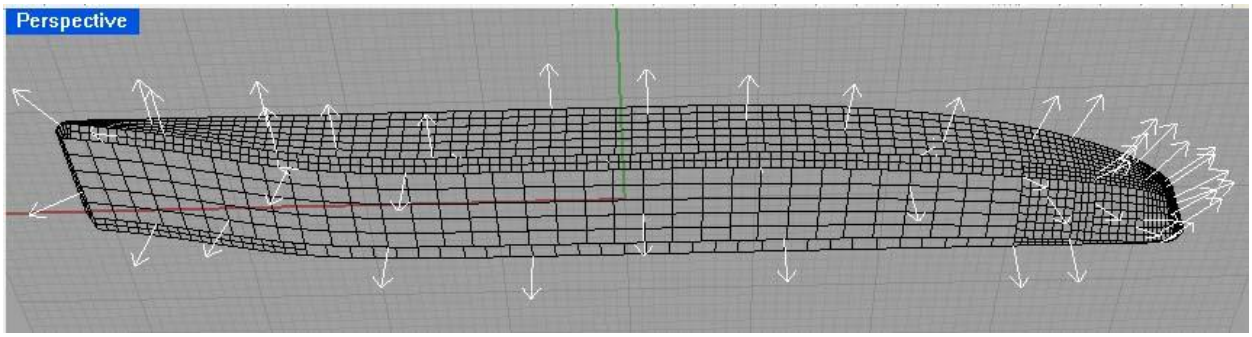

Figure 20: The arrow directions show the surface normal of mesh elements on hull Surface (view from bottom starboard side)

Now that the modeling has done and it is time to export our mesh as OBJ extension file to import Trawson Argos. We need to be sure that all meshes are joined together, then select them and go to File menu and follow the work order below.

- File menu > Export Selected

  On the opened dialog box save as the file as Wavefront (obj) file.
  - Save object as; Polygon mesh
  - Save surface trim curves as; Polylines
  - End of line character; Windows (CRLF)

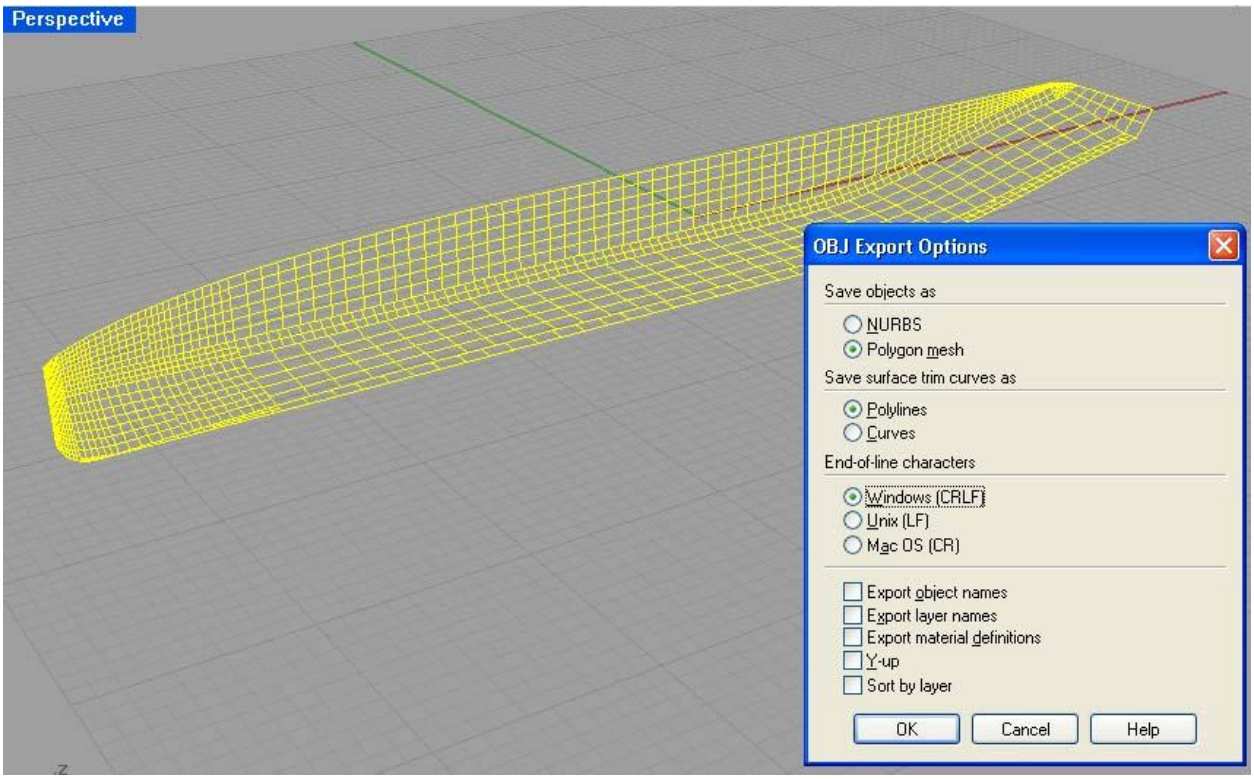

Figure 21: OBJ export dialog box of Rhinoceros 3D to export mesh elements

3.2.2. Running Trawson Argos for Parent hull PSV

After completing the necessary preparation of the model, it is time to run the wave resistance calculation solver program called ARGOS Trawson. This program will use the mesh modeled in the previous part . To run ARGOS Trawson, the following steps have been followed;

1. Argos program stay inside a file at windows operating system. Right click on ARGOS_GUI. Py and open with Python. The dialog box than appears can be seen at figure 22.
2. Click the OBJECT FILE 1 button and select the obj file.
3. SAVE DIRECTORY is to select a directory to write output files.
4. In the Hull Parameters section, hull type is defined as monohull. Catamaran, or barge are the other possible options for other projects
5. The delta option is for the hull spacing of catamarans. So it is not applicable.
6. Curved_transom parameter is NO.

7. Beause the curved_transom, option is no the curved_transom_x_offset is not applicable for us.
8. The Mesh Parameters section determines the free surface mesh. It is defined 50, 0.4, 0.3, and 0.5 for N_hull, beta, Rd, and Ru.
9. The Simulation Parameters define the operating constraints of the program. The tolerance is .0001 m defined
10. The water_density of water is 1025 kg/m3. It is for salt water for full scale model.

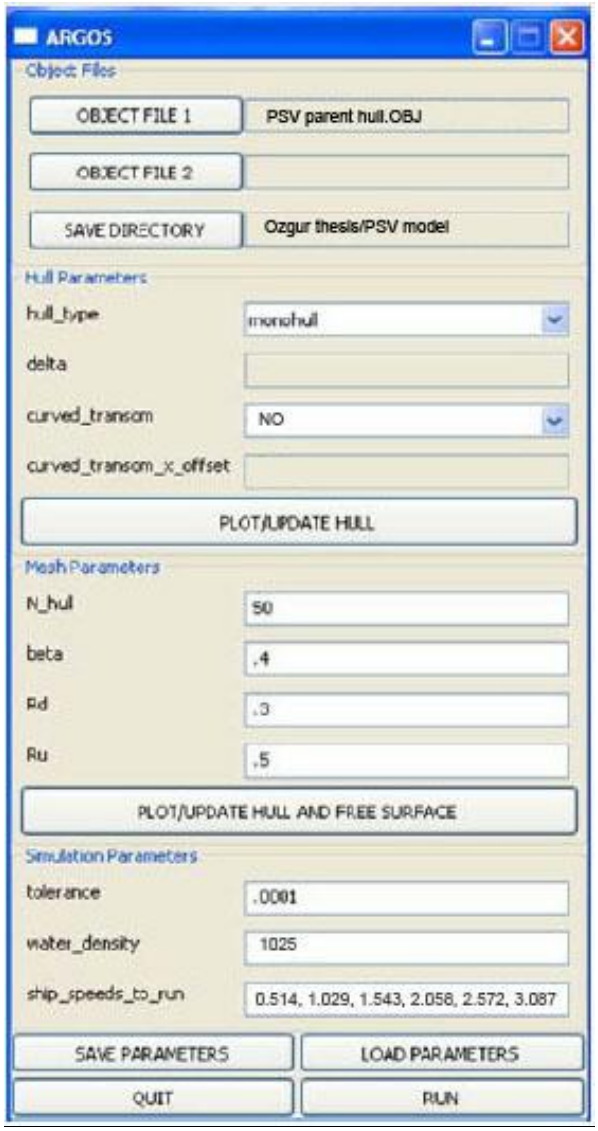

Figure 22: Trawson Argos data input dialog box

11. Ship_speeds_to_run is the speeds that we would like to run the model. I used speeds from 1 to 17 knots as speed for this study. The speeds must be in m/s and they are;

kts	**1**	**2**	**3**	**4**	**5**	**6**	**7**	**8**	**9**
m/s	0,514	1,029	1,543	2,058	2,572	3,087	3,601	4,116	4,630
kts	**10**	**11**	**12**	**13**	**14**	**15**	**16**	**17**	
m/s	5,144	5,659	6,173	6,688	7,202	7,717	8,231	8,745	

Table 2: Test Speeds in knots and m/s

12. SAVE PARAMETERS button saved all parameters entered.
13. It is time to run the program. The program will start working when pressing the the RUN button.

3.2.3. Trawson Argos results for parent hull

The results of Trawson Argos Software can are be seen at the following part. The Figure 23 presents the speed – wave resistance curve of parent hull PSV. Also the wave elevation can been seen at followings figures

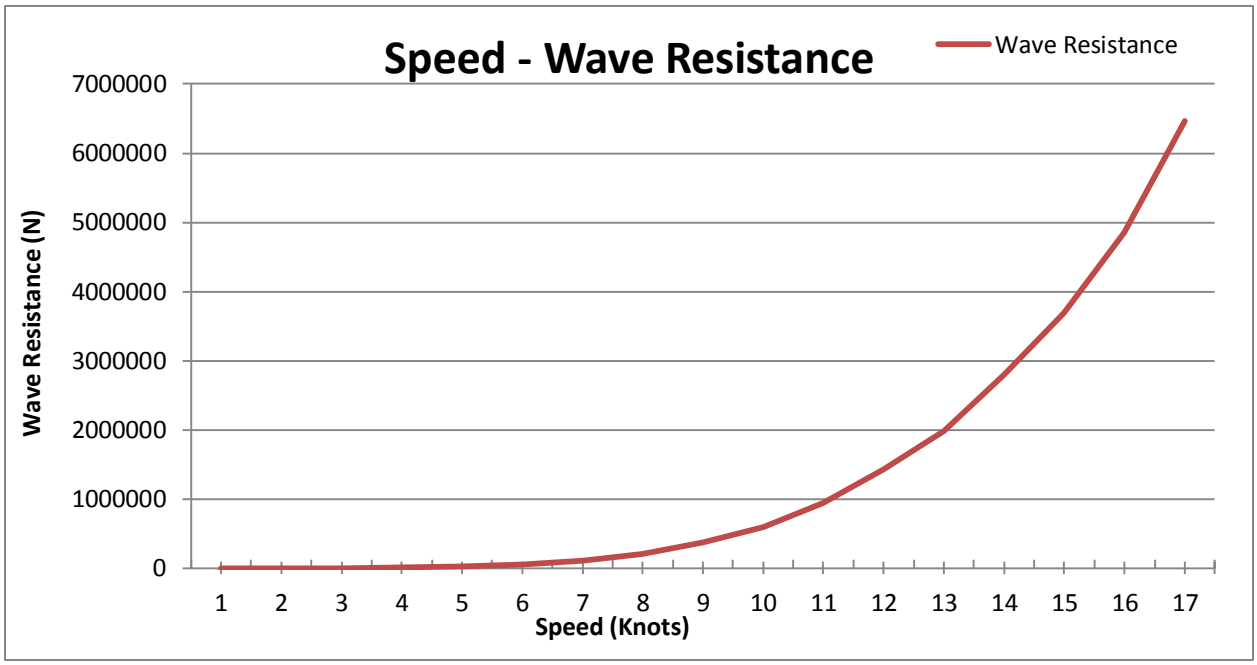

Figure 23: Speed – Wave Resistance curve of vessel for parent hull

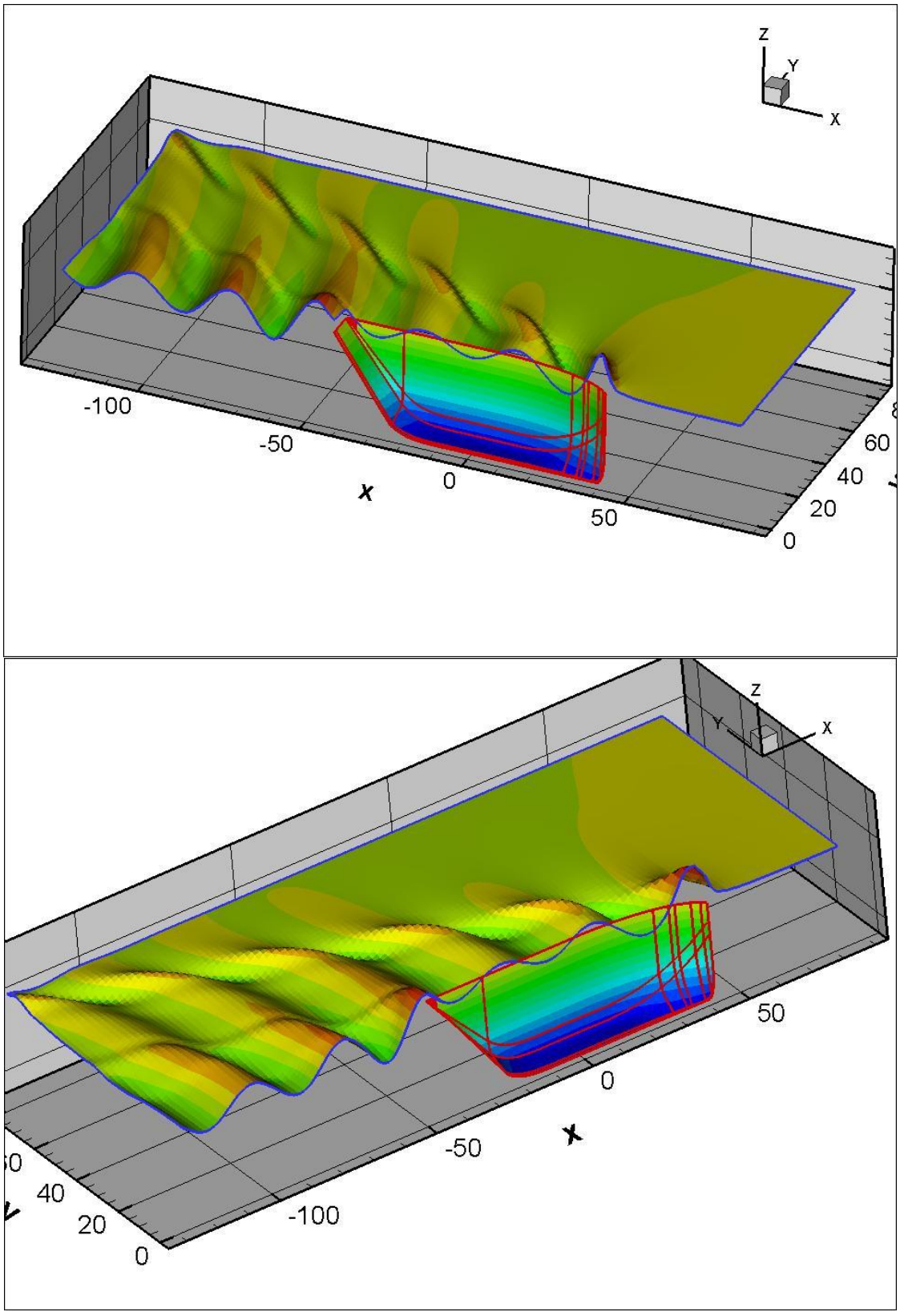

Figure 24: Wave elevation of parent hull Perspective view at 13,61 kts

3.3. ARGOS Optimization Software: Amidships Bulb Development

The Argos Software is a programs that makes the parabolization and create sidebulb on the predefined area of hull part. The software runs an algorithm and several iterations to reduce the wave resistance value.

The wave resistance is reduced using a gradient algorithm. The wave resistance is called the objective function, in optimization terminology. It is the quantity we wish to minimize (denote is as f).

We begin with a parent hull. A region of the hull amidship is defined with a single b-spline surface. The y-coordinates of the control points of this surface constitute the optimization variables x, i.e. the control point y-coordinates will be modified throughout the optimization process. This will change the shape of the hull amidship, and will consequently change the value of our objective, the wave resistance $f(x)$.

The parent hull is the starting point of the algorithm. The resistance is reduced iteratively, decreasing at every step, until a local minimum is reached. We need the gradient of the wave resistance with respect to the control point locations. The gradient tells the optimization algorithm how to move the control points in order to guarantee that the resistance is decreased at each iteration.

The gradient is calculated using the finite-difference method, specifically forward differences. Let N be the number of variables. Each variable is perturbed by some small quantity h, and the solver is run each time. The formula used to calculate the gradient is

$$\frac{\partial f(x)}{\partial x_i} \approx \frac{f(x + he_i) - f(x)}{h}$$

where f is the wave resistance, x is the vector of control point y-coordinates, and e_i is unit vector with 1 in the i-th coordinate and 0 everywhere else. Thus each time the gradient is calculated the solver must be run $N + 1$ times.

The gradient descent algorithm begins with some initial guess x_0. In our case this x_0 corresponds to the shape of the parent hull amidship, i.e. with no midship bulb. At each iteration the optimization determines a new x_k using the formula

$$x_k = x_{k-1} + \alpha_k p_k$$

where α_k is the step length and p_k is the step direction. The step length is determined using a line search algorithm. Many choices are possible for the step direction p_k. The steepest-descent method sets p_k to the negative of the gradient,

$$x_k = x_{k-1} - \alpha_k \nabla f_k$$

Newton's method looks at the second derivative of f, the Hessian $\nabla^2 f$. At each iteration the step direction is chosen to be

$$p_k = -(\nabla^2 f_k)^{-1} \nabla f_k$$

This uses much more information about the objective function, but the cost of calculating the Hessian of the wave resistance with respect to the control point coordinates using finite differences is prohibitive (on the order of N^2).

The quasi-Newton method approximates the Hessian using information accumulated over the course of several iterations. The step direction is

$$p_k = -B_k{}^{-1} \nabla f_k$$

where B_k is some approximation to the true Hessian. The rate of convergence of the quasi-Newton method is much faster than steepest-descent, though not as fast as Newton's method. However, the cost per iteration is much less.

Constraints on the variables are necessary. We want to ensure that the midship bulb surface is smooth, that it does not have a "bumpy" surface. We can do this by ensuring certain relationships between the control points.

Constraints make the optimization task more difficult, but there are free, high-quality implementations of many popular constrained optimization algorithms available. The gradient descent algorithm we use is implemented in the open source package IPOPT. IPOPT uses the interior-point method to guarantee constraints satisfaction.

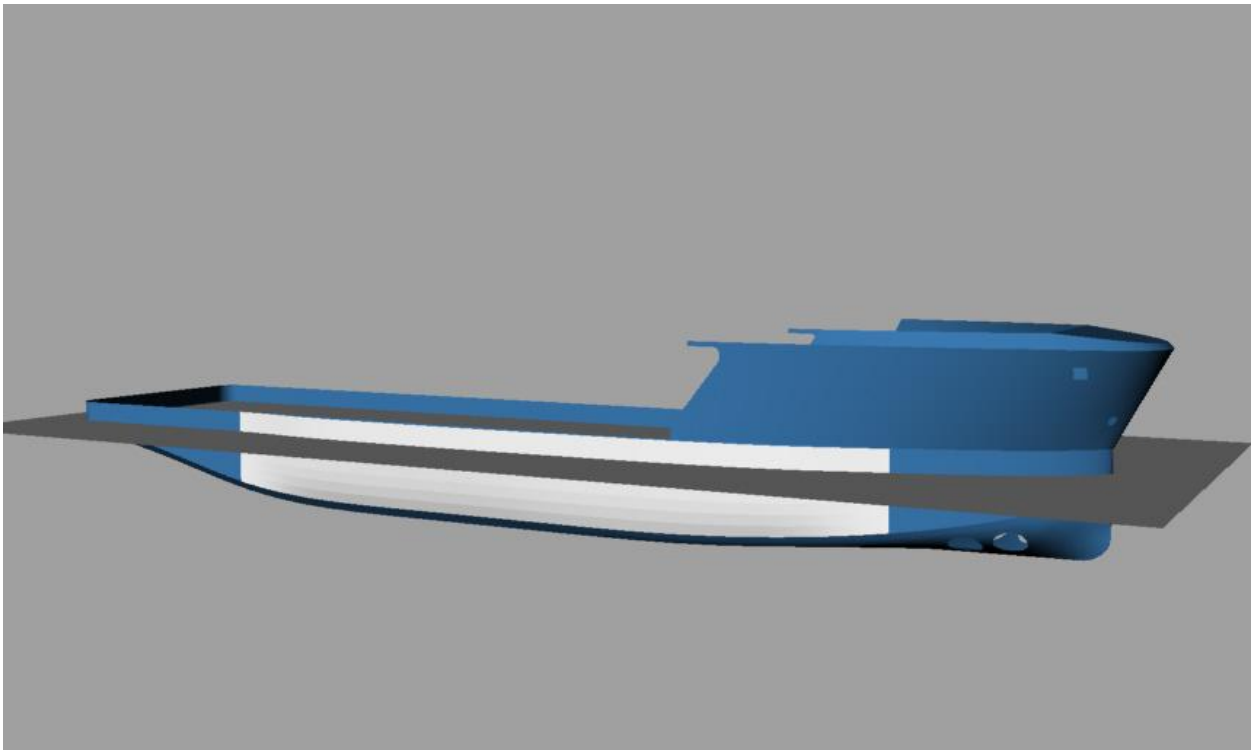

Figure25: 3D view pf parabolized retrofit hull. Created sidebulb is shown in grey and parent hull with blue color surfaces.

The theory explained above explains how sidebulb creation algorithm works inside the Trawson optimizer code and the result of the program created and appropriate sidebulb to our Platform supply vessel parent hull. The figure 26 show the side bulb placed on the flat wall structure of the hull. The sidebulb shape is usefull under the design waterline level (DWL). Regarding to design, the sidebulb shape can extend up to deck level like our PSV model or it can be finished at DWL.

The characteristics of the hull and sidebulb are presented in graphs and figures in the following part of the chapter.

3.3.1parabolized Hull Form, Wave Elevation And Results

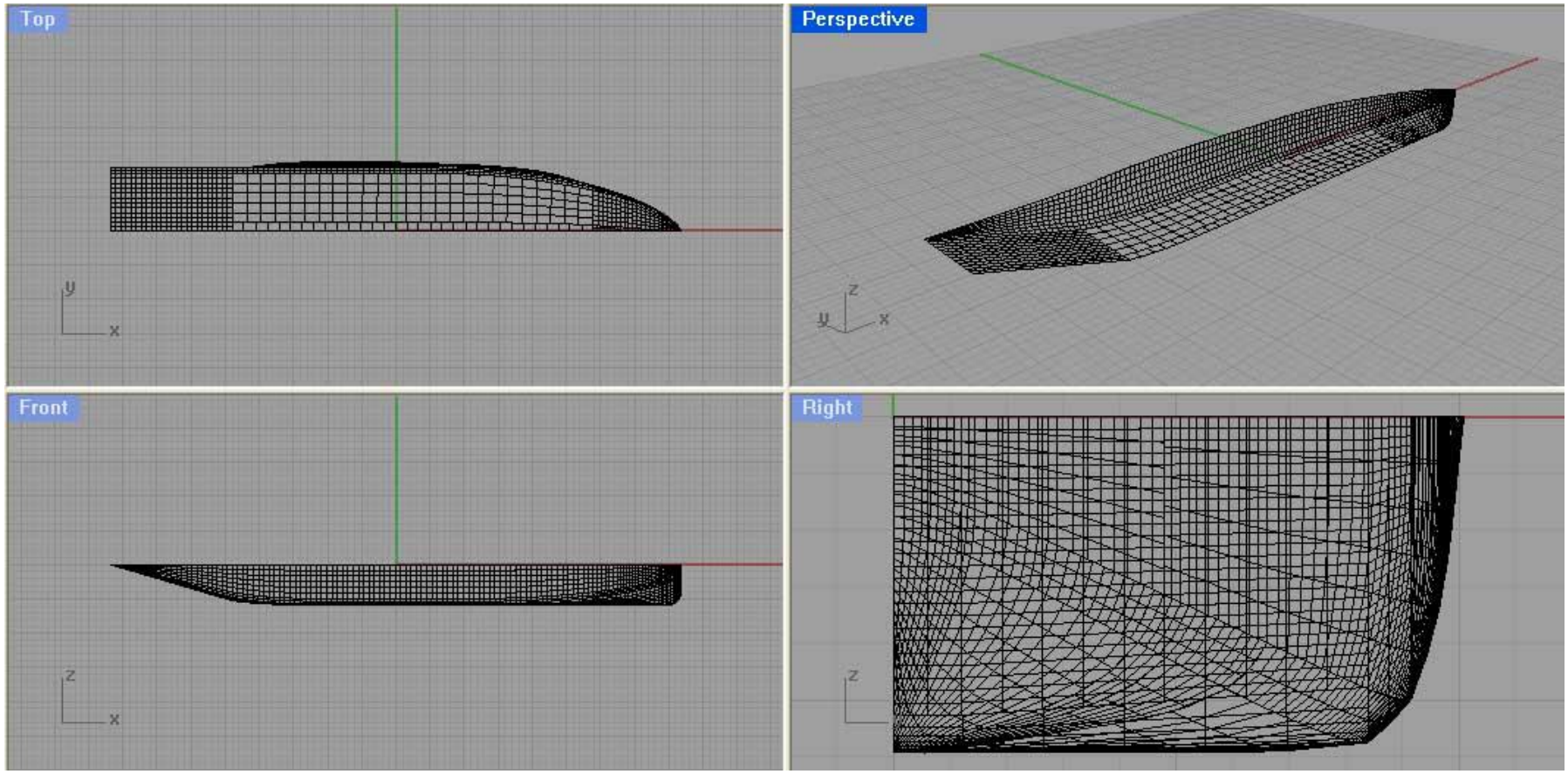

Figure26: 3D parabolized hull with mesh

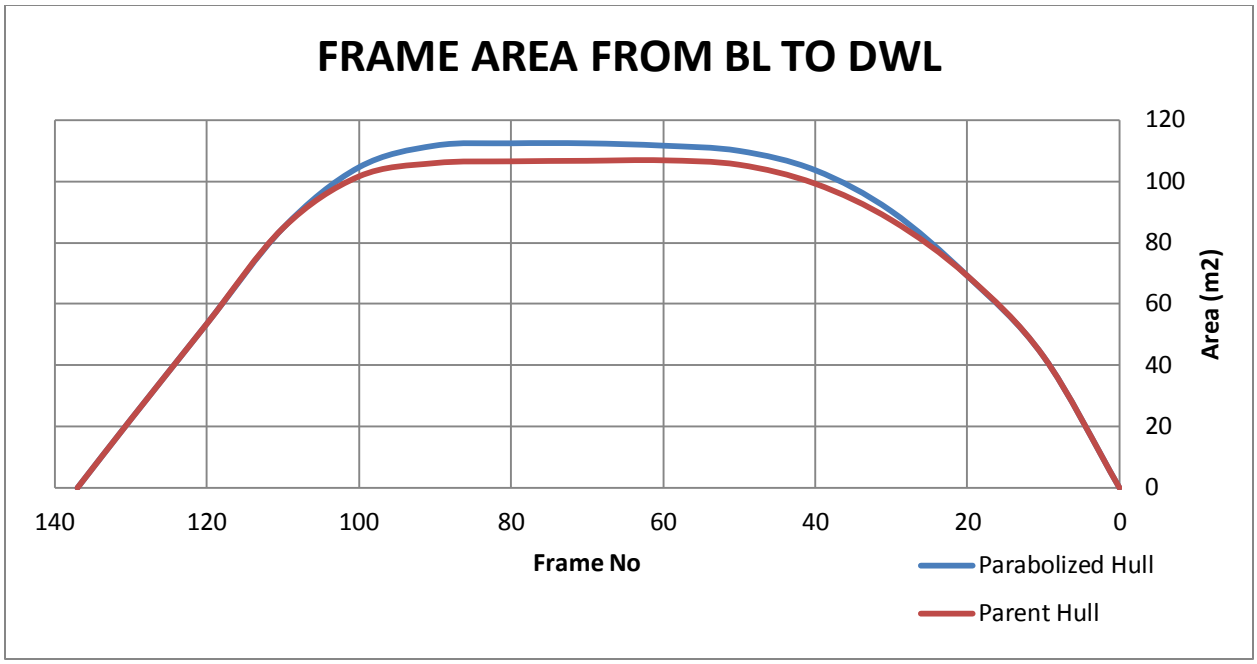

Figure 27: Frame cross section area of PSV from BL to DWL for parent and parabolized hull

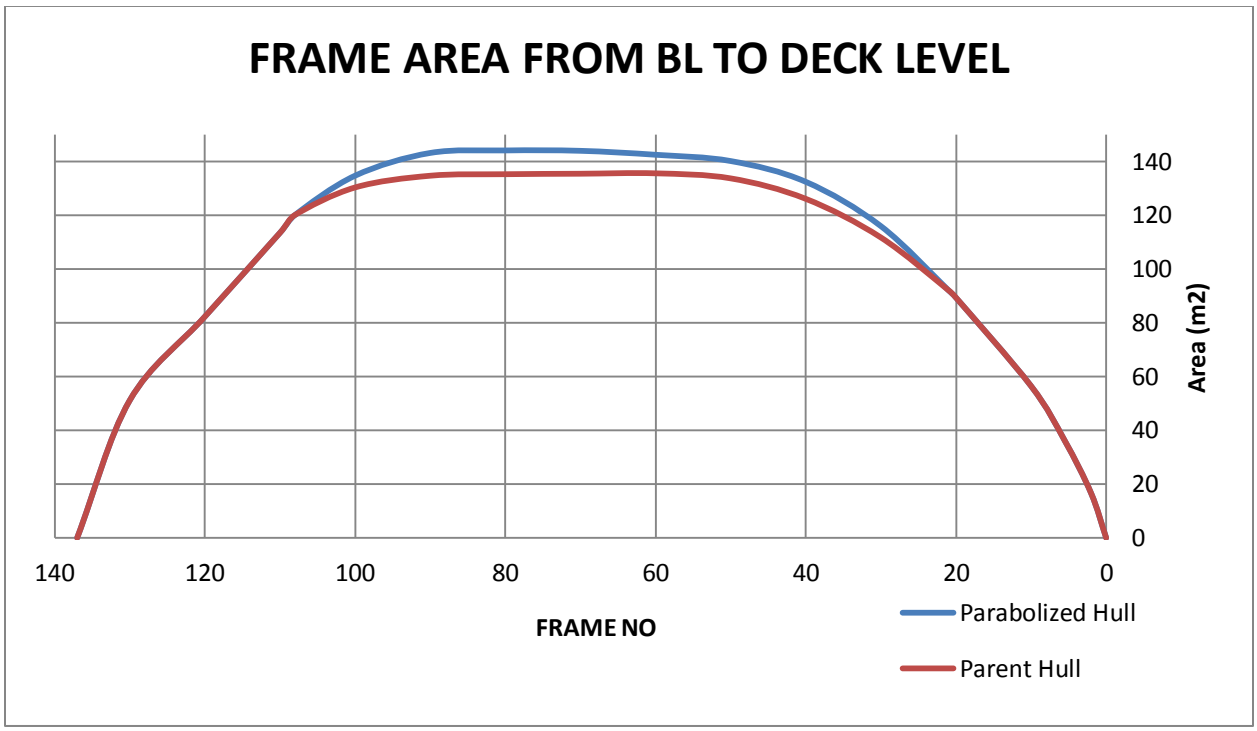

Figure 28: Frame cross section area of PSV from BL to Deck level for parent and parabolized hull

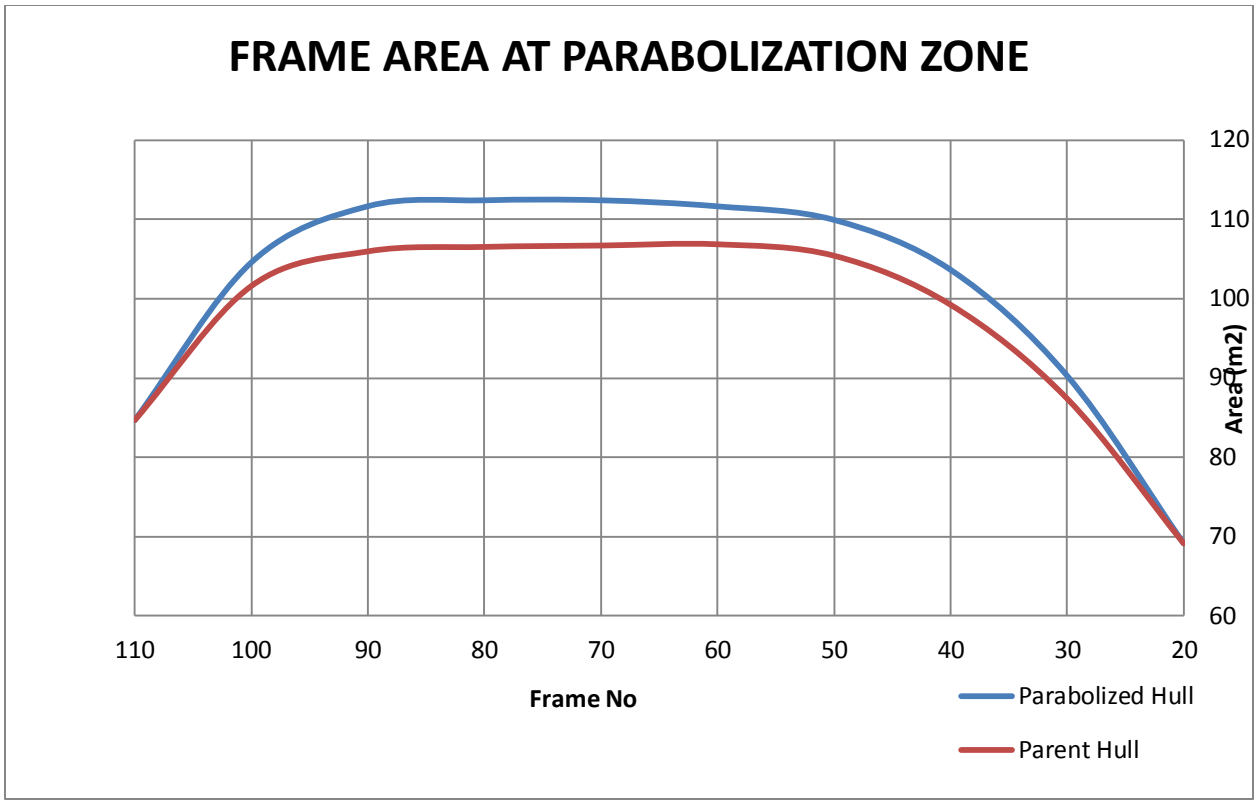

Figure 29: Frame cross section at parabolized area on the hull for parent and parabolized hull

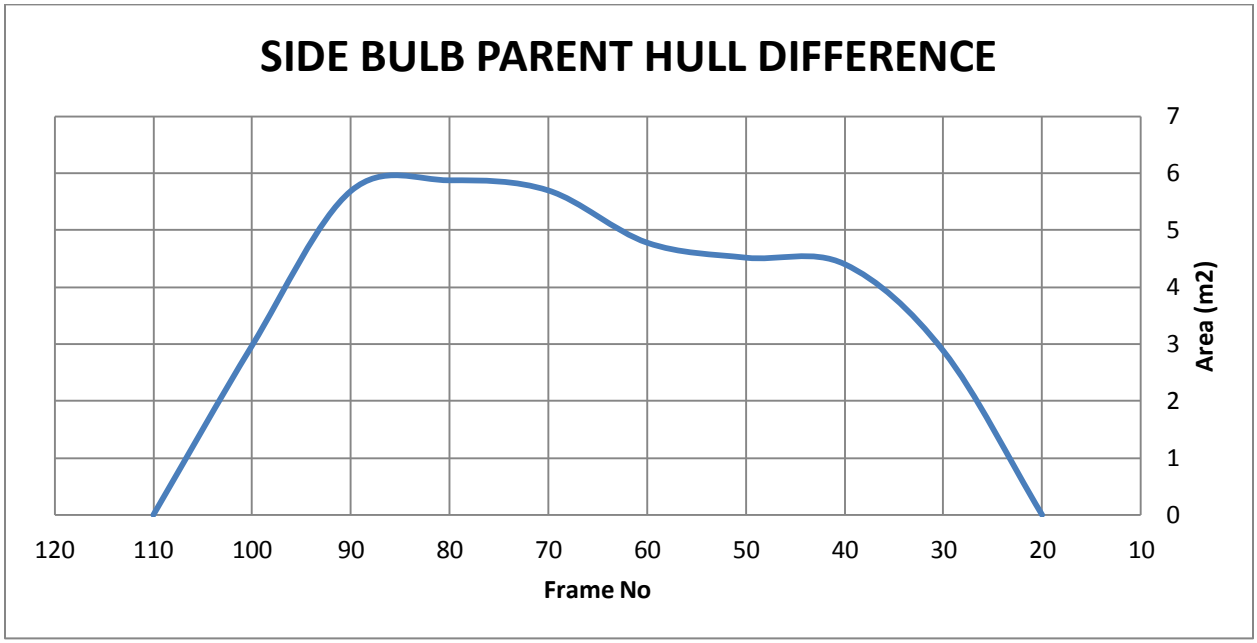

Figure 30: Frame cross section difference between parent and parabolized hull at parabolized area

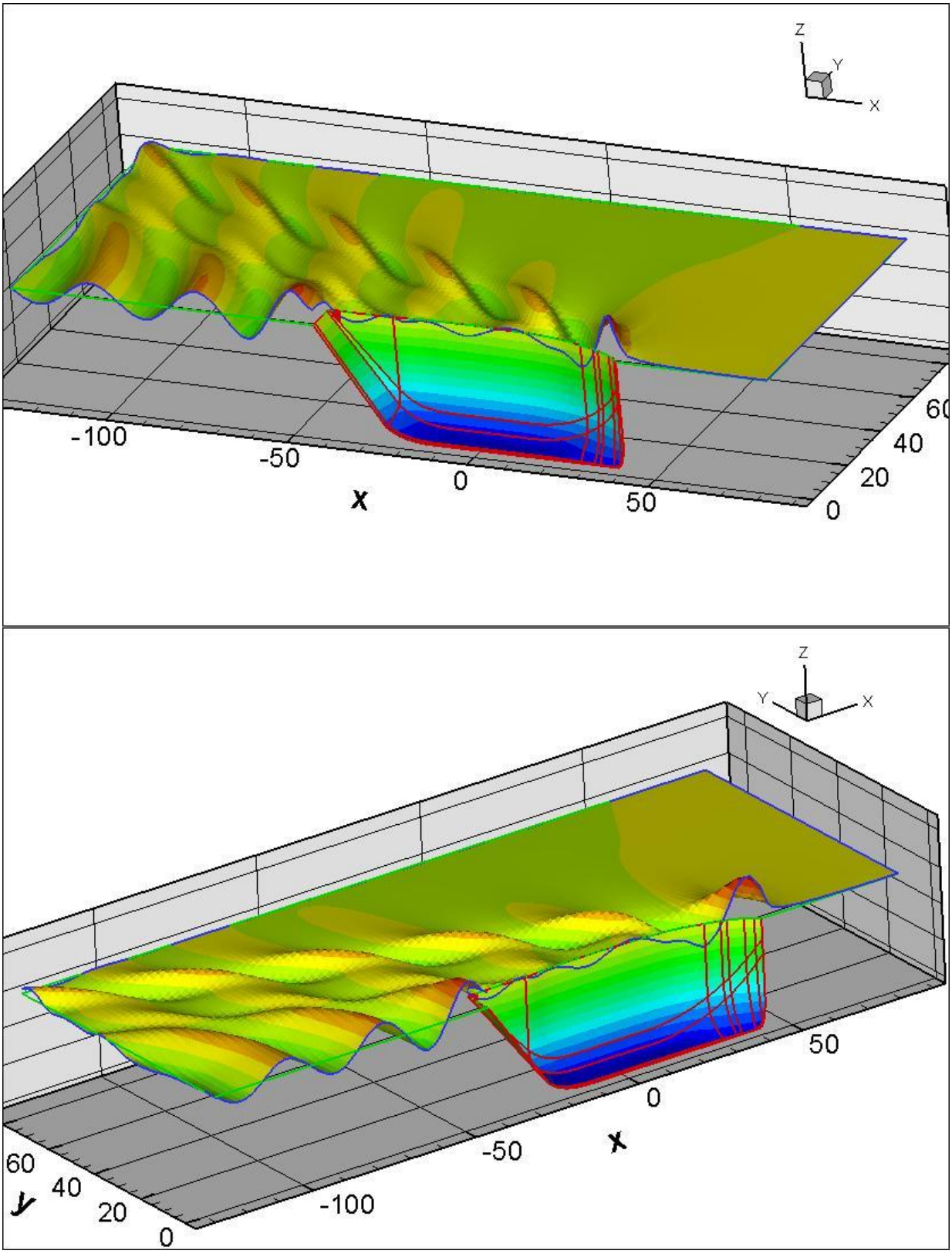

Figure 31: 3D wave elevation view of retrofit parabolic hull at 13,61kts

3.4. Parent And Parabolized Hull Forms Wave Elevation And Resistance Comparison

The wave height numerical analysis was done using **ARGOS Trawson** by modeling a full scale computer model for both parent and parent hull. The numerical wave height prediction is presented by using tecplot output image shown at figure 32. The speed of the analysis is 13,61kts for both hull and the wave heights are shown by color scale.

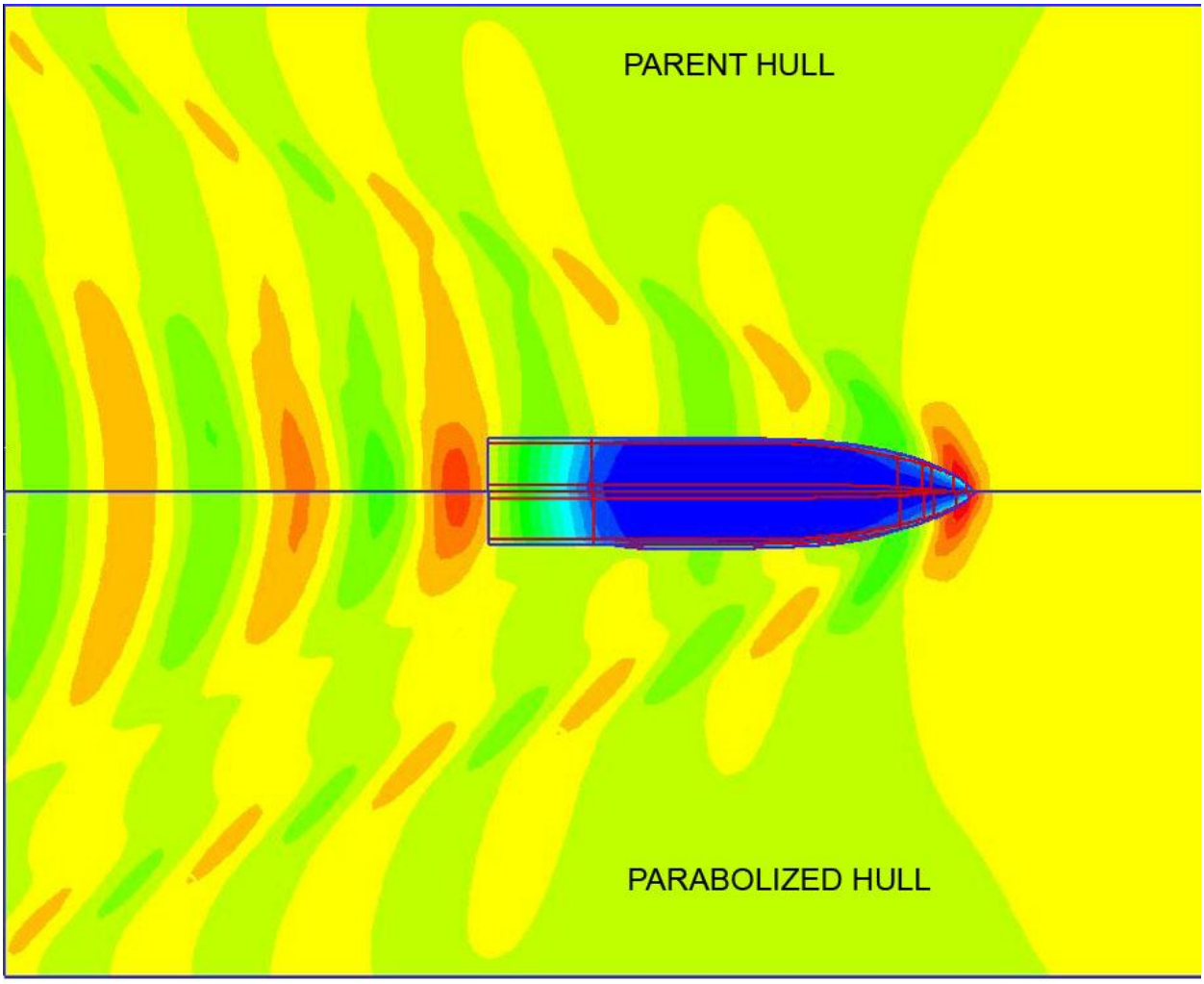

Figure 32: Wave elevation comparison of parent and parabolic hull at 13,61 kts

It can be easily seen that the bow wave is same up to sidebulb region of the hull. There is one peak and one trough is same at bow wave. The shoulder wave is slightly chancing the second peak and trough makes them less high and deep. It goes all the

way up to the stern of the vessel. The modification of hull wave also gives a positive effect on reducing the stern wave. The size of stern wave of the parabolized hull is slightly smaller but keeps the same height with parent hull at 13,61 kts.

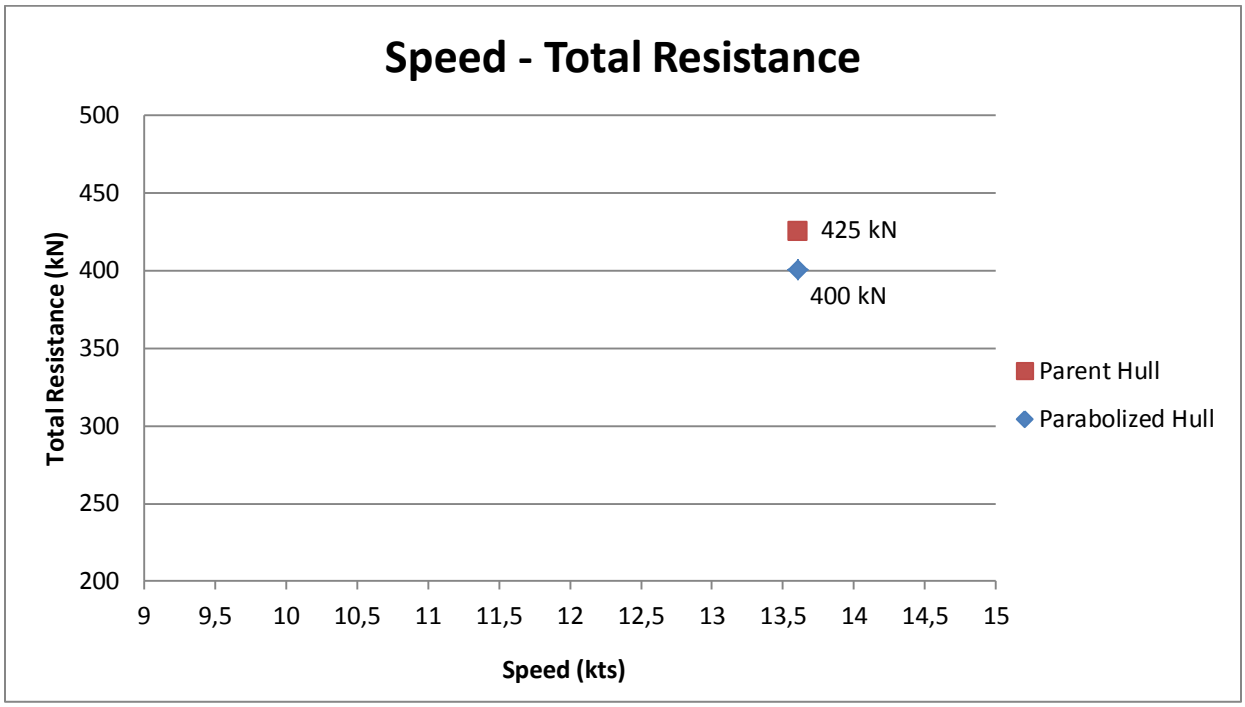

Figure 33: The total resistance values for parent and parabolized hull in 13,61 kts speed.

The total resistance values for retrofit parabolic hull and parent hull are shown at figure 33. The sidebulb reduces the total resistance which is sum of wave resistance plus ITTC 57, from 425 to 400 kN. The wetted surface and hull coefficient are both increased by amidship bulb geometry. Total resistance reduction is result of wave resistance reduction that made by the amidship bulb. The reduction ratio is calculated as below.

$$\boldsymbol{Total\ Reduction\ Ratio} = \frac{\boldsymbol{R_{T(Parent\ Hull)}} - \boldsymbol{R_{T(Parabolized\ Hull)}}}{\boldsymbol{R_{T(Parent\ Hull)}}} \%$$

$$\boldsymbol{Total\ Reduction\ Ratio} = \frac{\boldsymbol{425 - 400}}{\boldsymbol{425}} = \boldsymbol{0,0588 = 5,88\ \%}$$

4. SCANTLING OF PSV REGARDING TO ABS RULES

The principle dimensions of the vessel are the variables for scantling calculation of the ship structural members for every type of marine structures. If one of them change, the scantling has to be recalculated accordingly. The beam increased as well as the displacement as a result of “retro fit” waterline parabolization. So the scantling of the PSV is calculated and the required structural increase on size and thickness is calculated.

4.1. Deck Plating

Thickness: Generally, the thickness of deck plating is to be not less than obtained from the applicable equations specified in Table 3.
Also, the plating thickness of a deck or inner bottom on which cargo is carried is to be obtained from the following equations:

$$t = \frac{s\sqrt{h}}{254} + 1{,}5\ mm$$

where

t = thickness, in mm (in.)

s = beam or longitudinal spacing, in mm (in.)

p = uniform loading, in kN/m2 (kgf/m2, lbf/ft2)

h = height, in m (ft), as follows:

= p/7.01 m (p/715 m, p/44.7 ft) for an exposed deck intended to carry deck cargoes when load p exceeds 25.66 kN/m2

$$t = \frac{609{,}6\sqrt{6{,}997}}{254} + 1{,}5$$

t = 7,85 mm and t_{actual} = 10 mm

Deck Load = 5 ton/m^2 = 49,05 kN/m^2

h = 49,05/7,01 = 6,997 m

Decks	*Minimum Thickness Equation in Table 2*
A. Strength Deck Outside Line of Openings	
1. With Transverse Beams	1a and 1b (note 1)
2. With Longitudinal Beams	2a and 2b (note 1)
B. Exposed Strength Deck within Line of Openings	3 (note 2)
C. Enclosed Strength Deck within Line of Openings	5
D. Effective Lower Decks	
1. Second Deck:	
a. D_S > 15.2 m (50 ft)	1a
b. 15.2 m (50 ft) ≥ D_S ≥ 12.8 m (42 ft)	2a
c. D_S < 12.8 m (42 ft)	3
2. Third Deck:	
a. D_S > 17.7 m (58 ft)	1a
b. 17.7 m (58 ft) ≥ D_S ≥ 13.4 m (44 ft)	2a
c. 13.4 m (44 ft) ≥ D_S ≥ 9.8 m (32 ft)	3
d. D_S < 9.8 m (32 ft)	4
E. Exposed Forecastle Decks	
1. L > 122 m (400 ft)	2a
2. L ≤ 122 m (400 ft)	3
F. Exposed Poop Decks	
1. L > 100 m (330 ft)	3
2. L ≤ 100 m (330 ft)	5
G. Exposed Decks Above Poop/Forecastle Decks	4
H. Long Deckhouse Tops and other Enclosed Decks	5
I. Platform Decks in Enclosed Cargo Spaces	6
J. Enclosed decks in Accommodation spaces	7

Table 3: Applicable Thickness Equations

Notes:

1 *(1 July 2012)* In small vessels where the required area for longitudinal strength is relatively small, it may be disposed in the stringer plate and in the strake alongside openings in plating of thickness not less than that obtained from the equations in 1a and 1b. In such cases the remainder of the plating may be obtained from the equation in 5.

2 *(1 July 2012)* Equation 3 applies amidships. At the forward and aft ends, plating is to be as required for the exposed forecastle and poop deck

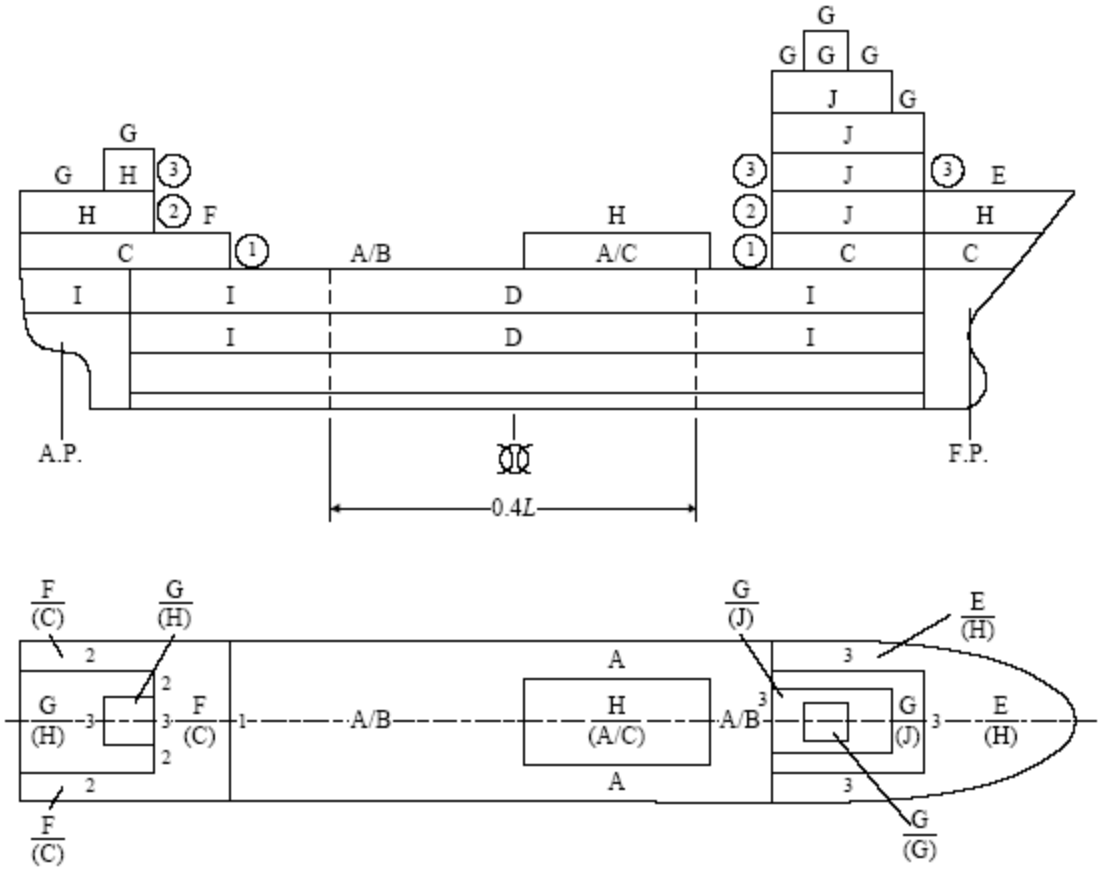

Figure 34: Decks and tiers allocation

4.2 Side Shell Plating

The minimum thickness, t, of the side shell plating throughout the amidship 0.4L is to be obtained from the following equations, whichever is greater:

$$t_{shell1} = \left(\frac{s}{645}\right)\sqrt{(L - 15{,}2)(\frac{d_s}{D_s})} + 2{,}5\ mm$$

$$\boldsymbol{t_{shell2} = 0,035\ (L + 29) + 0,009s\ \ mm}$$

Where

s = spacing of transverse frames or longitudinals, in mm, not greater than 610 mm for tshell2 only

L = length of vessel, in m

ds = scantling draft, in m

Ds = scantling depth, in m

The actual ratio of ds/Ds is to be used in the above equations, except that the ratio is not to be taken less than 0.67.

$$t_{shell1} = \left(\frac{609,6}{645}\right)\sqrt{(80,31 - 15,2)(\frac{5,9}{7,47})} + 2,5\ mm$$

$t_{shell\ 1}$ = 9,3 mm

$$\boldsymbol{t_{shell2} = 0,035\ (80,31 + 29) + 0,009x609,6\ \ mm}$$

t_{shell2} = 9,3 mm

t_{actual} = 12,7 mm

4.3 Beams and Longitudinals

Strength Requirement: Each beam and longitudinal, in association with the plating to which it is attached, is to have a section modulus SM as obtained from the following equation:

$$SM = 7,8chsl^2\ cm^3$$

C = 0,540 for half beams, for beams with centerline support only, for beams between longitudinal bulkheads, and for beams over tunnels or tunnel recesses..

= 0,585 for beams between longitudinal deck girders. For longitudinal beams of platform decks and between hatches at all decks

= 0,90 for beams at deep-tank tops supported at one or both ends at the shell or on longitudinal bulkheads

= 1,00 for beams at deep-tank tops between longitudinal girders

= 1/(1,709 -0,651k) for longitudinal beams of strength decks and of effective lower decks

k = $SM_R Y / I_A$

SM_R = Required hull girder section modulus amidships, in cm2-m

Y = distance, in m, from the neutral axis to the deck being considered, always to be taken positive

I_A = hull girder moment of inertia of the vessel amidships, in cm2-m2. The values of IA and Y are to be those obtained using the area of the longitudinal beams given by the above equation.

s = spacing of beams, in m

l = distance, in m, from the inner edge of the beam knee to the nearest line of girder support or between girder supports, whichever is greater. Under the top of deep tanks and in way of bulkhead recesses, the supports are to be arranged to limit the span to not exceeding 4.8 m

p = uniform loading, in kN/m^2

h = height, in m (ft), as follows:

= p/7.01 m (p/715 m, p/44.7 ft) for an exposed deck intended to carry deck cargoes when load p exceeds 25.66 kN/m2

Deck longitudinals

$$h = \frac{49,05}{7,01} = 6,997$$

$$k = \frac{SM_R Y}{I_A} = \frac{13234,5X4,267}{31917,8} = 1,7693$$

$$c = \frac{1}{1,709 - 0,651k} = \frac{1}{1,709 - 0,651x1,7693} = 1,7947$$

$$SM = 7{,}8x1{,}7947x6{,}997x0{,}6096x2{,}4384^2\ cm^3$$

$$SM = 355\ cm^3$$

Deck Beams

$$h = \frac{49{,}05}{7{,}01} = 6{,}997$$

$$k = \frac{SM_R\, Y}{I_A} = \frac{13234{,}5X6{,}096}{31917{,}8} = 2{,}5276$$

$$c = \frac{1}{1{,}709 - 0{,}651k} = \frac{1}{1{,}709 - 0{,}651x2{,}5276} = 15{,}7505$$

$$SM = 7{,}8x15{,}7505x6{,}997x0{,}6096x4{,}572^2\ cm^3$$

$$SM = 10953{,}6\ cm^3$$

4.4 Longitudinal Frames

Strength Requirement: Each beam and longitudinal, in association with the plating to which it is attached, is to have a section modulus SM as obtained from the following equation:

$$SM = 7{,}8chsl^2\ cm^3$$

s = spacing of longitudinal frames, in m

c = 0,95

h = above 0.5D from the keel, the vertical distance, in m, from the longitudinal frame to the bulkhead or freeboard deck, but is not to be taken as less than 2.1m

= at and below 0.5D from the keel, 0.75 times the vertical distance, in m (ft), from the longitudinal frame to the bulkhead or freeboard deck, but not less than 0.5Ds.

l = the unsupported span, in m

Side longitudinal above

$$SM = 7{,}8x0{,}95x2{,}52x0{,}63x2{,}44^2\ cm^3$$

SM = 70 cm^3

SM_{actual} = 103,5 cm^3

Side longitudinal below

$$SM = 7{,}8x0{,}95x6{,}3x0{,}63x2{,}44^2\ cm^3$$

SM = 175 cm^3

SM_{actual} = 221 cm^3

4.5 Bottom Shell plating

Each beam Shell plating is to be of not less thickness than is required for purposes of longitudinal hull girder strength; including buckling strength, nor is it to be less than is required by this Section.

The shell plating is not to be less than:

$$t_{shmin} = \frac{sk\sqrt{qh}}{254} + 2{,}5\ mm$$

but not less than 8.5 mm for side shell and 6.5 mm for bottom shell, or (s/150 + 2.5) mm, whichever is greater

Where

t = thickness, in mm
s = stiffener spacing, in mm
k = 1,0 where α > 2
α = aspect ratio of the panel (longer edge/shorter edge)
q = 235/Y N/mm^2
Y = specified minimum yield point or yield strength, in 235/Y N/mm^2
h = the greatest of the following distances, in m
depth, D,
no less than 0.1L or 1.18d,whichever is greater,if L is less than 90m

$$t_{shmin} = \frac{609{,}6x1x\sqrt{235/235x7{,}47}}{254} + 2{,}5$$

$$t_{shmin} = 9{,}06\ mm \qquad t_{actual} = 11{,}11\ mm$$

4.6 Central Girder Thickness and Side Girder Thickness

The depths of center girder and side girders are to comply with the double bottom depth, center girder plates are to be of the thickness given by the following equations, between the peak bulkheads. In peaks, the center girder plates are to be of the thickness of the peak floors. Where longitudinal framing is adopted, the center girder plate is to be suitably stiffened between floors and docking brackets are to be provided. Where the length of the cargo hold is greater than 1.2B or exceeds 0.25L, or where the vessel is intended to carry heavy cargoes on double bottom, the thickness of center girder plates is to be specially considered based on the results of a direct structural calculations.

Thickness amidships

$$t = 0{,}056\,L + 5{,}5\ mm$$

Thickness at ends

85% of the thickness required amidships

$$t = 0{,}056\, x80{,}31 + 5{,}5$$

$$t = 10{,}0\, mm$$

4.7 Solid Floor Thickness

Solid floors (see Figure 35) of the thickness obtained from the following equations, are to be fitted on every frame (600 mm to 800 mm) under machinery, under the outer ends bulkhead stiffener brackets and at the forward end. Elsewhere, they may have a maximum spacing of 3.66 m in association with intermediate open floors, or longitudinal framing of the bottom and/or inner bottom plating. With the latter, the floors are to have stiffeners and/or brackets supporting each longitudinal or an equivalent arrangement is to be provided.

$$t = 0{,}036\, L + 4{,}7 + c\ \ mm$$

t	=	thickness, in mm (in.), but need not exceed 14 mm (0.55 in.) when floors are fitted at every frame
L	=	length of vessel, in m
c	=	1.5 mm for floors where the bottom shell and inner bottom are longitudinally framed o be taken as less than 2.1m

$$t = 0{,}036x80{,}31 + 4{,}7 + 1{,}5\ \ mm$$

$$t = 9{,}1\ \ mm$$

$$t_{actual} = 9{,}525\ \ mm$$

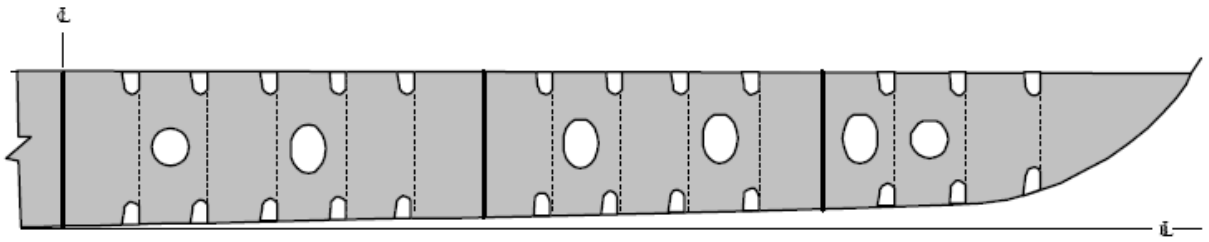

Figure 35: Double bottom solid floors

4.8 Bottom Shell Frames

Each frame and reverse frame similar to that shown in Figure 36, in association with the plating to which it is attached, is to have a section modulus SM as obtained from the following equation:

$$SM = 7{,}8chsl^2\ cm^3$$

s = spacing of longitudinal frames, in m

c = 0,5 with struds

h = ds or 0.67D in m, whichever is greater. For reverse frames without struts, the distance may be measured from the top of the inner bottom

l = the greatest distance, in m, between the connecting brackets or intercostals, as shown in Figure 36. Where effective struts are fitted and the tank top is intended to be uniformly loaded with cargo, l may be taken as 85% of the distance between supports, as determined above.

$$SM = 7{,}8x0{,}5x5{,}90x0{,}6096x5{,}49^2\ cm^3$$

$$SM = 423\ cm^3$$

$$SM_{actual} = 4111\ cm^3$$

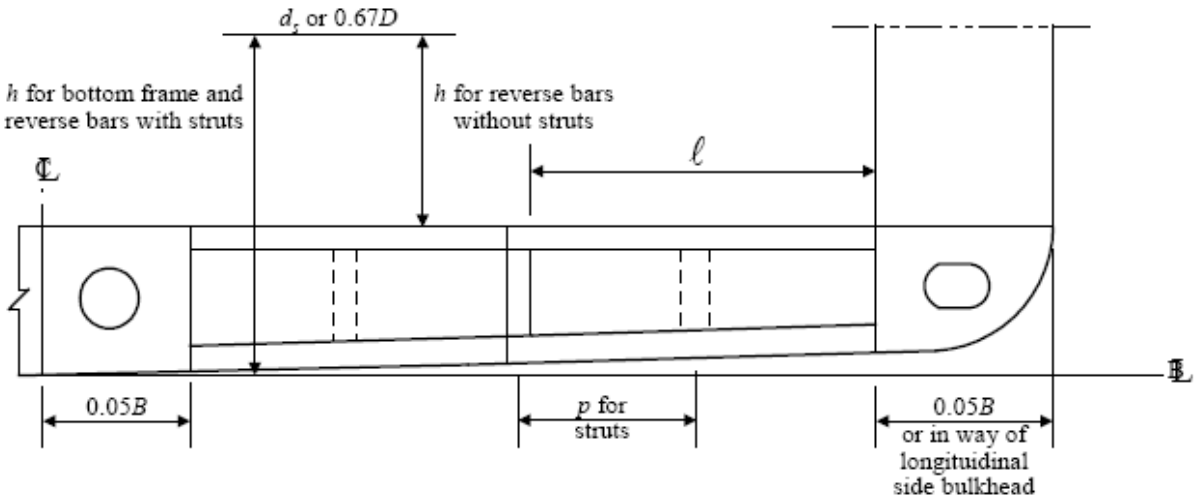

Figure 36: Double bottom open floors

4.9 Bottom Ordinary Shell Longitudinals Between CL and 3657,6 CL

Each bottom longitudinal frame similar to that shown in Figure 37, in association with the plating to which it is attached, is to have a section modulus SM not less than that obtained from the following equation:

$$SM = a(7{,}8chsl^2)R_l \; cm^3$$

a = 1.0 for bottom longitudinals

c = 0,715 with effective struts

h = ds or 0.67D in m, whichever is greater.

s = spacing of longitudinals, in m

l = distance, in m, between the supports, but is not to be taken as less than 1.83 m without struts or 2.44 m with struts. Where effective struts are fitted and the tank top is intended to be uniformly loaded with cargo, l may be taken as 85% of the distance between supports subject above minimum.

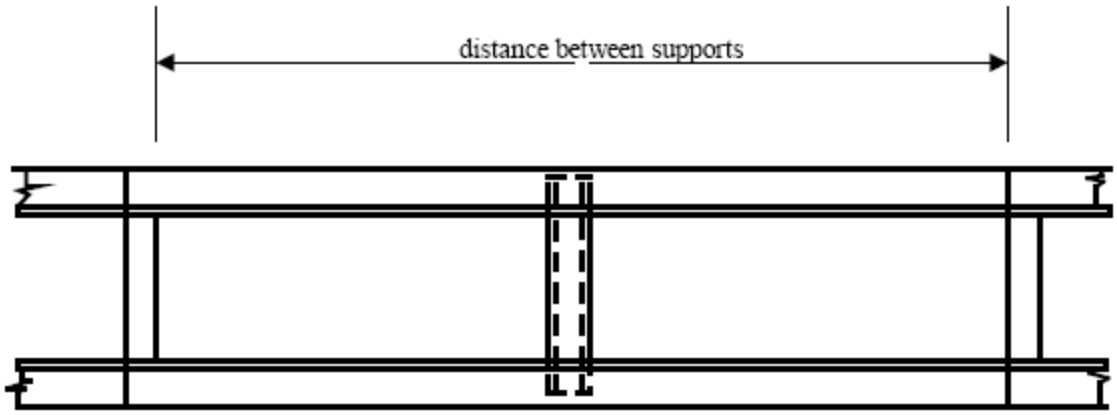

Figure 37: Longitudinal Framing

The section modulus (SM)of the bottom longitudinals may be obtained from the above equations multiplied by the factor R_ℓ where,

i) The actual bottom hull girder section modulus SMA is greater than required at least throughout 0.4L amidships,

ii) Still-water bending moment calculations are submitted, and

iii) Adequate buckling strength is maintained.

$R_\ell = n/\left[n + f_p(1 - SM_R/SM_A)\right]$ but is not to be taken less than 0.69

n = 8,278

f_p = 17,5 kN/cm^2

SM_R = required hull girder section modulus required, in cm^2-m

SM_A = actual bottom hull girder section modulus, in cm^2-m

$R_\ell = 1 \;\; Assumed\; SM_R = SM_A$

$$SM = 1(7{,}8x0{,}715x5{,}9x0{,}597x2{,}44^2)x1\ cm^3$$

$$SM = 116{,}8\ cm^3$$

$$SM_{Actual} = 168\ cm^3$$

4.10 Bottom ordinary Shell Longitudinals between 3657,6 CL and out

The section modulus, SM, of each bottom frame to the chine or upper turn of bilge, in association with the plating to which it is attached, is not to be less than that obtained from the following equation:

$$SM = 7{,}8chsl^2\ cm^3$$

c = 1,0 for longitudinal frames clear of tanks, and in way of tanks

s = spacing frames, in m

l = unsupported span, in m

h = vertical distance, in m, from the middle of l to the deck at side. In way of a deep tank, h is the greatest of the distances, in m, from the middle of l to a point located at two-thirds of the distance from the top of the tank to the top of the overflow, a point located above the top of the tank not less than 0.01L + 0.15 m or 0.46 m, whichever is greatest.

$$SM = 7{,}8x1x5{,}90x0{,}6096x2{,}44^2\ cm^3$$

$$SM = 167\ cm^3$$

$$SM_{Actual} = 168\ cm^3$$

4.11 The Scantling Results Summary

The additional beam and displacement didn't chance the scantling of the vessel structure much. The beam has increased less and it didn't cause increase much at structural members thickness and size. The scantling calculation results are presented at table 4.

	Actual	Calculated	New Scantling
Deck plating	10mm	7,85 mm	10 mm
Side shell plating	12,7 mm	9,3 mm	12,7 mm
Deck longitudinals		355 cm3	
Deck beams		10953,6 cm3	
Side longitudinals above	103,5 cm3	70 cm3	103,5 cm3
Side longitudinal below	221 cm3	175 cm3	221cm3
Bottom shell plating	11,11 mm	9,06 mm	11,11 mm
Central Girder	12 mm	10 mm	12 mm
Solid floor	9,525 mm	9,1 mm	9,525 mm
Bottom Shell Frames	4111 cm3	423 cm3	4111 cm3
Bottom ordinary Shell Longitudinals between CL and 3657,6 CL	168 cm3	167 cm3	168 cm3
Bottom ordinary Shell Longitudinals between 3657,6 CL and out	168 cm3	167 cm3	168 cm3

Table 4: The scantling of structural members

As it seen at table 4, scantling values for some structural members are calculated less than the original design. On the original design the naval architects might be using safety factors on structural stiffness for the ship construction. The ship owner may ask for using material more closer to calculated values of scantling to reduce the steel material used on construction of vessel. This will also make ship owner gain some profit by using less steel both labor and material.

5. FINITE ELEMENT ANALYSIS

5.1 Introduction To FEA

The Finite Element method is a numerical technique which is uses solving wide range of engineering problems. This method first introduced in the 1950s, and then continually developed and improved since then. FEA is an extremely complicated tool that works by ordinary or partial differential equations. Although it was developed for structural analysis firstly, it is used for solving heat transfer, fluid mechanics, acoustic and electromagnetic problems as well. This development made finite element technique widely accepted and used in different branches of industry like car design, climate and heating system manufacturers, aircraft and aerospace companies like many others.

The areas of application and potential of usage of finite element method are enormous. Today we can see all kinds of industrial works with FEA. As an example, car industry analyses and develops their products with using Finite Element Analysis mainly. The structural integrity and performance of cars are doing by analyses with this method before building prototype. They analyse the strength of car components of car body as whole part for safe drive in fine conditions and safety of users in crash cases with structural analysis. The companies are using FEA for aerodynamic testing of car, testing vibration of every single part of car engine and affection of engine to total structure. The heat transfer techniques to estimate the temperature distribution in the engine block, pistons, the mechanical affection of heat on structures and climate control effect at seating area. The marine industry is also using FEA technique mainly for structural integrity of vessel. Vibration and heat transfer analysis are also common use of it.

The growth and development of technique has gone rapidly, parallel to improve of computer and programming techniques. As the power of computers has increased and it has been possible to analyse complex shapes and structures. In the past this new but effective solution technique was used by big companies because of the lack of powerful computer hardware and high prices of software. Depending on the fast development on the computer technology increasing availability and power and decreasing prices made

computer hardware and software more common and made small companies had access to finite element analysis.

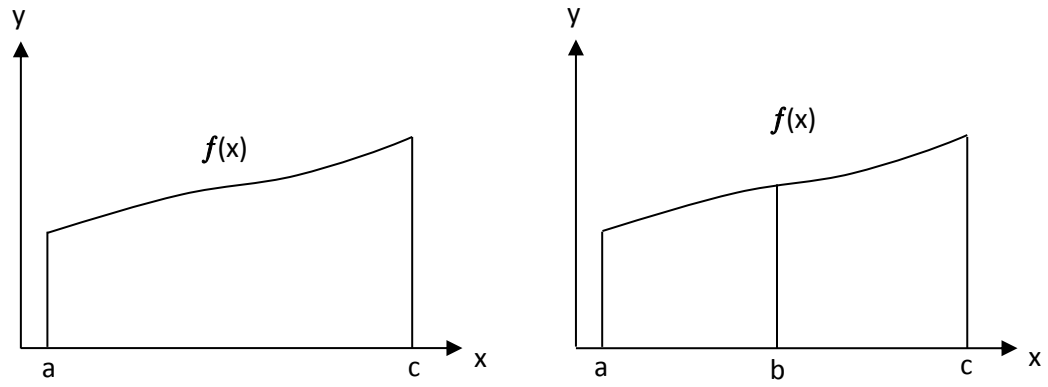

$$\int_a^c f(x)\,dx = \int_a^b f(x)\,dx + \int_b^c f(x)\,dx$$

Figure 38: FEA integral expression

5.1.1 Fundamentals

We have to remember something about FEA program that they are just tools and computer programs which runs on user's commands. The user must be someone who has knowledge about complex engineering problems to solve it by FEA programs. The user first makes model part where he needs to calculate parameters, apply boundary conditions and runs it with appropriate solver. This part he needs to explain the basics of structural analysis theory.

5.2 STRUCTURAL MECHANICS

5.2.1 Principles

All engineering problems go through a cycle before converging solution in obtained. This cycle start from theory, model and analysis than goes up to the construction and fabrication. The cycle is illustrated in figure. 39

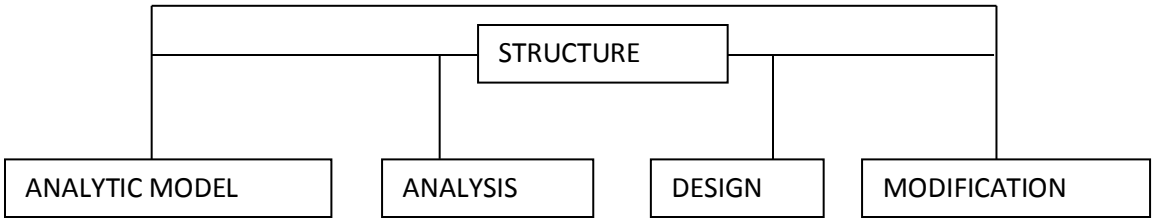

Figure 39: Analysis design cycle

This is a cycle for a structure of a usual manufacturing product of independent need and urgency. The cycle is continued till a satisfactory profile of the structure is obtained. Analysis of structures always rests in certain basic principles and assumptions. These principles mainly relate to equilibrium, compatibility, material behaviours and boundary conditions.

5.2.2 Equilibrium

A structure has to be in equilibrium both internally and externally to be of functional value. These equilibrium properties relates to (a) overall equilibrium (b) joint equilibrium and (c) member equilibrium for the structure as shown in figure 40. These conditions must be obtained and put in the form of equations.

a) Overall Equilibrium

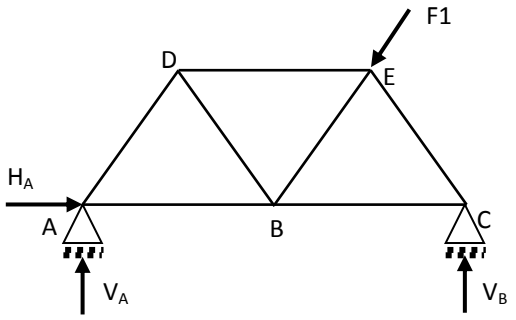

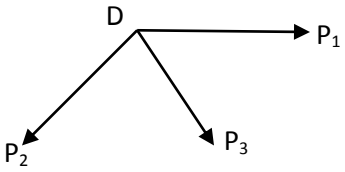

b) Joint Equilibrium

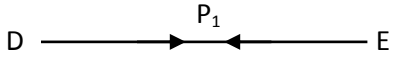

c) Member Equilibrium

Figure 40: Structural equilibrium types

5.2.3 Compatibility

All parts of the structure should act cohesively to resist the external loads. So as a result of solution all structure deformations term compatible. The conditions of compatibility relate to deformations/strains and degrees to freedom (see figure 41). Degrees of freedom or kinematic degree of indeterminacy is the independent degree of freedom with which one can define the deformed shape of the structure.

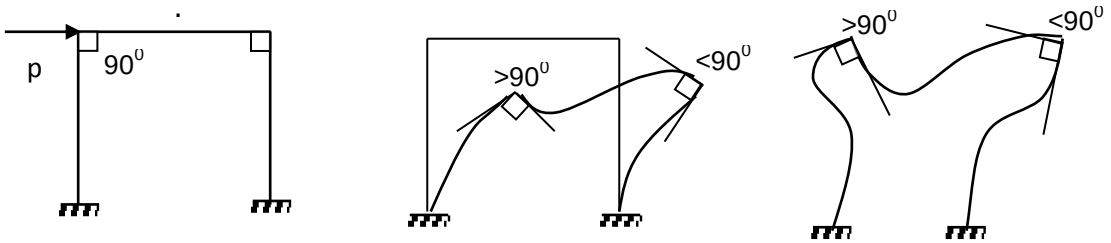

a) Flame subjected to load | b) Compatible Displacement | c)Incompatible Displacement

Figure 41: Conditions of compatibility

5.2.4 Metal behaviours

There are some experimental knowledge about deformations, related to the structure of materials under external loads. These loads have characteristics that relate forces/stresses with displacements/strains. These are obtained from experiments. But as a theory most of the time Hooke's Law provides the basis of the linear relationship between force/stress to displacements/ strains as shown in figure 42.

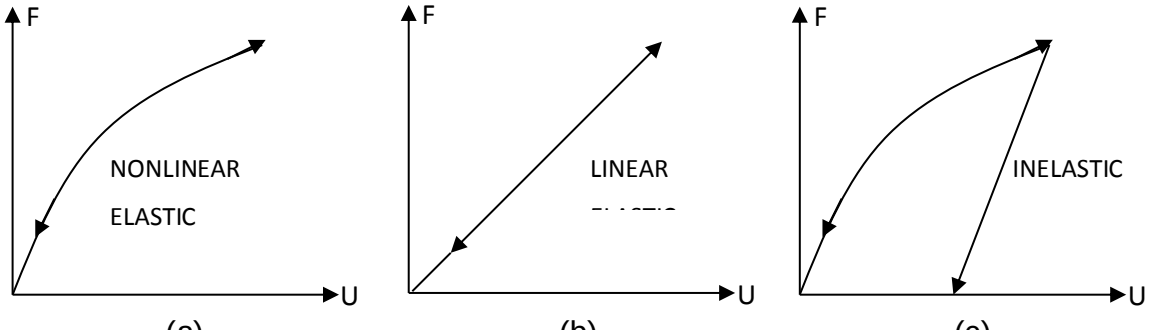

(a) (b) (c)

Figure 42: Stress and Strain laws

5.2.5 Boundary Conditions

A structure cannot resist any external load or its own self-weight without proper boundary conditions. Because of these essentially all the problems in structural mechanics fall into boundary value problems.

5.2.6 Degrees of Freedom

Degree of freedom of a structure shows the possibility of the joint to move. Depending on the type of structure generally, degree of freedom can be classified as

(i) Discrete Structures, those having discrete elements only (Fig. 43 a).

(ii) The structures which are continuum (Fig. 43 b)

(iii) The structures that are both discrete and continuum (Fig. 43 c).

By this classification, a certain amount of case is brought in degrees of freedom as discrete elements or deemed to possess a set of known deformations and forces. In a continuum, discretion using finite elements is effective to the extent of degrees of freedom. This extension associated with each demoralized element as it is very difficult to treat infinite degrees of freedom.

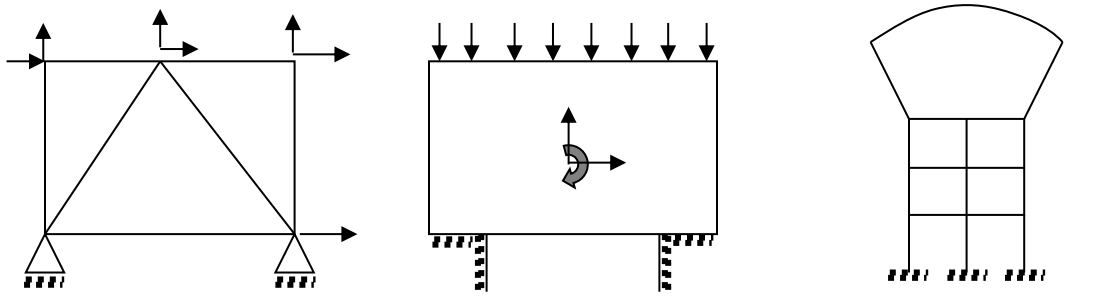

Figure 43: Discrete and continuum of structures

5.3 Concept

FEA models are represented by piecewise linear, quadratic or cubic fields over the models. Here in first figure you see an idea of a model that used as a cantilever beam. If

only the length is the dominant dimension for a linear beam element, resultants are developed in terms of displacements earlier. If the dimension of the structure warrants two dimensional approximations, then figure 44 b gives the physical model, figure 44 c gives the reduced model and figure 44 d gives, the single element.

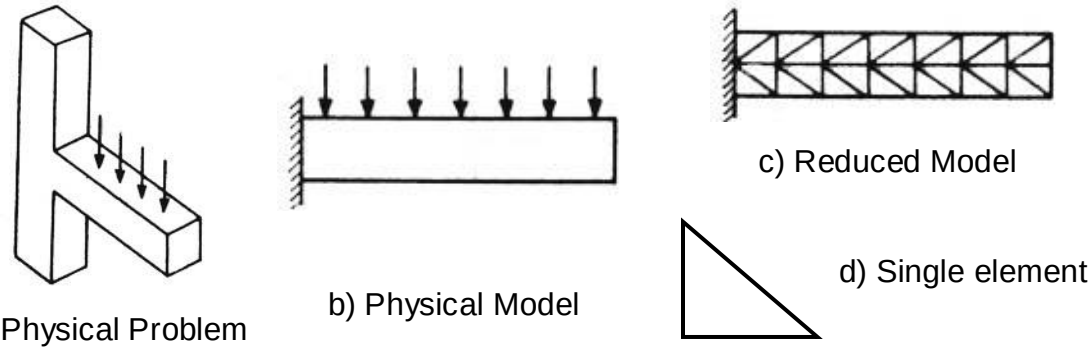

Figure 44: Beam models and element

This feature, contrasts with other classical methods that deal with formulated differential equations on the physical model.

Stress and Strain laws of the continuum with infinite degrees of freedom, is brought to a tractable problem with finite degrees of freedom with the reduced model. In figure 45 one can see modelling of these as unknowns and assumption linear, parabolic of cubic variation.

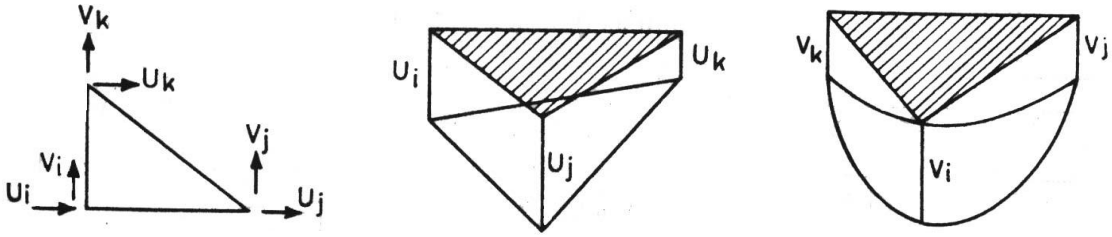

Figure 45: Degree of freedom on models

When matrix methods are applied to one dimensional structures or skeletal structures, they considered one structures member at a time. The member was the discrete element. If we think about a continuum such as plates and shells, we see a choice discretization. In such cases the continuum is also divides into finite elements as shown in figure 46. In FEA, therefore, the continuum is divided into a finite number of elements

having finite dimensions and reducing the continuum having infinite degree of freedom to a model with finite degrees of freedom.

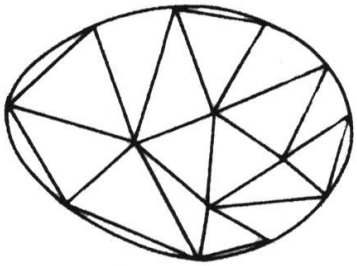

Figure 46: Discretization into finite elements

5.4 Basic Theory Of FEA Method

The finite element method can be discussed in heaps of different ways. One of these ways is to consider it as a process of transformation between force displacement coordinate systems. This cycle is shown in figure 47.

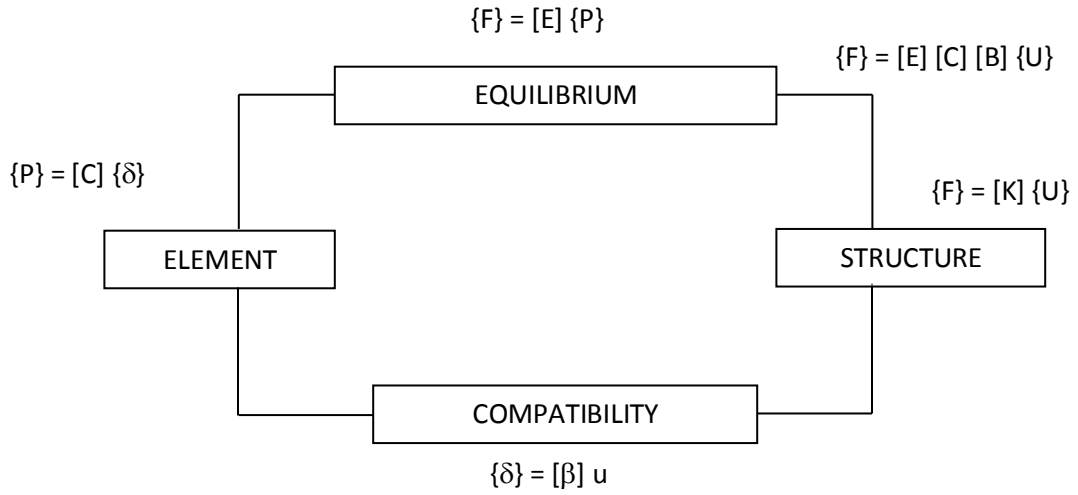

Figure 47: Stiffness approach

In finite element method, the actual structure is replaced by a conceptual model that we can call as a finite element model. What we are analysing is not the actual structure but the approximate finite element model. The accuracy of the solution that we get depends on how we have created the finite element models of the structure. This phase of the analysis work requires lot of experience, judgement, intuitive thinking on the part of the

structural analyst. One of the ways to master this art of finite element modeling is to make case studies of the real life problems that have been analysed successfully by the finite element methods.

5.5 Advantages And Disadvantages Of FEA

There are so many advantages of finite element analysis. The main advantage of the FEA is analysing intractable physical problems and complex closed bound problems.

The other advantages of FEA are listed like below.

1. The method can be applied to irregular geometries.
2. It can take care of any type of boundary.
3. Material anisotropy and inhomogeneous can be treated without much difficulty.
4. Any type of loading can be handled.

The disadvantages of this method are,

1. Some other solution methods may be more accurate than the finite element method in some problems.
2. FEA is not simple as theory and there is cost involved in the solution of the problem.
3. For vibration and stability problems in many cases the cost of analysis by Finite Element method may be too prohibitive.
4. Another problem of finite element method is that the approximations used in the development of the element stiffness. No element can represent all possible behaviour patterns equally well and compensation in one aspect causes distribution of another. We should know what a particular element is capable of and must not expect more from it. For example one might run a large number of lower order elements and still not get as accurate answer obtained with less number of more refined elements.
5. Results may change depending on the mesh technique and mesh size. If you have a fine mesh you can get fine results.

6. There are some other difficulties such as aspect ratio that means ratio of longer to smaller dimension of the elements. If you can use proper aspect ratios when it is necessary, you get more accuracy. So aspect ratio also affect the final results.

7. Interpretation of output is another disadvantage of FEA. It occurs when all the decisions are made and all the analysis is done. Analysis of a multi store building would be meaningful but a smaller problem would generate so many numbers that very few would have patience to look at all of them. Selection of post processors particularly graphical representation of displacements and stresses would be very useful but post processors must be tailored to specific applications and also require special expertise to develop.

6. SHIP HULL SCANTLING DESIGN BY ANALYSIS

6.1 General

Classification rules have traditionally been the mainstay of ship design practices. These rules are primarily semi-empirical in nature and have been calibrated to ensure successful operational experience. They have obvious advantages. They are simple in format and familiar to most ship designers. Nevertheless, the ship sizes have increased dramatically and the ship designs have changed remarkably in the past 20 years. The conventional design approach that relied on the "Rule Book, has been seriously challenged with the development of unconventional ship types and complex ship structures such as high speed vessels, large opening container ships with considerably increased capacity, large LNG-carriers, drilling ships, FPSOs, etc. The conventional design rule formulae involve a number of simplification assumptions and can only be used within certain limits. Moreover, scantlings based on rules are not necessarily the most cost efficient designs. Hence, the application of rational stress analysis using FEM has gained increasing attention in the shipbuilding industry. With the rapid growth of information technology, computational complexity is no longer a big issue and numerical efficiency is not the main concern in the design procedure. The actual design approach includes the overall strength analysis by accounting for both static and dynamic loads and evaluation of the fatigue life of all critical structural details. This approach provides a well-designed and uniformly utilized structure, which ensures a higher degree of reliability than past structures.

The analysis procedure is starting from design loads, strength criteria, FEM analysis, up to the assessment of the obtained calculation results. The summarized procedure of strength analysis can be seen in figure 48.

6.2 Design Loads

The design loads acting on the overall ship structure consist of static and dynamic loads. Static loads include dead and live loads, such as hydrostatic loads, and wind loads. Dynamic loads include wave induced hydrodynamic loads, inertia loads due to vessel motion, and impact loads. The various loading conditions and patterns, which are likely to impose the most onerous local and global regimes, are to be investigated to capture the maximum local and global loads in structural analysis. Sloshing and slamming loads should also be taken into account where applicable. When designing ocean-going ships, environmental loads are usually based on global seastate criteria due to their mobility. While for offshore structures, environmental loads are calculated in accordance with specifically designed routes and/or site data.

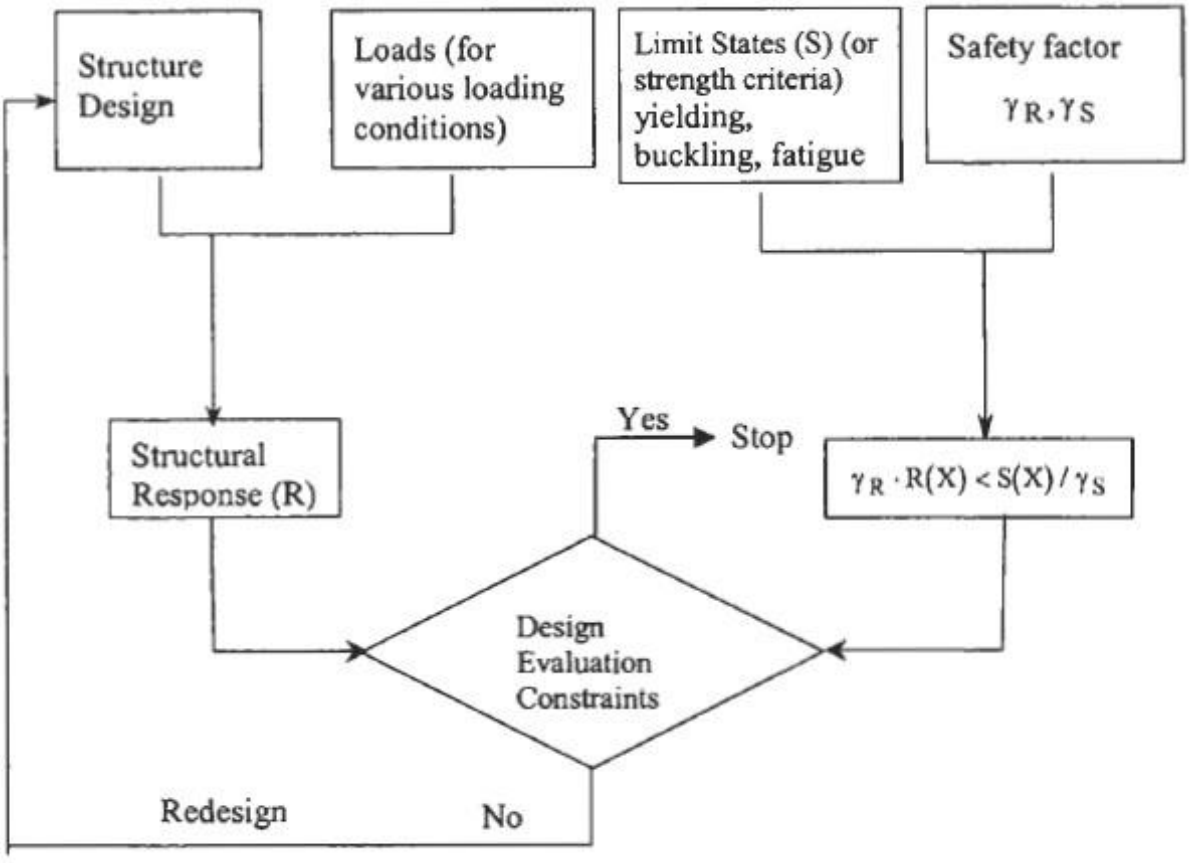

Figure 48: Stress Analysis Procedure (Yong Bai, 2003)

Liu et a1 (1992) developed a Dynamic Load Approach (DLA) for ship design, where the loads experienced by a tanker were calculated, including wave induced loads, ship motions, internal, structural, and cargo inertial loads etc. Three loading conditions are analyzed, namely, full load condition, ballast load condition, and partial load condition.

- Static Loads

The distribution of hull girder shear forces and bending moments is calculated by providing the vessel's hull geometry, lightship (i.e. the weight of the steel structure, outfitting and machinery), and deadweight (i.e. cargoes and consumables such as fuel oil, water and stores), as input for each loading condition. An analysis of a cross-sectional member along the length of the ship is required in order to account for the discontinuities in the weight distribution.

- Hydrodynamic Coefficients

Each loading condition requires hydrodynamic coefficients to determine the ship's motions and dynamic loads. It is important that a significantly broad range of wave frequencies are considered in this calculation.

- Ship Motion and Short-term /Long-term Response

Ship motion analysis should be carried out using a suitable method, e.g. linear seakeeping theory and strip theory. Frequency response functions are to be calculated for each load case. Short-term response is then obtained by multiplying the frequency response functions by the wave spectra. The long-term response is calculated by using the short-term response and wave statistics, which consist of wave scatter diagrams

6.3 Strength Analysis Using Finite Element Method

6.3.1 Modeling

In principle, strength analysis by means of finite element methods should be performed with the following model levels:

- Global Analysis

A global analysis models the whole structure with a relatively coarse mesh. For a large

structure like ships, the global model mesh must be quite rough; otherwise too many degrees of freedom may consume unnecessary man-hours and cause computational difficulty. The overall stiffness and global stresses of primary members of the hull should be reflected in the main features of the structure. Stiffeners may be lumped, as the mesh size is normally greater than the stiffener spacing. It is important to have a good representation of the overall membrane panel stiffness in the longitudinal and transverse directions. This model should be used to study the global response of the structure under the effects of functional and environmental loads, to calculate global stresses due to hull girder bending, and to provide boundary conditions for local FE models. Design loads should reflect extreme sagging and hogging conditions imposed by relevant operation modes such as transit, operating, storm survival, installation, etc.

- Local Structural Models

For instance, cargo hold and ballast tank models for ship shaped structures may be analyzed based on the requirements of classification rules.

- Cargo Hold and Ballast Tank Model

The local response of the primary hull's structural members in the cargo and ballast area is analyzed, for relevant internal and external load combinations. The extent of the structural model shall be decided on, by considering structural arrangements and load conditions. Normally, the extent covered is the tank itself, and one half the tank outside each end of the considered structure (figure 49).

The mesh fineness shall be determined based on the method of load application. The model normally includes plating, stiffeners, girders, stringers, web-frames, and major brackets. Additional stiffness may be employed in the structure for units with topsides, and should be considered in the tank modeling.

From the results of the global analysis, the boundary conditions for the cargo hold and ballast model may be defined. The analysis results of the cargo hold/ballast model may be used as the boundary conditions for the frame and girder models.

The following basic loads are to be considered in the model:

1 Static and dynamic loading from cargo and ballast,

2 Static and dynamic external sea pressure,

3 Dead weight, topside loading, and inertia loads

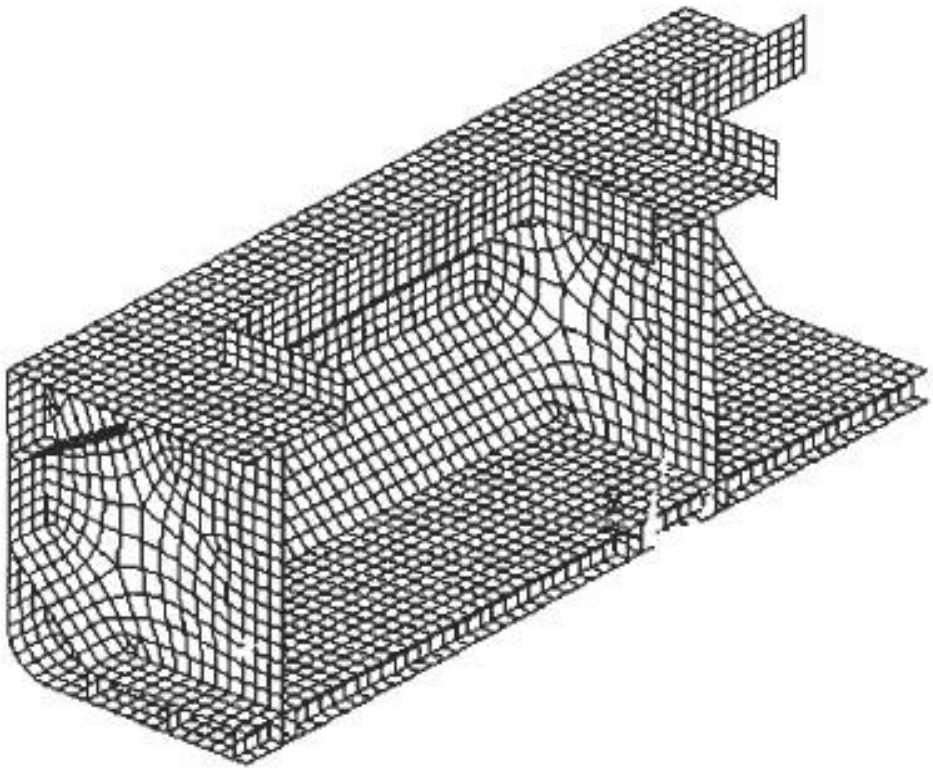

Figure 49: Half tank model with bulkheads and cargo hatch

Frame and Girder Model

The frame and girder analysis is used to analyze the stresses and deformations in the mainframe or girder system. The results will be more illustrative if the calculations include bending, shear and torsion. The minimum requirements are a function of the type of vessel being analyzed, but should include at least one transverse web in the forward cargo hold or tank (Figure 50)

The model may be included in the cargo hold and ballast tank models or run separately using the boundary conditions from that model analysis.

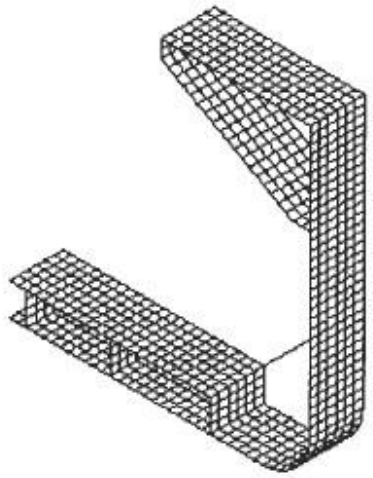

Figure 50: Frame model

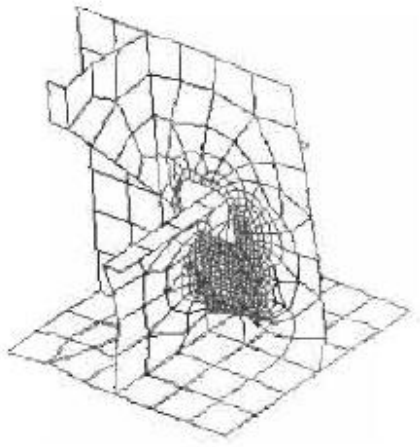

Figure 51: Stress concentration model

Stress Concentration Area:

In the areas where high stress concentrations may take place, local fine mesh models are to be applied by using forces or forced deformations as boundary conditions based on the results obtained in the global analysis. Alternatively, sub-modeling, super-element techniques or direct mesh refinement may be introduced.

Attention should be paid particularly to the following areas:

- Areas around large openings,
- Longitudinal stiffeners between transverse bulkheads and the first frame at each side of the bulkhead,
- Vertical stiffeners at transverse bulkheads with horizontal stringers in the way of the inner bottom and deck connections,
- Horizontal stiffeners at transverse bulkheads with vertical stringers in the way of the inner side and longitudinal bulkhead connections (Figure 51),
- Corrugated bulkhead connections.

Fatigue Model

If fatigue is of concern, analysis of critical structural details should be performed. Fine mesh models shall be completed for critical structural details in the areas such as the following:

- Hopper knuckles in way of web frames,
- Topside support stools,
- Details in way of the moonpool,
- Other large penetrations in longitudinal load bearing elements,
- Longitudinal bulkhead terminations,
- Stiffener terminations,
- Pontoon to column or column to deck connections,
- Other transition areas when large changes in stiffness occur

The size of the model should be such that the calculated hot spot stresses are not affected significantly by the assumptions made for the boundary conditions. Element sizes for stress concentration analysis should be of the same order of magnitude as the plate thickness. Normally, shell elements may be used for the analysis. Only dynamic loads are to be applied on the model, because only these affect the fatigue life of the structure. The correlation between different loads such as global bending, external and internal pressure, and acceleration of the topside should be considered in the fatigue assessment.

6.3.2 Boundary Conditions

Defining boundary conditions is one of the most important steps in FEM analysis. For local analysis models, the boundary conditions imposed by the surrounding structures should be based on the deformation or forces calculated from the global model.
The boundary conditions, for a global model, have no other purpose than to restrict the rigid body motion. Fixing 6 degrees of freedom (DOF) at both ends (and corners) of the model should be good enough. The total loading must be balanced so that the reaction forces at the boundaries approach zero.
When modeling, the model length of the ship structure should be sufficient to minimize boundary condition effects over the analyzed area. ABS (2002) requires 3 cargo holds to be covered for models of tankers, bulk carriers, or container ships; LR "Direct calculation - Guidance Notes" (1996) requires that 2 cargo holds be covered for the

model of a bulk carrier. All continuous longitudinal elements should be restrained to remain plane under the effects of the hull girder bending and must be rotationally fixed about the vertical axis if the calculated deformations or forces are not available at the free ends of the model. Conditions of symmetry should be applied at each end of the finite element model. Rotation about the two axes in the plane of symmetry is to be constrained where there is symmetry imposed at the centerline or at the ends of the model. The model should be supported vertically by distributed springs with ship sides and longitudinal bulkheads at the intersections of the transverse bulkheads.

6.3.3 Type of Elements

The types of elements are chosen to provide a satisfactory representation of the deflections and stress distributions within the structure. The conventional frame analysis may be carried out with a beam model. It has significant advantages for its modeling simplicity and computational efficiency. However, thanks to the availability of powerful computers, computational efficiency is no longer a concern. More refined and accurate element types can be used.

In a research conducted by the ISSC, Zillottto et al. (1991), nine different finite element models were applied to different combinations of beams, trusses, rods, membranes, planes, and shell elements. A considerable scatter was observed in the results. The conclusion was that a detailed analysis of the deformations and stress levels in all the elements of the transverse frames should be performed using a refined finite element model for all the different types of structures and ships.

In "Direct Calculation-Guidance Notes", LR (1996) suggests that all areas of the plating should be modeled by shell elements, secondary stiffeners by line elements (bars or rods), double bottom girders and floors by three or more plate elements over the depth of these members, and side shells by plate or bar elements.

In general, if the structure is not subjected to lateral bending, membrane and rod elements may be applied. Otherwise, plate and beam elements, which have both bending and membrane resistance, should be employed. The selection of element types depends on many aspects, such as the type of structure, the load application

approach, the type of analysis performed, the results generated, and the accuracy expected. There is no substitute for engineering judgement.

6.3.4 Post-Processing

The design is a complicated and iterative process in which building and solving a FE model is simply the first step. A more important step is that designers use their knowledge and judgment to analyze the results and, if necessary, redesign or reinforce the structure.

First, the engineer must ensure that the results calculated by the FE program are reasonable, and that the model and the load application are correct. This can be achieved by plotting stress contour, the deformation, the reactions & applied load equilibrium, force & moment diagrams, etc. The next step is to check the strength of the structure against relevant design criteria. Load combinations and stress combinations are not always straightforward. Assumptions are usually made to certain degrees both in creating the model and in solving the model. Yong Bai mention in his book that the designers must bear this in mind and be familiar with the FE program being used, in order to account for the assumptions adopted, to evaluate the calculated results, and, if necessary, to modify the results.

Yielding Check

The yield check ensures that the stress level on each structural member is below the allowable stress. The allowable stress is defined as the yield limit of the material divided by a safety factor. Stresses calculated from different models are combined to derive the equivalent von Mises stress and evaluated against the yield criterion. Component stresses, such as axial stress, bending stress, normal stress in x-direction, normal stress in y-direction, shear stress, etc. as well as combined stresses, are to be evaluated. The combination of global and local stresses should account for actual stress distributions and phases. If the phase information is limited or uncertain, the maximum design value for each component may be combined as the worst scenario. Possible

load offset due to the simplified assumptions made in the FE analysis should be accounted for in the stress combinations.

Buckling Check

Structural members subjected to compressive loads may normally buckle before reaching the yield limit. Various buckling modes should therefore be evaluated. Four different modes of buckling are usually recognized:

Mode 1: simple buckling of the plate panel between stiffeners and girders.

Mode 2: flexural buckling of the individual stiffener along with its effective width of plating in a manner analogous to a simple column.

Mode 3: lateral-torsion or tripping mode. The stiffener is relatively weak in torsion, and failure may be initiated by twisting the stiffener in such a way that the joint between stiffener and plate does not move laterally.

Mode 4: overall grillage buckling, panel buckling

To ensure that the local bending stress resulting from loads, acting directly on stiffeners, are included in the buckling code check, the lateral pressure should be explicitly included in the capacity check, combined with membrane stresses calculated from the FE analysis. Relevant combinations of buckling load checks should include evaluation of the capacity with relevant lateral pressure applied to either side of the plate. Compressive stresses calculated from global and local models are to be superimposed. Each structural member is to be designed to withstand the maximum combined buckling loads, of which the critical load cases and wave phases may be different to those pertaining to the yield check.

6.4 Fatigue Damage Evaluation

General

The fatigue strength of welded joints in highly dynamically stressed areas needs to be assessed to ensure structural integrity and to optimize the inspection effort. The analysis of fatigue strength should be based on the combined effects of loading, material properties, and flaw characteristics. At the global scantling design level, the

fatigue strength check for hull-girder members can be conducted for screening purposes. At the final design level, analysis for structural notches, cutouts, bracket toes, and abrupt changes of structural sections need to be performed.

Stress types commonly used in fatigue analysis based on S-N curves include nominal stress, hot-spot stress, and notch stress. Each of these methods has specific applicable conditions. Although only the nominal stress is used in the examples, the analysis approach is not limited to any stress type.

Spectral Fatigue Analysis (SFA) based on the S-N curve and Palmgren-Miner's cumulative damage hypothesis has been widely applied in the fatigue damage assessment of marine structures. Figure 52 shows the procedure for spectral fatigue assessment.

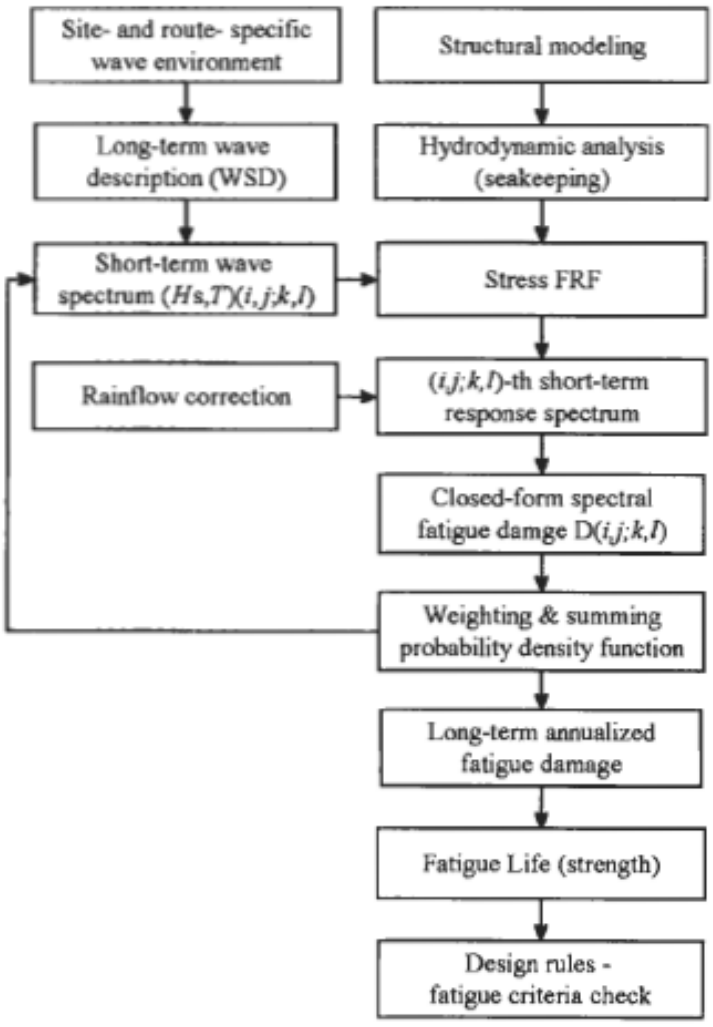

Figure 52: Procedure of Spectral Fatigue Analysis (Zhao, Bai&Shin, 2001)

7. FINITE ELEMENT MODELLING AND SOLUTIONS BY ANSYS

7.1 Modelling

The finite element modeling and analysis of the ship structure is carried out using a commercial software package, the ANSYS 13.0, which is based on finite element method.

The overall exterior hull has been obtained by importing the lines as IGES format file from Autocad and Rhinoceros 3D to the ANSYS. Therefore, intersecting the exterior hull with the double bottom, main deck level, the interior structures were developed at ANSYS. Afterwards, all structural components were modeled by area and beam modeling. A specific shell element, SHELL181, was adopted for all plating parts, BEAM188 element for longitudinal stiffeners.

SHELL181 has both bending and membrane capabilities. Both in-plane and normal loads are permitted. The element has six degrees of freedom at each node: translations in the nodal x, y, and z directions and rotations about the nodal x, y, and z-axes. Stress stiffening and large deflection capabilities are included. A consistent tangent stiffness matrix option is available for use in large deflection (finite rotation) analyses. This element can be seen in figure 3-1.

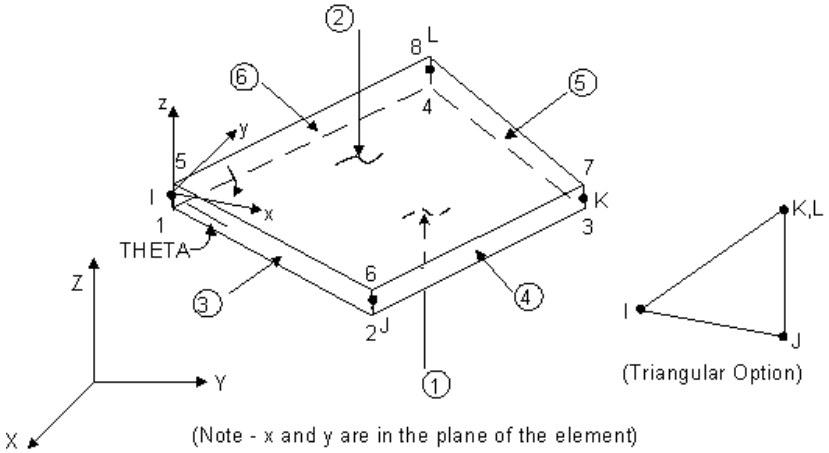

Figure 53: SHELL181 element

BEAM188 is a linear (2-node) beam element in 3-D. BEAM188 has six degrees of freedom at each node. These include translations in the x, y, and z directions and rotations about the x, y, and z directions. Warping of cross sections is assumed to be unrestrained. The beam elements are well suited for linear, large rotation, and/or large strain non-linear applications. This element can be seen in figure 54.

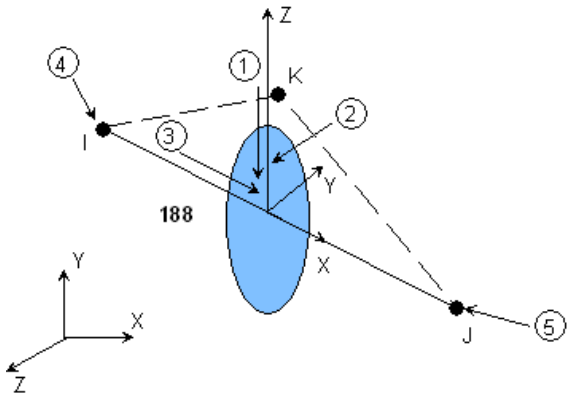

Figure 54: BEAM188 element

The material used in this ship construction is A Grade St-42 general-purpose shipbuilding steel and its properties are given as follows,

Yielding Stress	: 235 N / mm^2
Elasticity Modulus	: 210000 N / mm^2
Density	: 7850 kg / m^3
Poisson Ratio	: 0.29

The parent hull model has 104695 units of shell 181 element at various thickness and 12940 units of beam 188 element at various section. The parabolized hull has 109481 shell 181 and 13532 beam 188 elements. The mesh we use at our elements are quadratic mesh. The Finite Element Model used in this study is shown below.

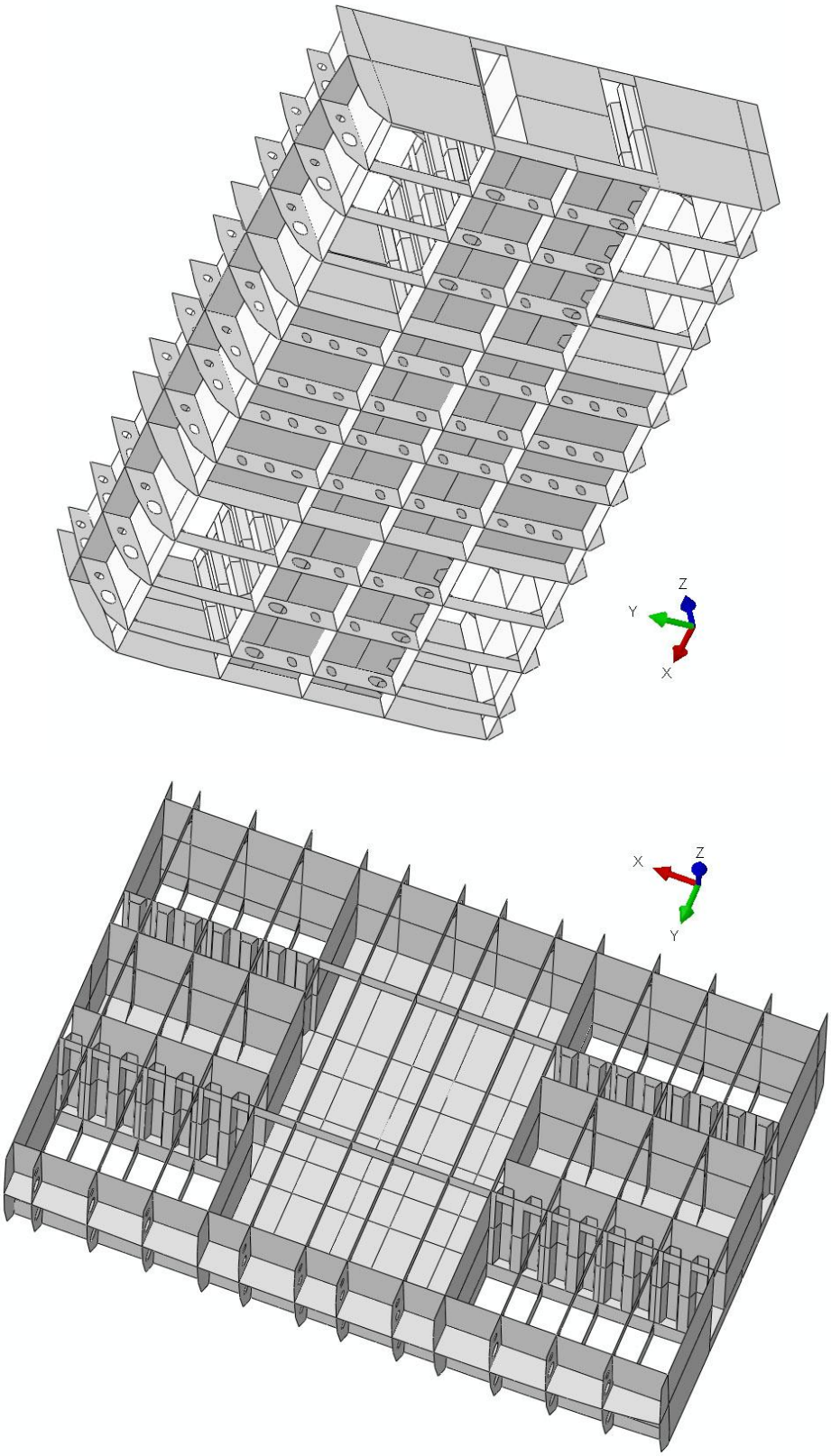

Figure 55: 3D modelling PSV, Surfaces top and bottom view

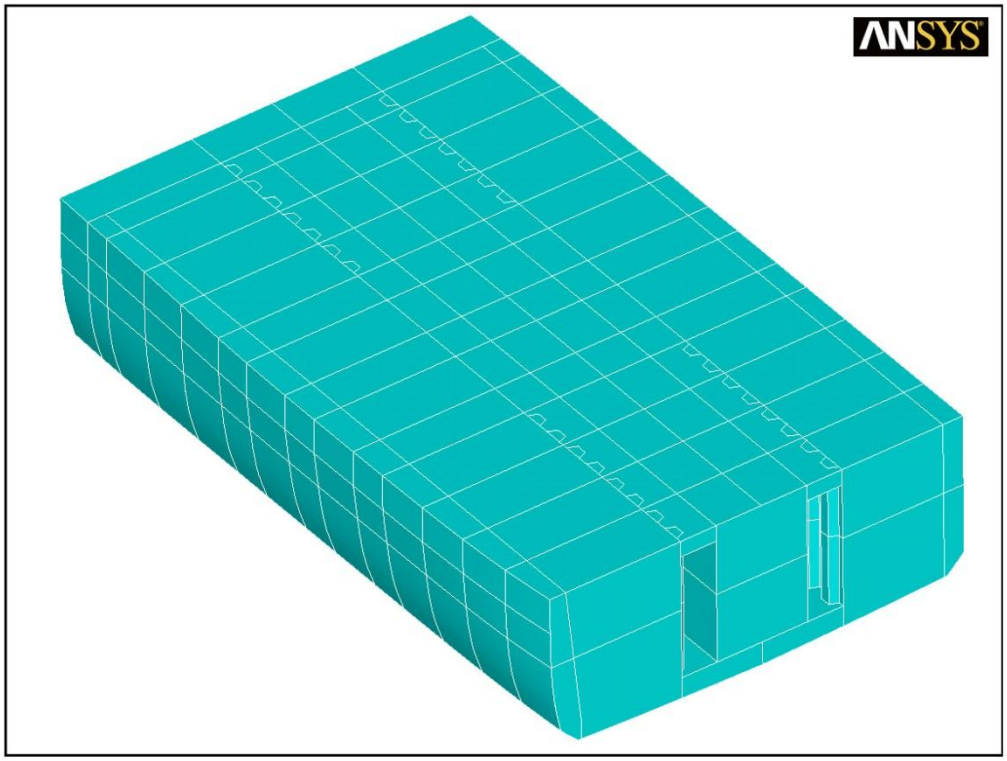

Figure 56: 3D modelling PSV at ANSYS, Surfaces top view on deck

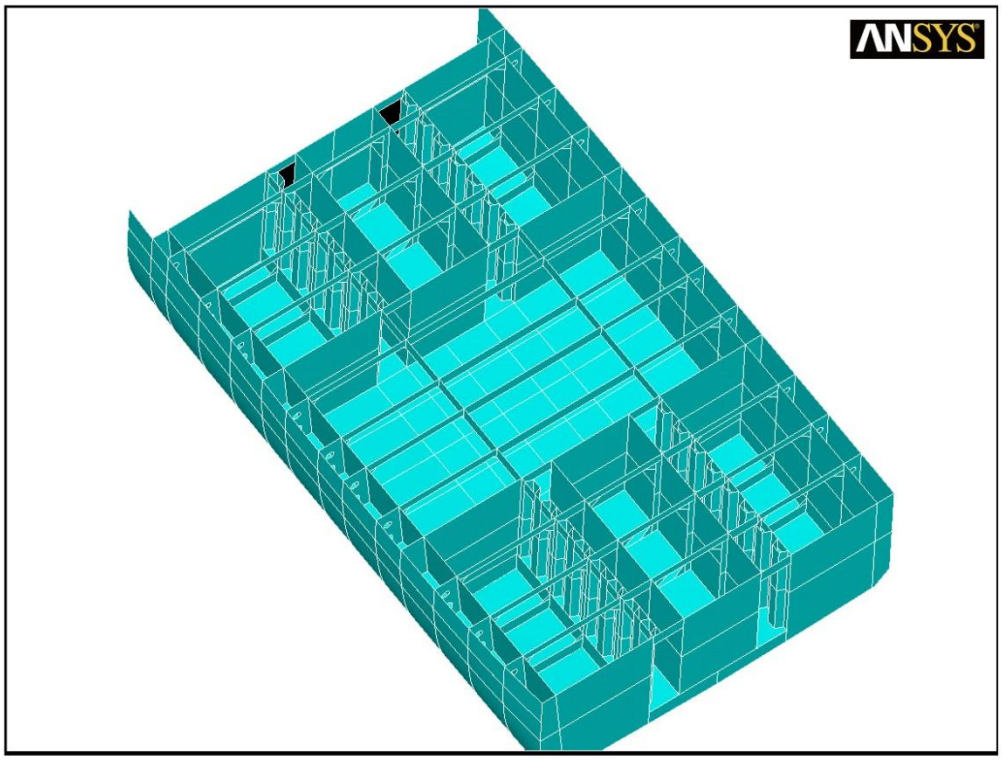

Figure 57: 3D modelling PSV at ANSYS, Surfaces top views on deck

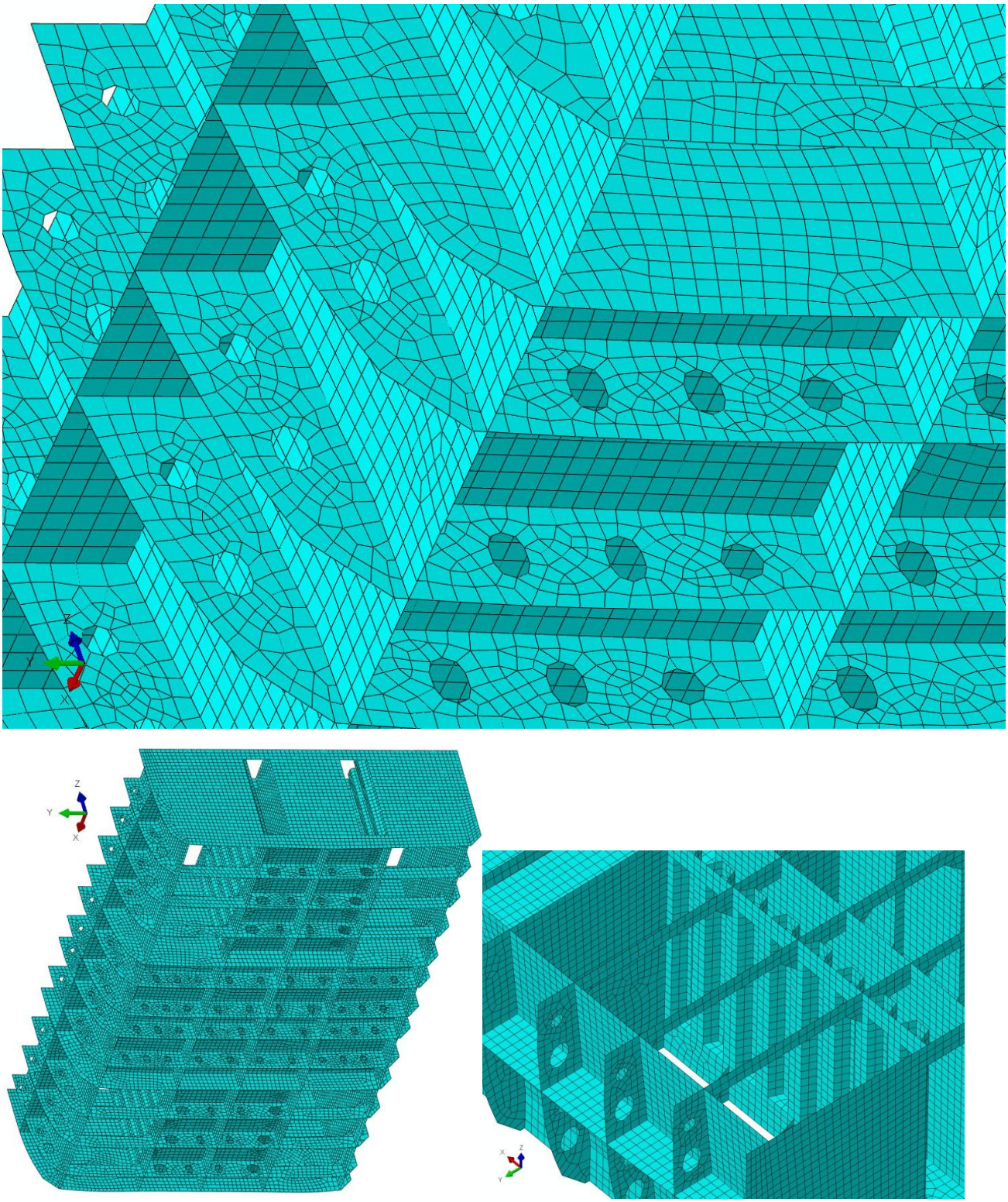

Figure 58: ANSYS model, Mesh elements internal structure at various views.

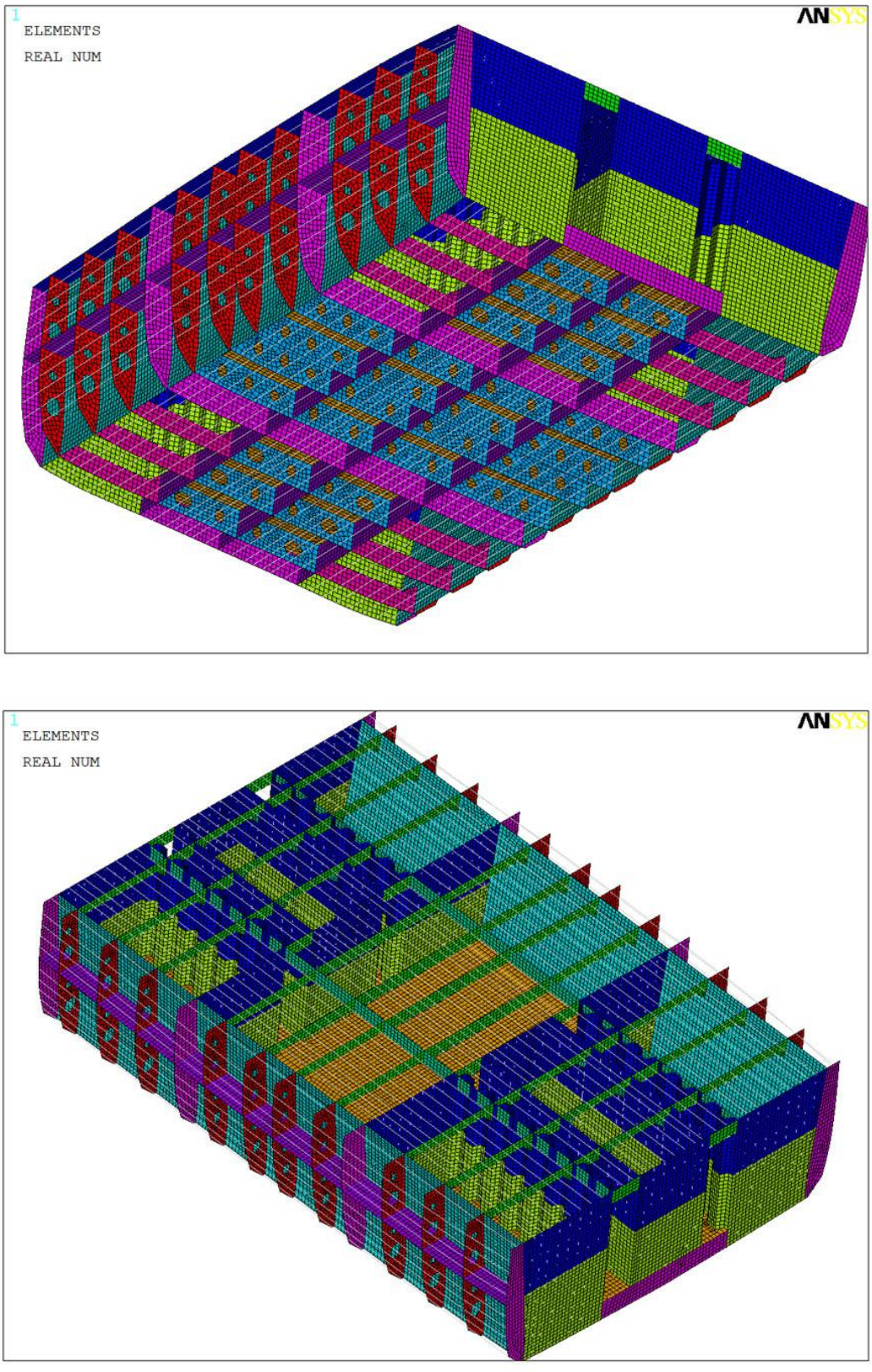

Figure 59: ANSYS model, Mesh elements internal structure and double bottom.

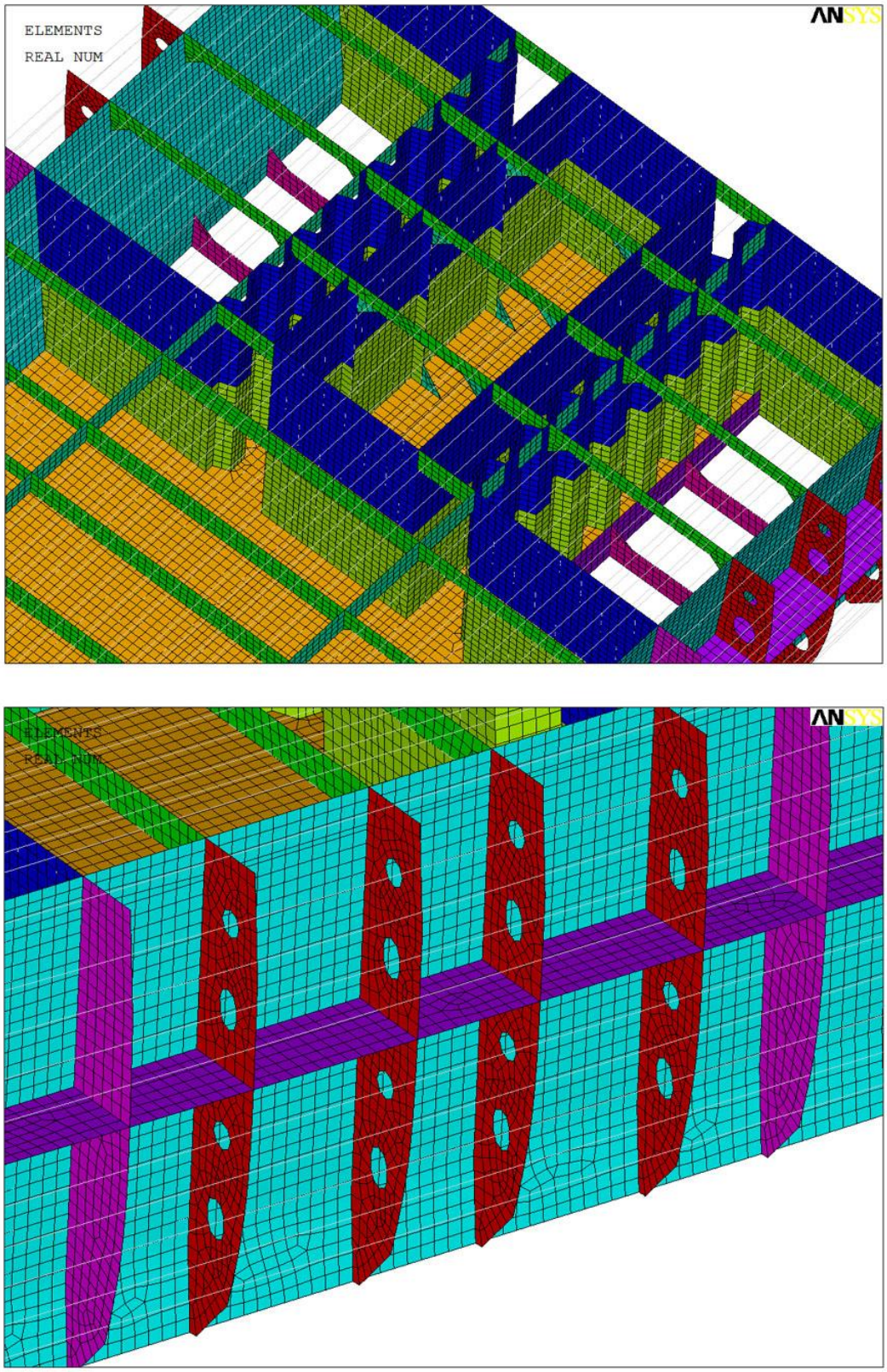

Figure 60: ANSYS model, Mesh elements internal structure and side frames.

7.2 Loads Calculation

The load calculations are done according to American Bureau of Shipping (ABS) Rules for building and classing, Offshore Support Vessel 2013, Part 3 Hull construction and equipment.

7.2.1 Longitudinal Strength for Vessels 61 m (200 ft) in Length and Over

7.2.1.1 Sign Convention of Bending Moment and Shear Force

The sign convention for bending moment and shear force is shown in Figure 61

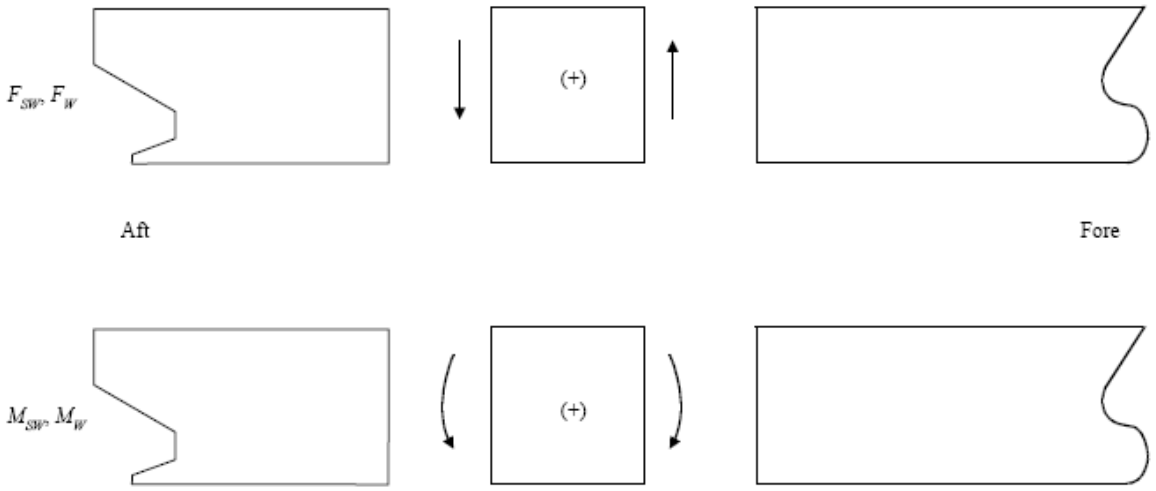

Figure 61: Sign convention

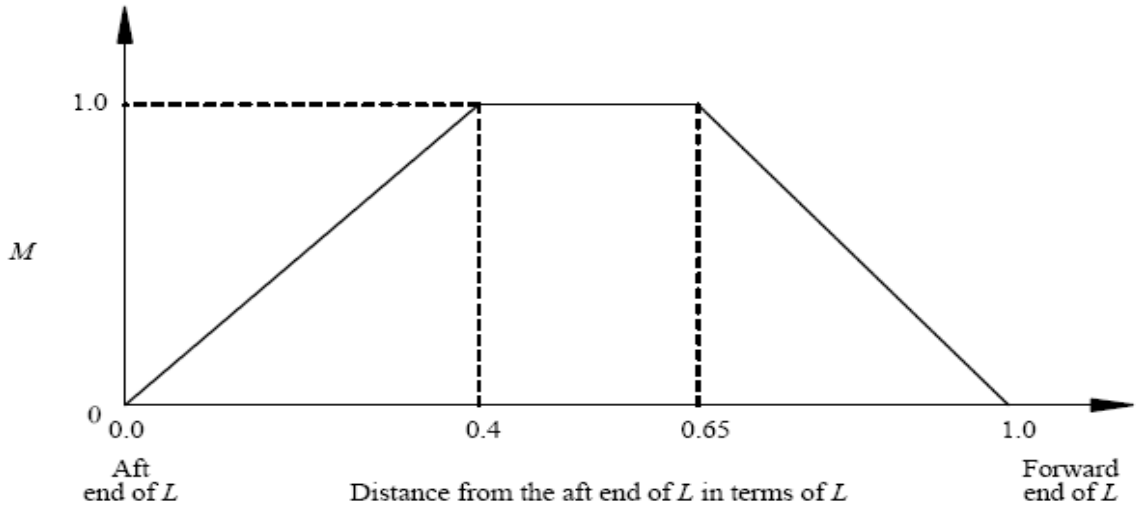

Figure 62: Bending moment distribution factor M

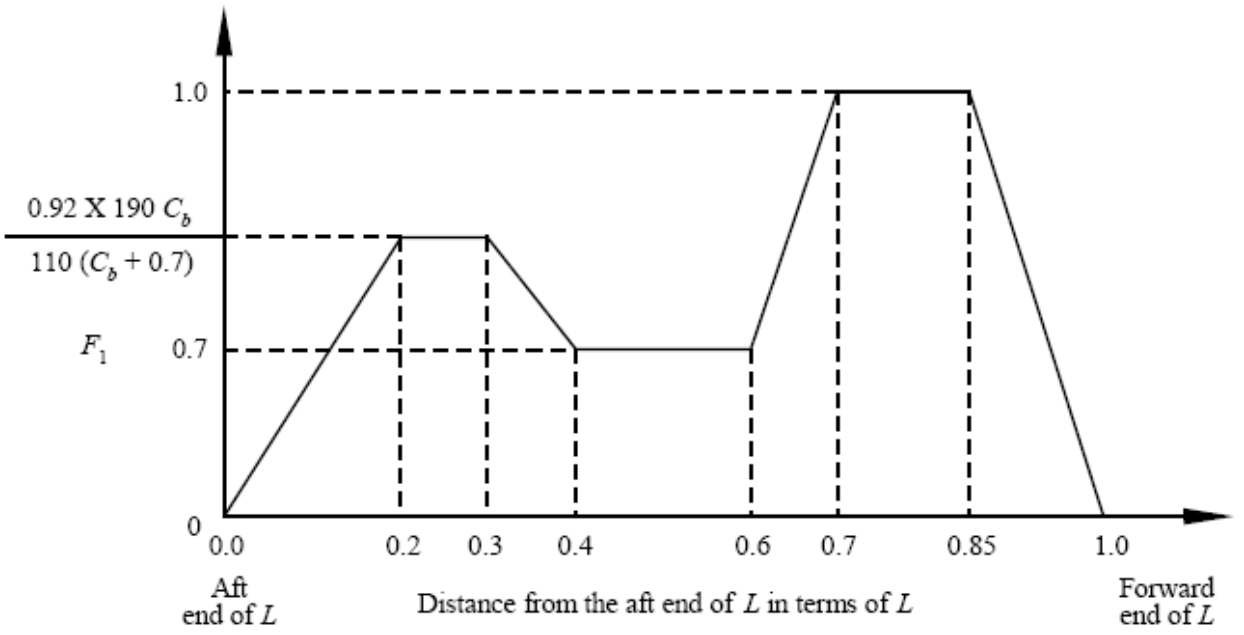

Figure 63: Positive shear force distribution factor F1 (Wave shear force)

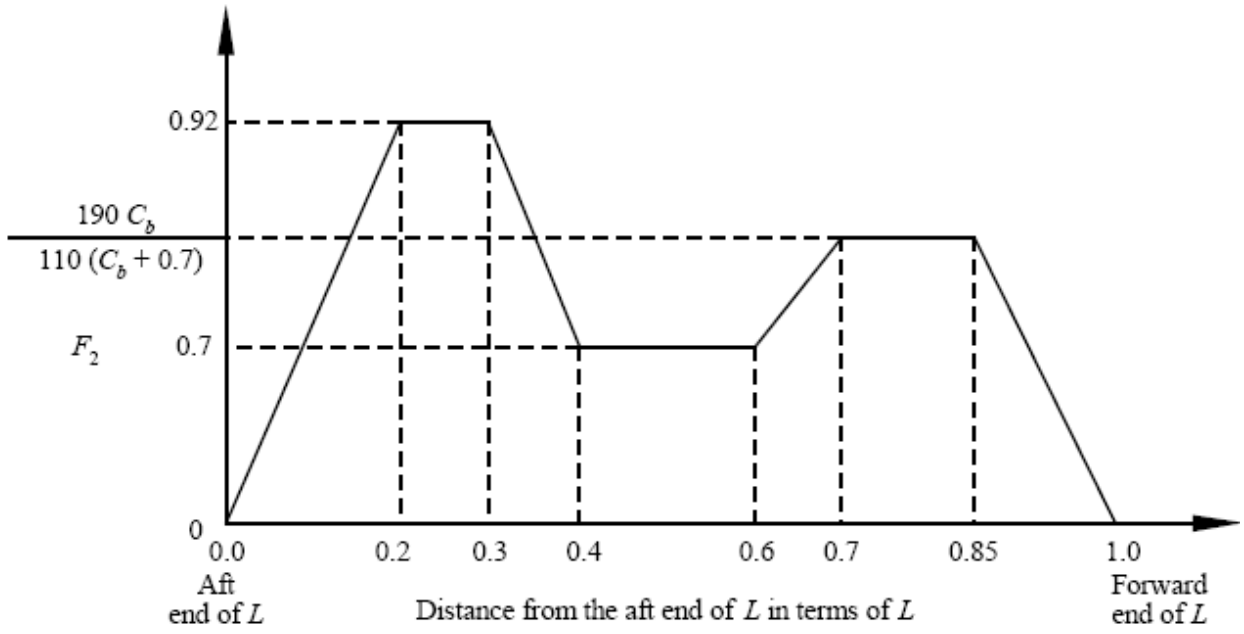

Figure 64: Negative shear force distribution factor F2 (Wave shear force)

7.2.1.2 Still-water Bending Moment and Shear Force

7.2.1.2 (a) General. Still-water bending moment and shear force calculations, determining the bending moment and hull girder shear force values along the vessel's entire length, are to be submitted together with the distribution of lightship weights. The distribution factor are shown at figure 62,63,64.

7.2.2 Wave Loads

7.2.2.1 Wave Bending Moment Amidships

The wave bending moment, expressed in kN-m, may be obtained from the following equations.

$$M_{ws} = -k_1 C_1 L^2 B(C_b + 0{,}7)x10^{-3}$$ Sagging Moment

$$M_{wh} = k_2 C_1 L^2 B x 10^{-3}$$ Hogging Moment

where

k_1 = 110

k_2 = 190

C_1= 0.044L + 3.75 for ships $61 \leq L < 90\ m$

L = length of vessel, in m

B = breadth of vessel, in m

C_b = block coefficient, but not to be taken less than 0.6

Calculations for parabolized hull

For Sagging

M_{ws} = - 110 x 7,284x $80{,}31^2$ x 20,122 x (0,7+0,7) x 10^{-3}

= - 145579.8 kN-m

C_1 = 0,044 x 80,31 + 3.75

= 7,284

For Hogging

M_{wh} = 190 x 7,284 x 80,31^2 x 20,122 x 10^{-3}

= 179611,4 kN-m

Calculations for parent hull

For Sagging

M_{ws} = - 110 x 7,284x 80,31^2 x 18,3 x (0,74+0,7) x 10^{-3}

= - 136180.7 kN-m

C_1 = 0,044 x 80,31 + 3.75

= 7,284

For Hogging

M_{wh} = 190 x 7,284 x 80,31^2 x 18,3 x 10^{-3}

= 163348,0 kN-m

7.2.3 Bending Strength

7.2.3.1 Hull Girder Section Modulus

7.2.3.1 (a) Section Modulus. The required hull girder section modulus for 0.4L amidships is to be the greater of the values obtained from the following equation or 7.2.3.1 (b):

$$SM = M_t / f_p \qquad \text{cm}^2\text{-m}$$

M_t = total bending moment, as obtained below

f_p = nominal permissible bending stress, 17.5 kN/cm2

The total bending moment, Mt, is to be considered as the maximum algebraic sum (see sign convention in Figure 61) of still-water bending moment and wave-induced bending moment, as follows:

$$M_t = M_{sw} + M_w$$

M_{sw} = Still water bending moment, kN-m

M_w = Maximum wave-induced bending moment

7.2.3.1 (b) Minimum Section Modulus. The minimum hull girder section modulus amidships is not to be less than obtained from the following equation:

$$SM = C_1 C_2 L^2 B(C_b + 0{,}7) \qquad \text{cm}^2\text{-m}$$

C_1= as defined in 7.2.2.1

C_2 = 0.01

L = length of vessel, in m

B = breadth of vessel, in m

C_b = block coefficient, but not to be taken less than 0.6

Calculations for parabolized hull

SM = 7,284 x 0,01 x $80{,}31^2$ x 20,122 x (0,7+0,7)

= 13234.5 cm^2-m

$$SM = M_t / f_p$$

13234.5 = M_t / 17,5

M_t = 231603.8 kN-m

$$M_t = M_{sw} + M_w$$

For hogging

231603.8 = M_{sw} + 179611,4

M_{sw} = 51992.4 kN-m

For Sagging

231603.8 = M_{sw} + 145579.8

M_{sw} = 86024.0 kN-m

Calculations for parent hull

SM = 7,284 x 0,01 x $80,31^2$ x 18,3 x (0,74+0,7)

= 12380.0 cm^2-m

$$SM = M_t / f_p$$

12380.0 = M_t / 17,5

M_t = 216650.0 kN-m

$$M_t = M_{sw} + M_w$$

For hogging

216650.0 = M_{sw} + 163348,0

M_{sw} = 53302,0 kN-m

For Sagging

216650.0 = M_{sw} + 136180,7

M_{sw} = 80469,3 kN-m

7.2.4 Hull girder moments of Inertia

The hull girder moments of Inertia, I, amidship is to be not less than:

$$I = L.SM/33.3 \text{ cm}^2 \text{ m}^2$$

Where

L = Length of Vessel, m

SM = Required hull girder section modulus in, cm^2 m

Calculations for parabolized hull

I = 80,31 x 13234,5 / 33.3

= 31917.8 cm^2 m

Calculations for parent hull

I = 80,31 x 12380.0 / 33.3

= 29857.0 cm^2 m

The Horizontal Wave Bending Moment calculations are done according to American Bureau of Shipping (ABS) Rules for building and classing, Steel Vessels 2014, Part 5C Specific Vessel Types.

7.2.5 Horizontal Wave Bending Moment

Horizontal Wave Bending Moment The horizontal wave bending moment, positive (tension port) or negative (tension starboard), may be obtained from the following equation:

$$M_H = \pm m_h K_3 C_1 L^2 D C_b \, x10^{-3} \text{ kN-m}$$

m_h= distribution factor, as given by Figure 65

K_3 = 180

C_1 = As given above

L = length of vessel, in m

D = Depth of vessel, in m

C_b = block coefficient, but not to be taken less than 0.6

Parabolized hull

M_H = 1 x 180 x 7,284 x $80,31^2$ x 7,47 x 0,7 x 10^{-3}

= 44218,1 kN-m

Parent hull

M_H = 1 x 180 x 7,284 x $80,31^2$ x 7,47 x 0,74 x 10^{-3}

= 46744.9 kN-m

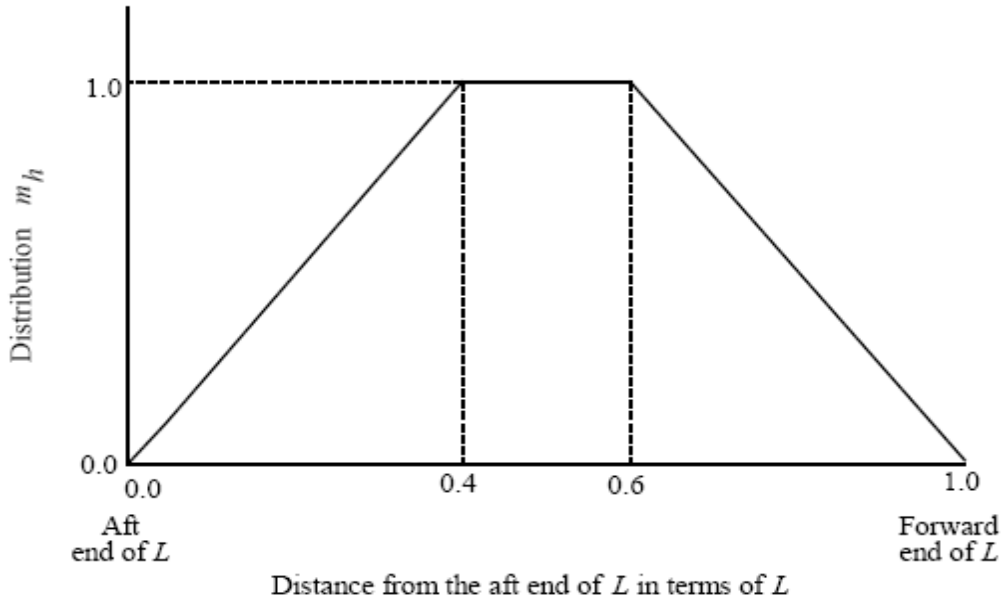

Figure 65: Horizontal wave bending moment distribution factor M_h

7.2.6 Deck Load

The deck load is given by design company as 5 ton/m^2

7.2.7 Moments Calculations Summary

The moments used for loads applied to FEA model is listed at table

Type of Moment	Hull	Load
Wave Bending Moment Amidship	Parabolized	145579,8 kN-m Sagging
		179611,4 kN-m Hogging
	Parent	136180,7 kN-m Sagging
		163348,0 kN-m Hogging
Total Bending Moment	Parabolized	231603,8 kN-m
	Parent	216650,0 kN-m
Still Water Bending Moment	Parabolized	51992,4 kN-m Hogging
		86024,0 kN-m Sagging
	Parent	53302,0 kN-m Hogging
		80469,3 kN-m Sagging
Horizontal Wave Bending Moment	Parabolized	44218,1 kN-m
	Parent	46744,9 kN-m
Deck Load	Parabolized	5 ton/m^2
	Parent	5 ton/m^2

Table 5: Loads Calculated for FEA

7.3 Solutions and Results

The results from finite element analysis are presented in this part of the thesis. The results are showing the von misses stress values, longitudinal component stress values, longitudinal- horizontal shear stress values and displacement values for each analysis. The design loads used for FEA are shown at table 5. The results are showing the hogging values are higher for wave bending moment and still water bending moment. So the hogging moments are applied for both bending moments. The deck load, horizontal wave bending moment and total bending moment are applied regarding to calculation. The maximum stress value is appeared at deck load analysis with 5 ton/m^2 load vertically applied to ship's deck. It appeared at beams and longitudinal structure below the deck shell plate. It is quite high as we consider tensile strength of st 42 steel material is 235 MPa. The stress is local and it can be easily drop down by increasing the thickness of the structure or installing additional bracket below high stress area. The highest stress value appeared at structure under deck shell plate of parabolized hull at the wave bending moment analysis. The maximum stress value is 118,24 MPa which is acceptable for st 42 steel material.

7.3.1 Parent Hull Wave Bending Moment

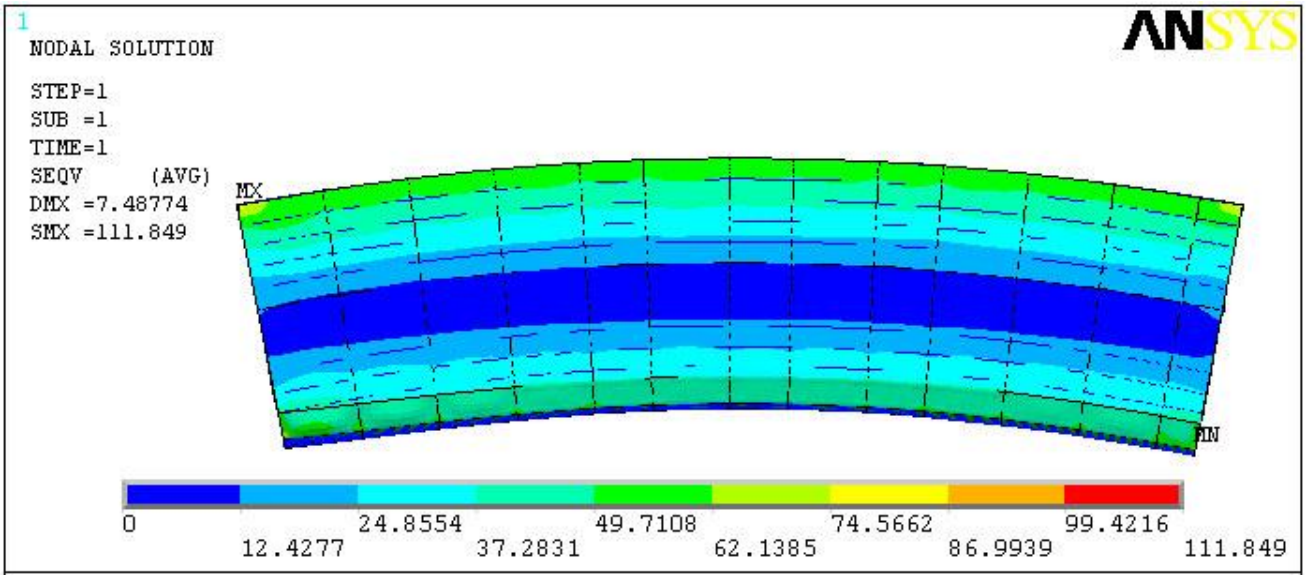

Figure 66: Parent Hull Wave Bending Moment Von Mises Stress, (MPa)

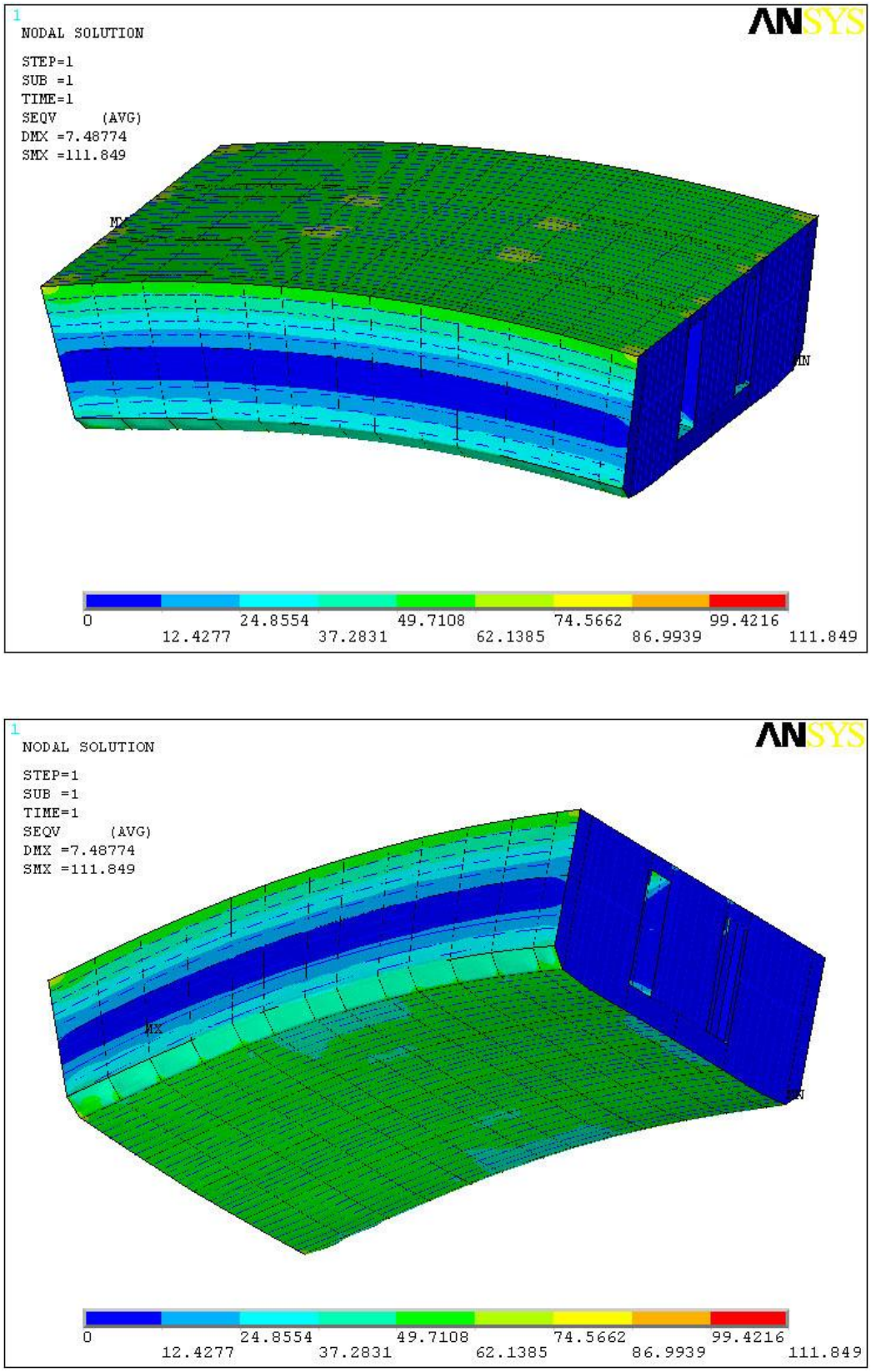

Figure 67: Parent Hull Wave Bending Moment Von Mises Stress, (MPa)

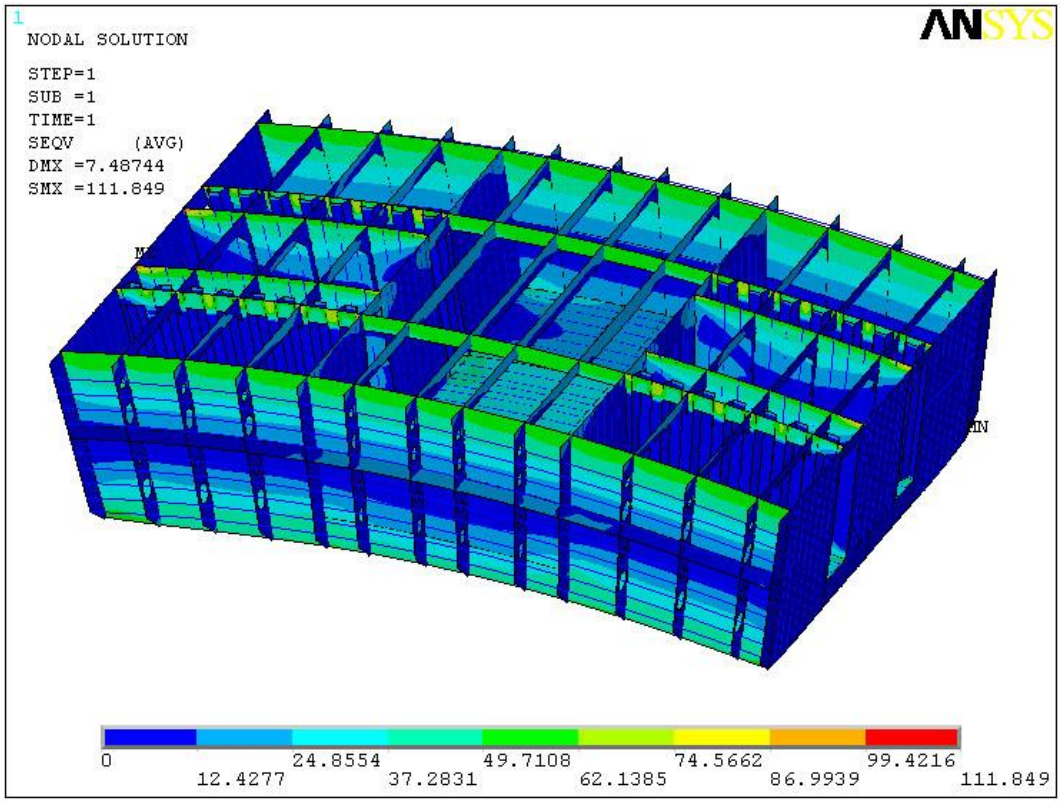

Figure 68: Parent Hull Wave Bending Moment Von Mises Stress, (MPa)

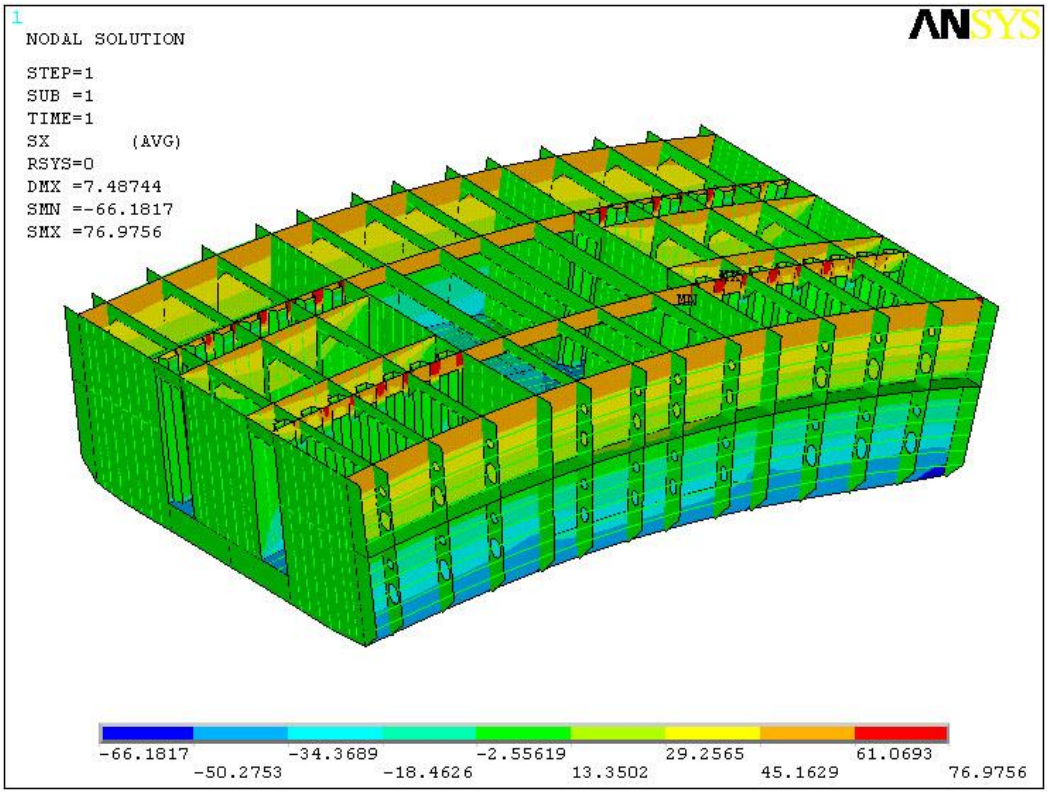

Figure 69: Parent Hull Wave Bending Moment Longitudinal Component Stress, (MPa)

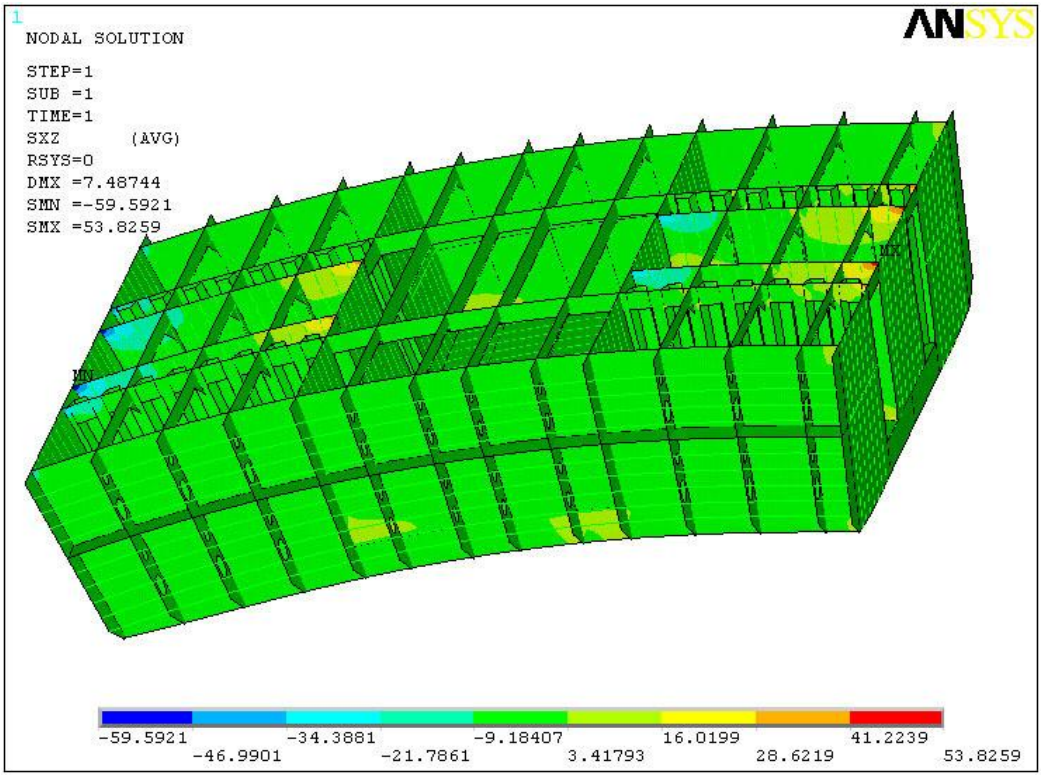

Figure 70: Parent Hull Wave Bending moment Longitudinal- horizontal Shear Stress, (MPa)

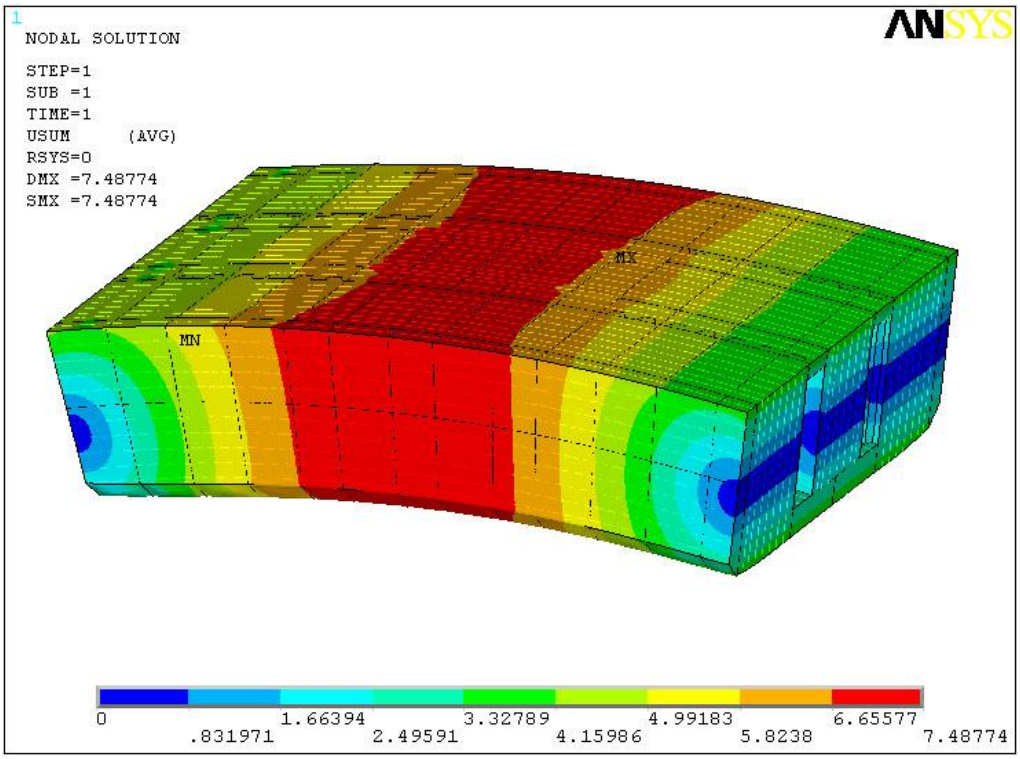

Figure 71: Parent Hull Wave Bending Moment Displacement Values, (mm)

7.3.2 Parent hull Horizontal Wave Bending Moment

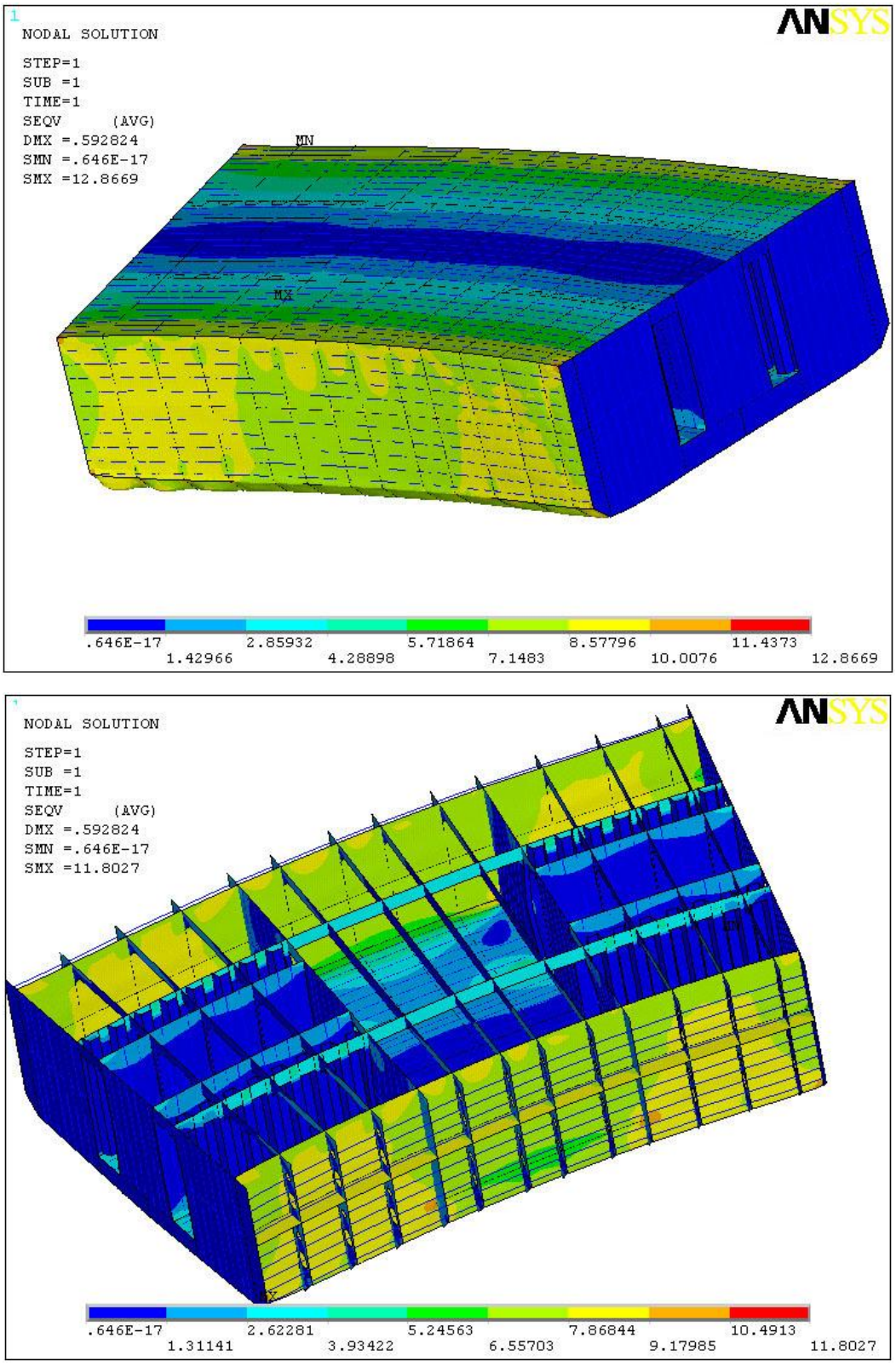

Figure 72: Parent Hull Horizontal Wave Bending Moment Von Mises Stress, (MPa)

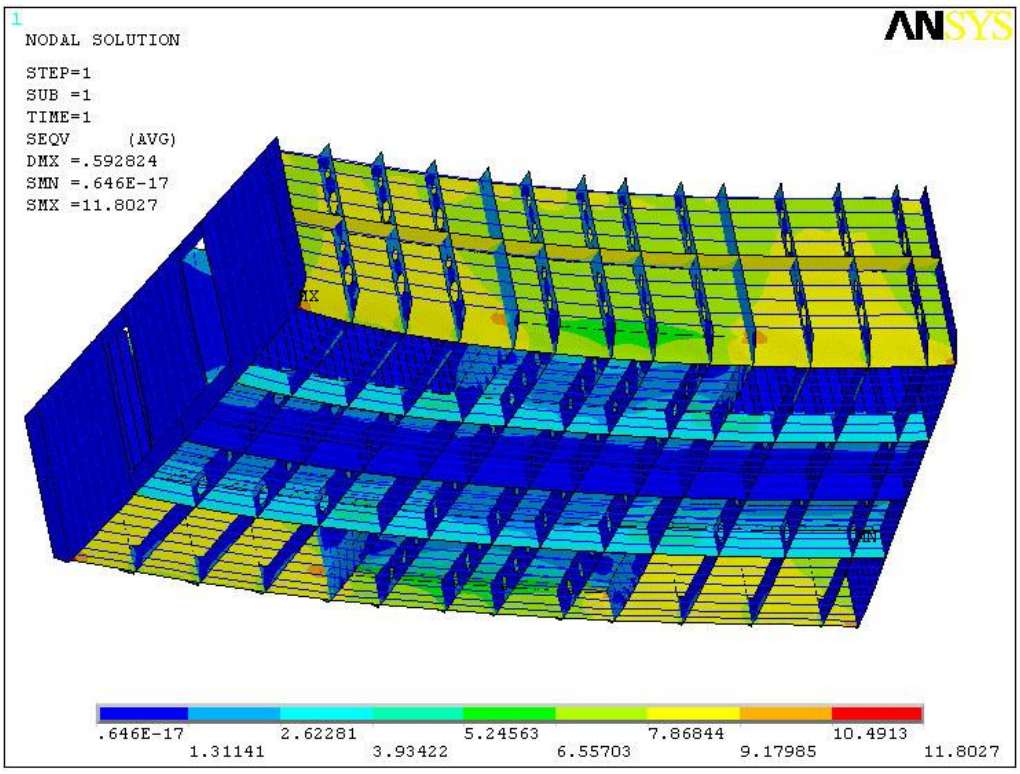

Figure 73: Parent Hull Horizontal Wave Bending Moment Von Mises Stress, (MPa)

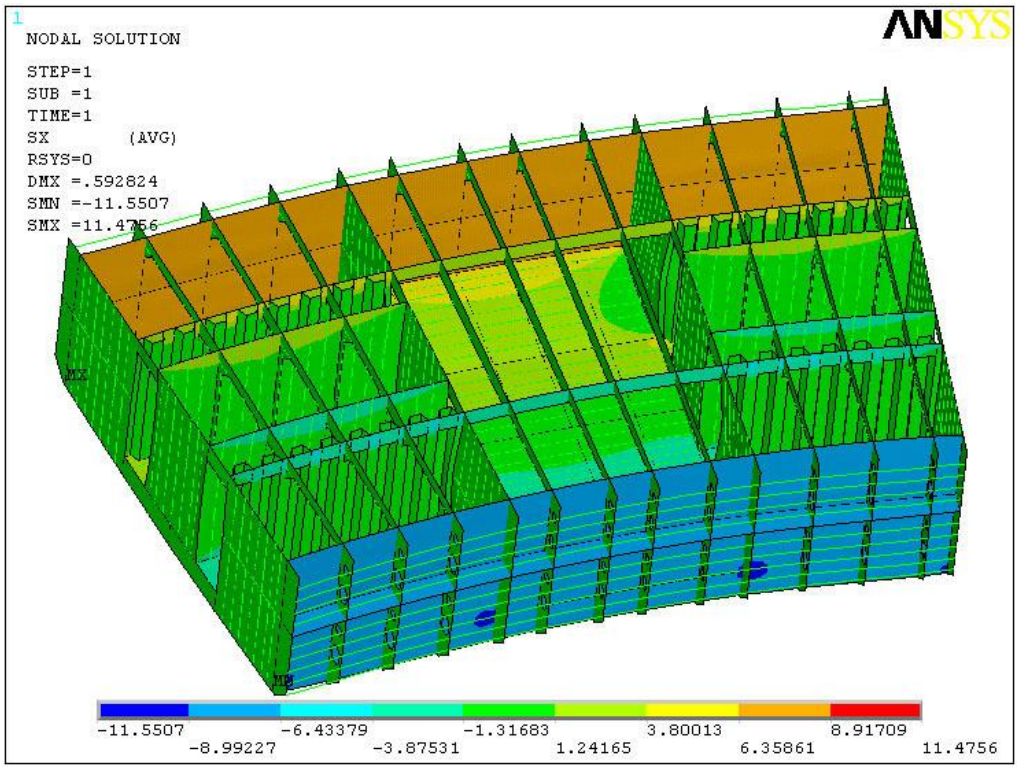

Figure 74: Parent Hull Horizontal Wave Bending Moment longitudinal Component Stress, (MPa)

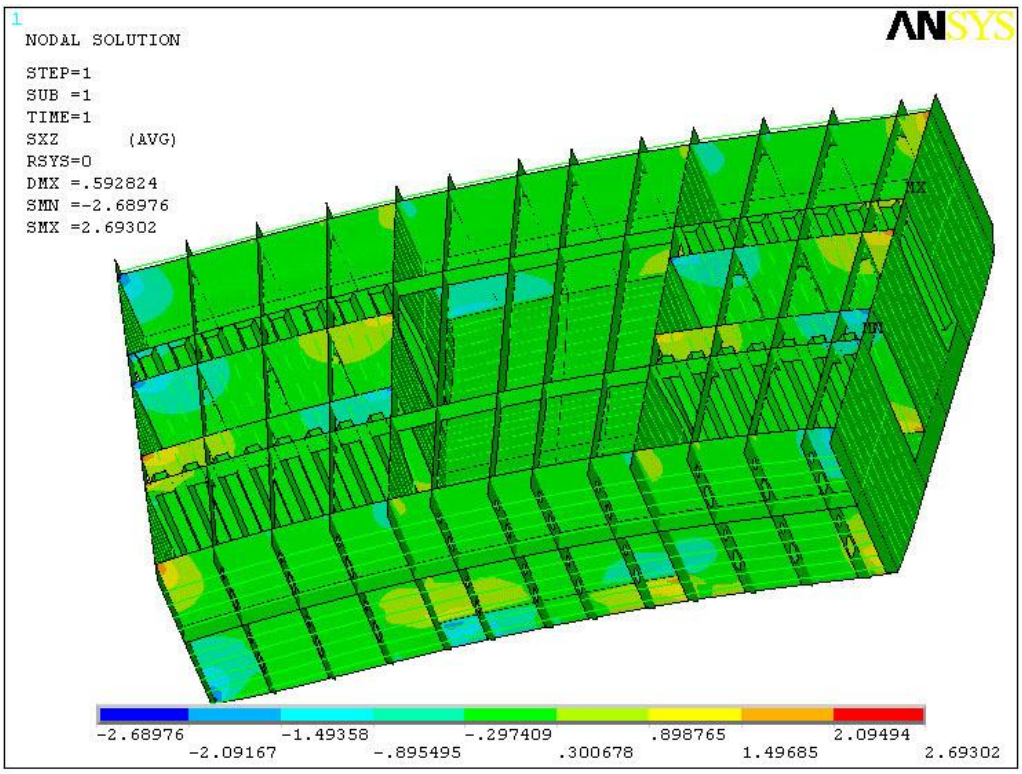

Figure 75: Parent Hull Horizontal Wave Bending moment Longitudinal- horizontal Shear Stress, (MPa)

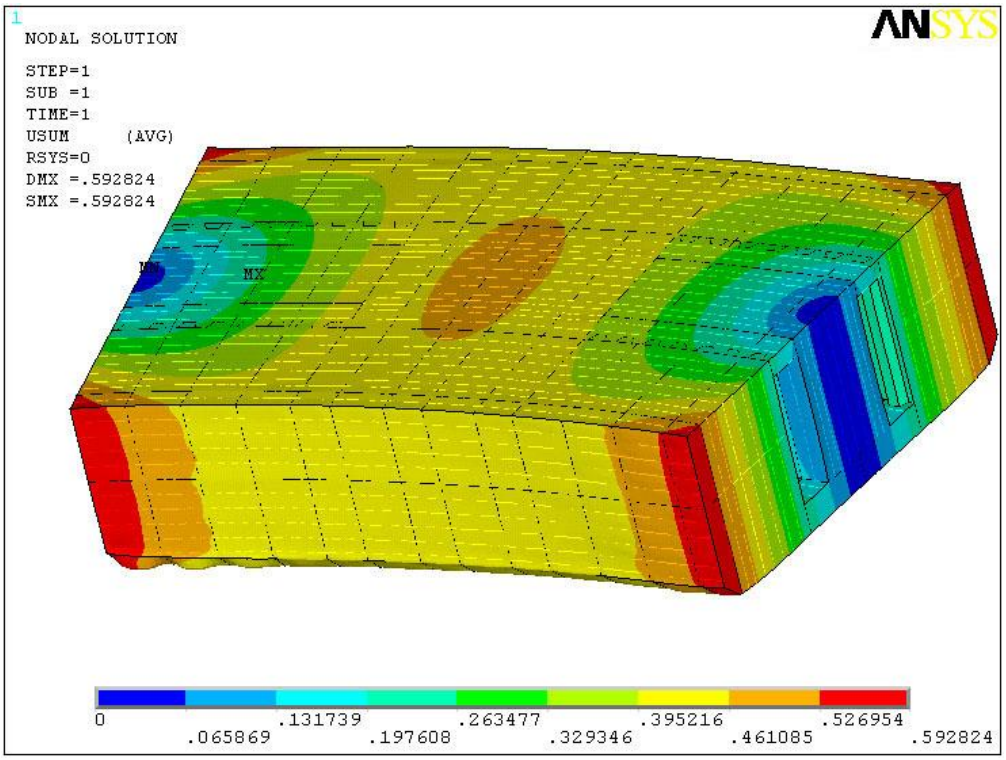

Figure 76: Parent Hull Horizontal Wave Bending Moment Displacement Values,(mm)

7.3.3 Parabolized Hull Deck Load

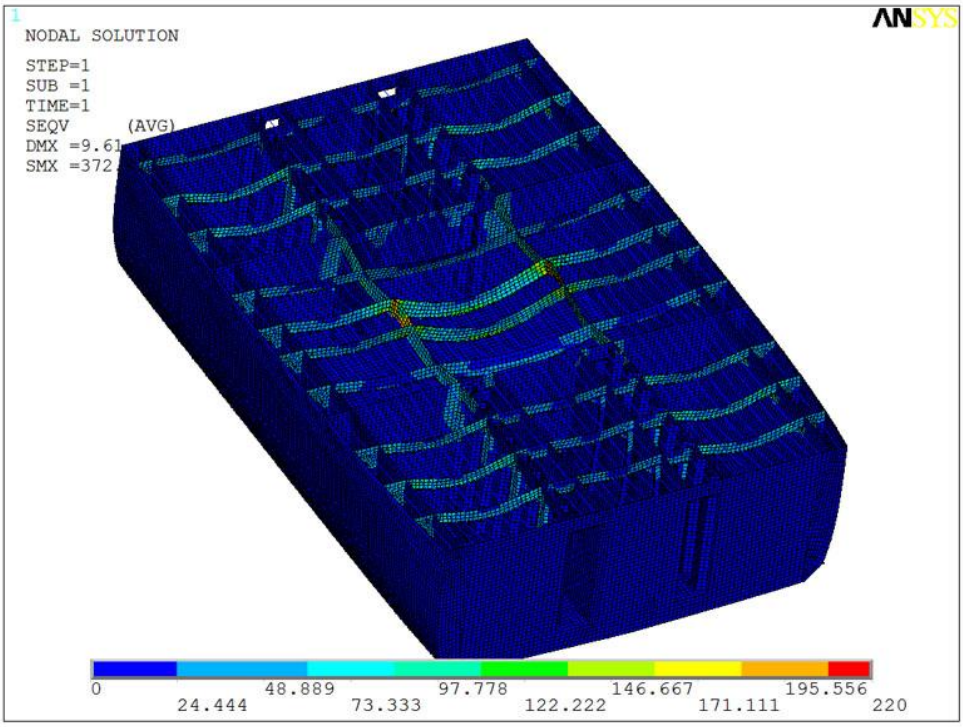

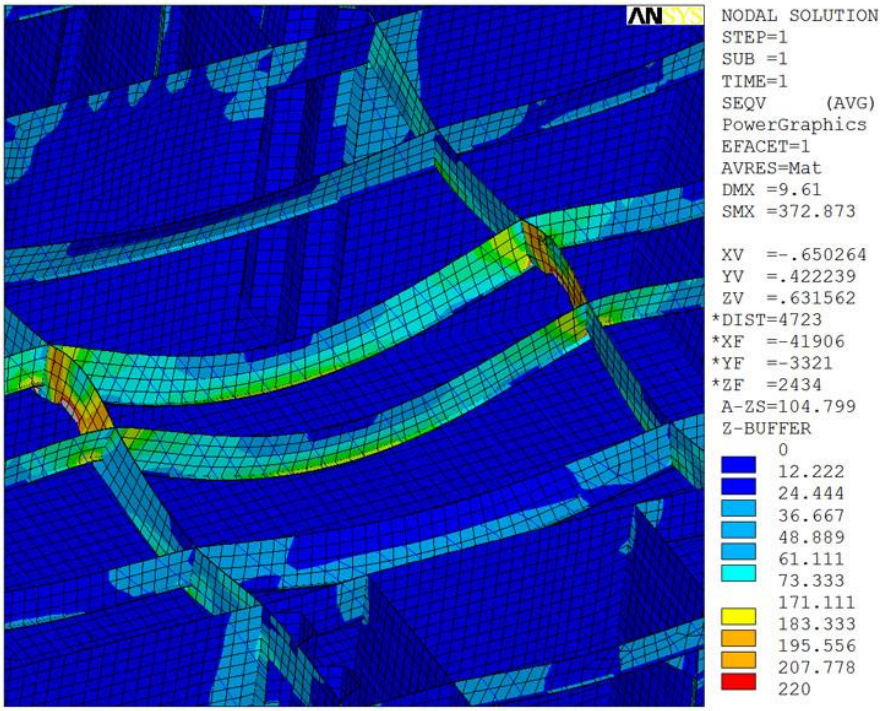

Figure 77: Deck Load Solutions. Internal structure Von Misses values, (MPa)

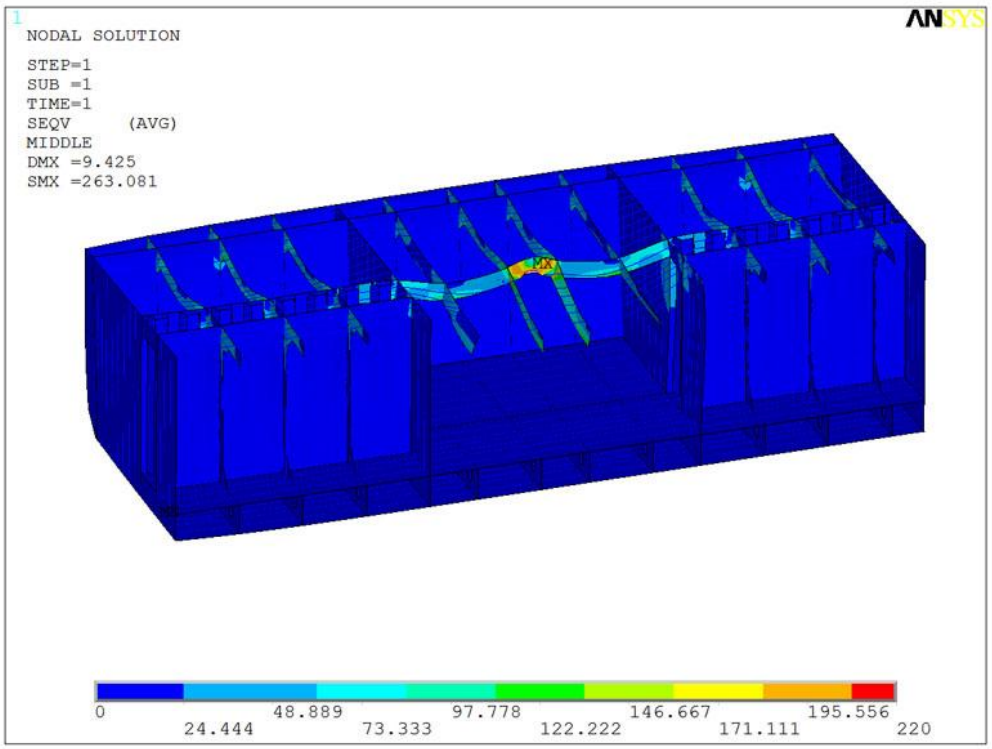

Figure 78: Deck Load Solutions. Internal structure Von Misses values, (MPa)

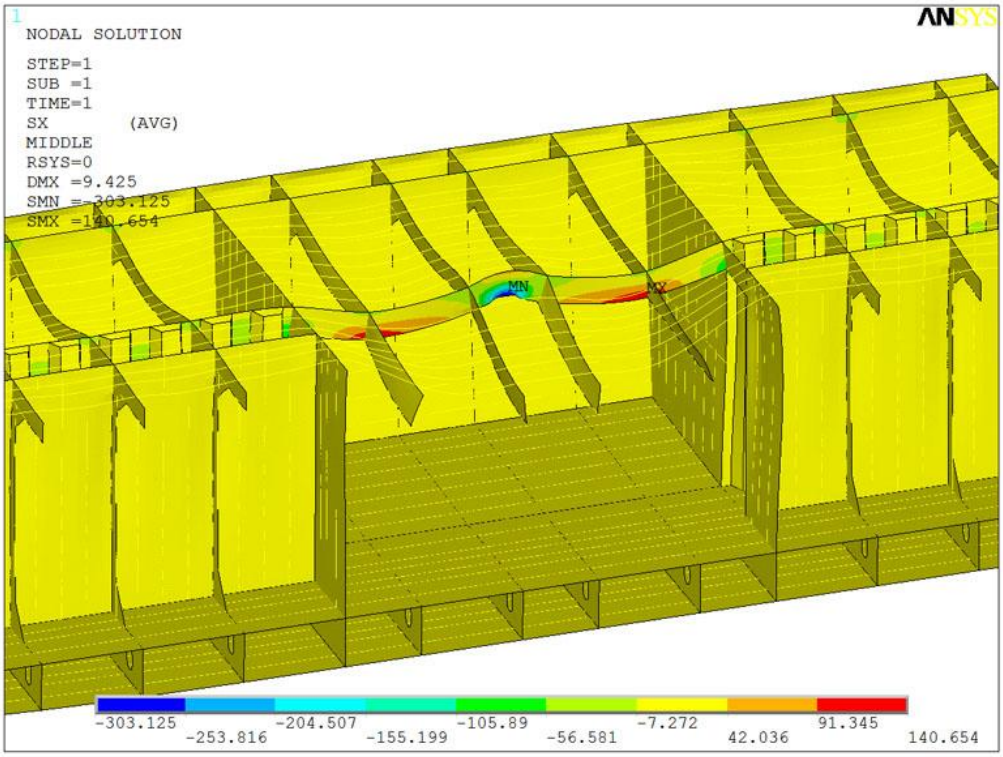

Figure 79: Deck Load Solutions. Shear stress values at longitudinal orientation, (MPa)

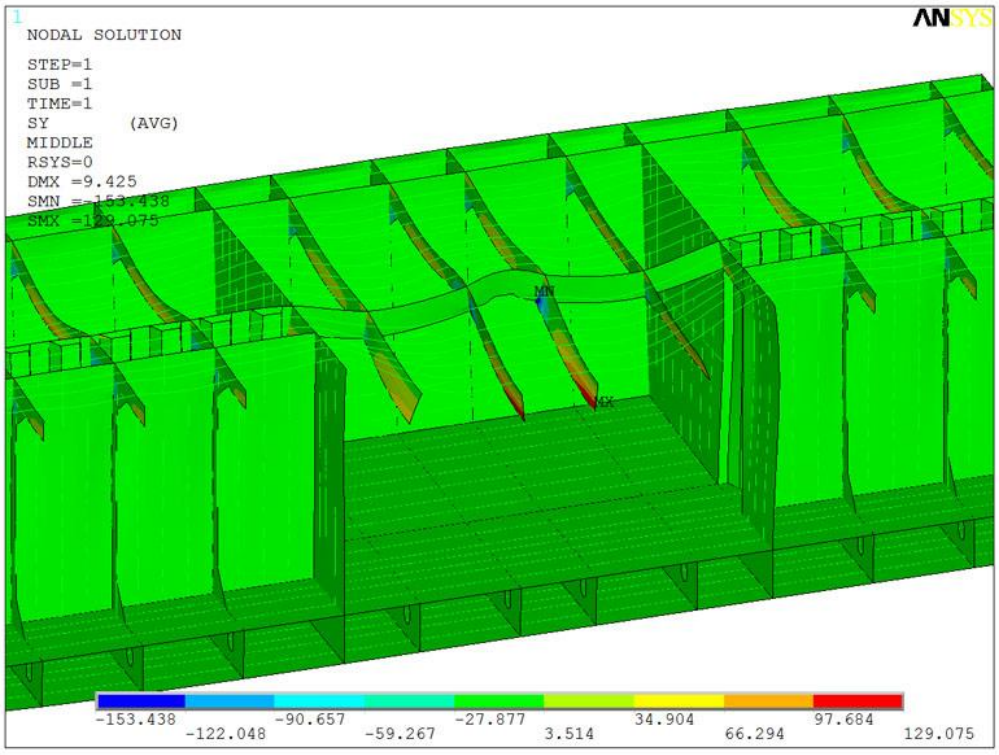

Figure 80: Deck Load Solutions. Shear stress values at transversal orientation, (MPa)

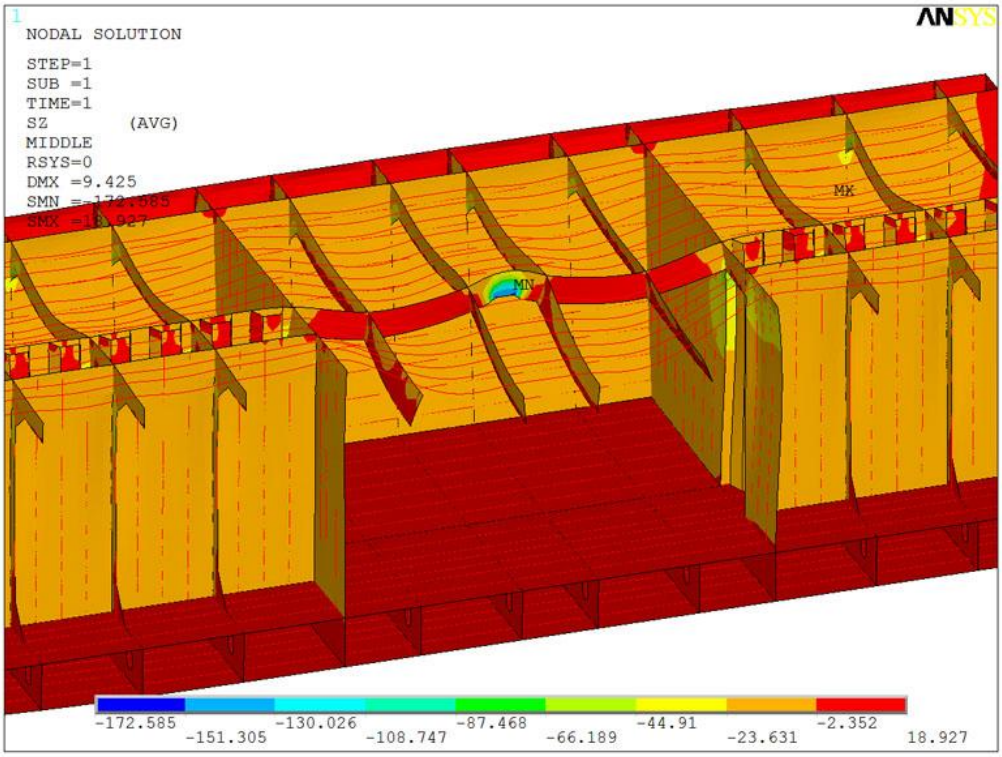

Figure 81: Deck Load Solutions. Shear stress values at vertical orientation, (MPa)

7.3.4 Parabolized hull Wave Bending Moment

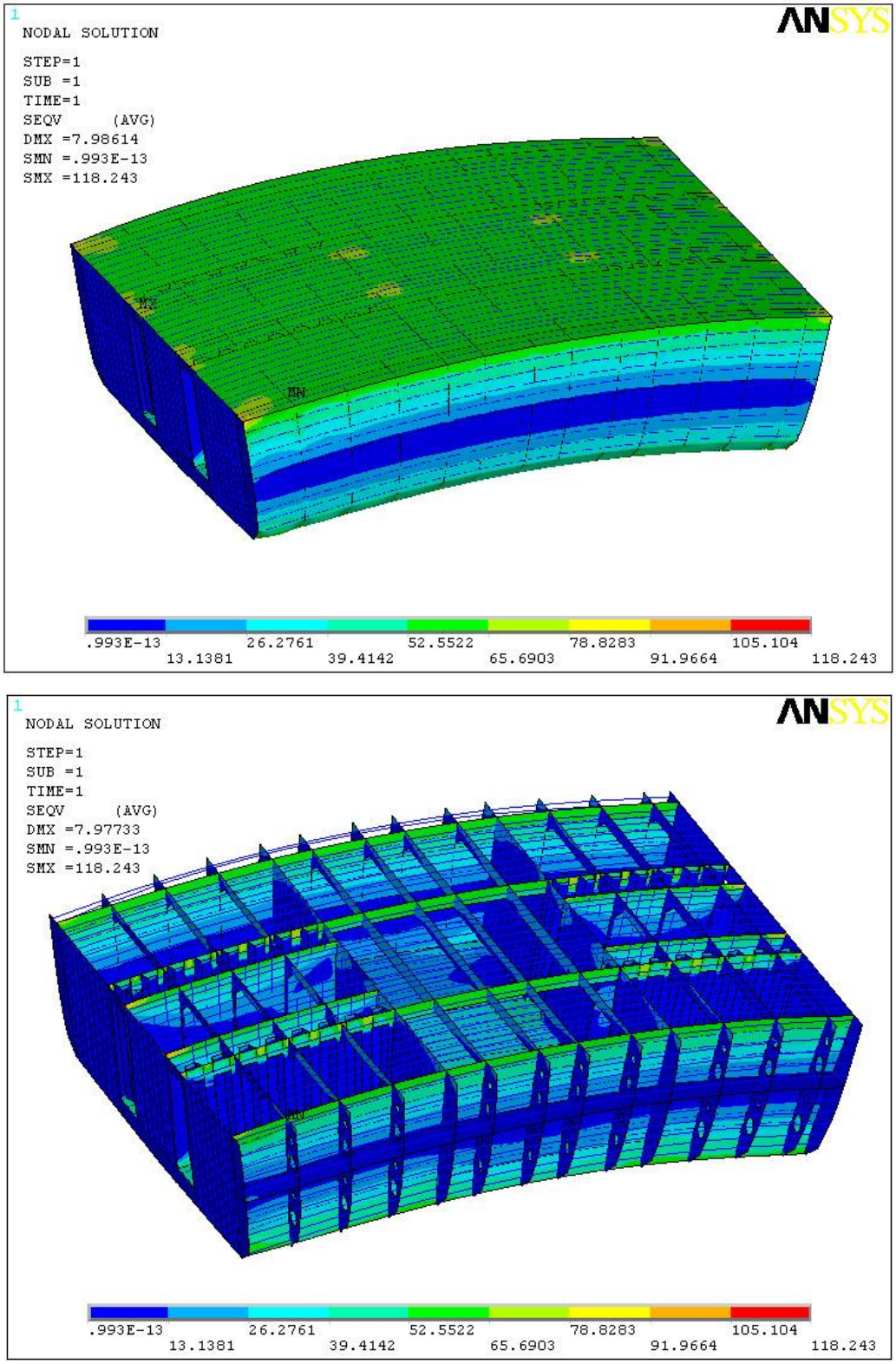

Figure 82: Parabolized Hull Wave Bending Moment Von Mises Stress values, (MPa)

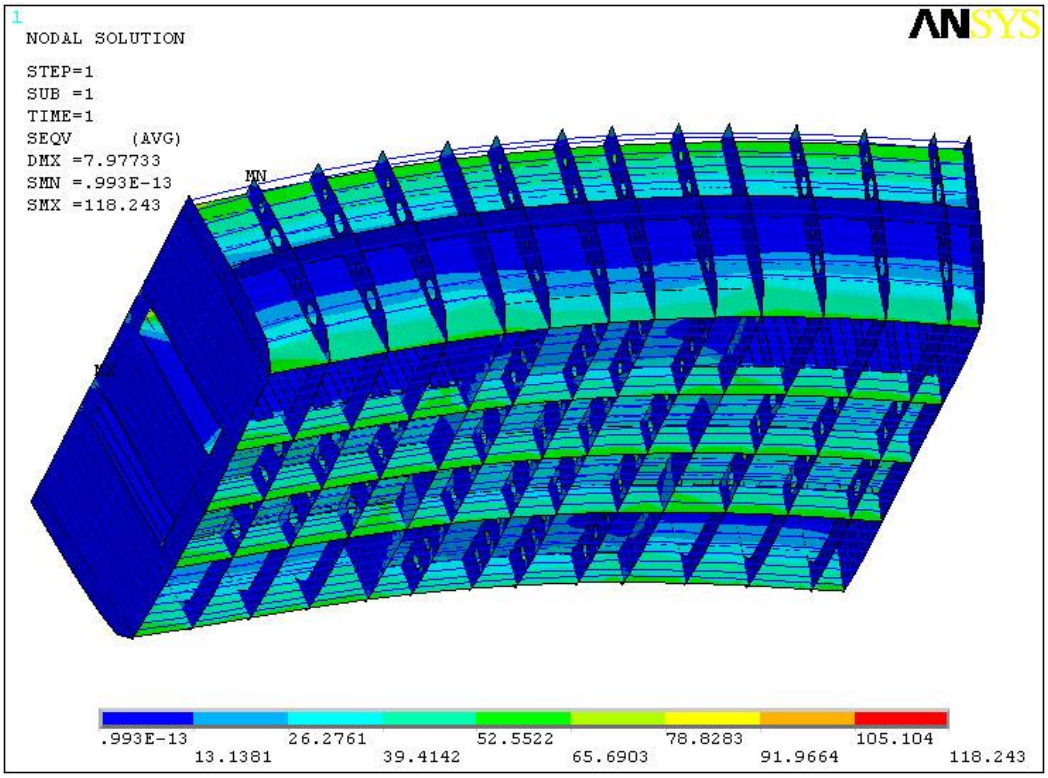

Figure 83: Parabolized Hull Wave Bending Moment Von Mises Stress values, (MPa)

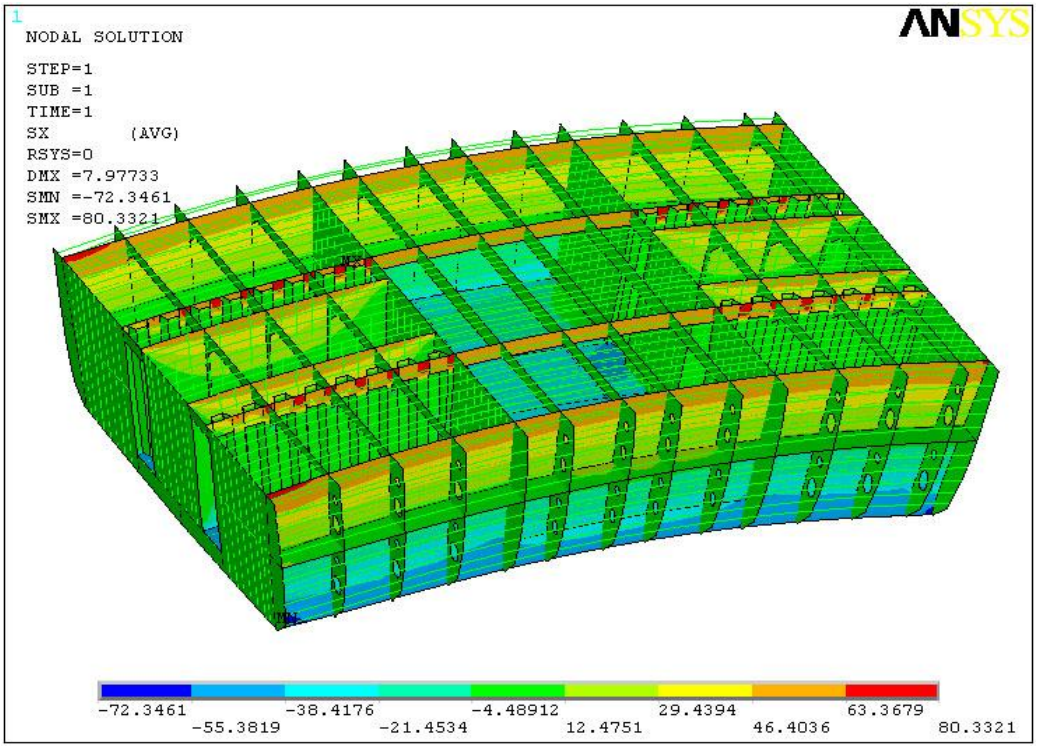

Figure 84: Parabolized Hull Wave Bending Moment Longitudinal Component Stress, (MPa)

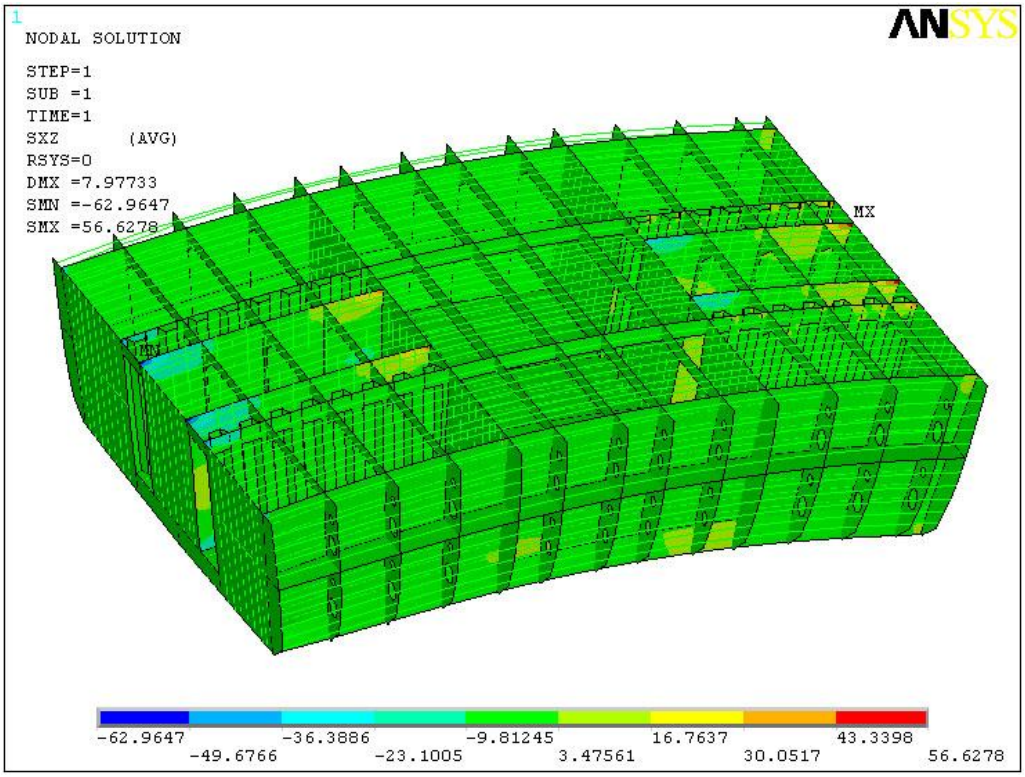

Figure 85: Parabolized Hull Wave Bending Moment Longitudinal- Horizontal Shear Stress, (MPa)

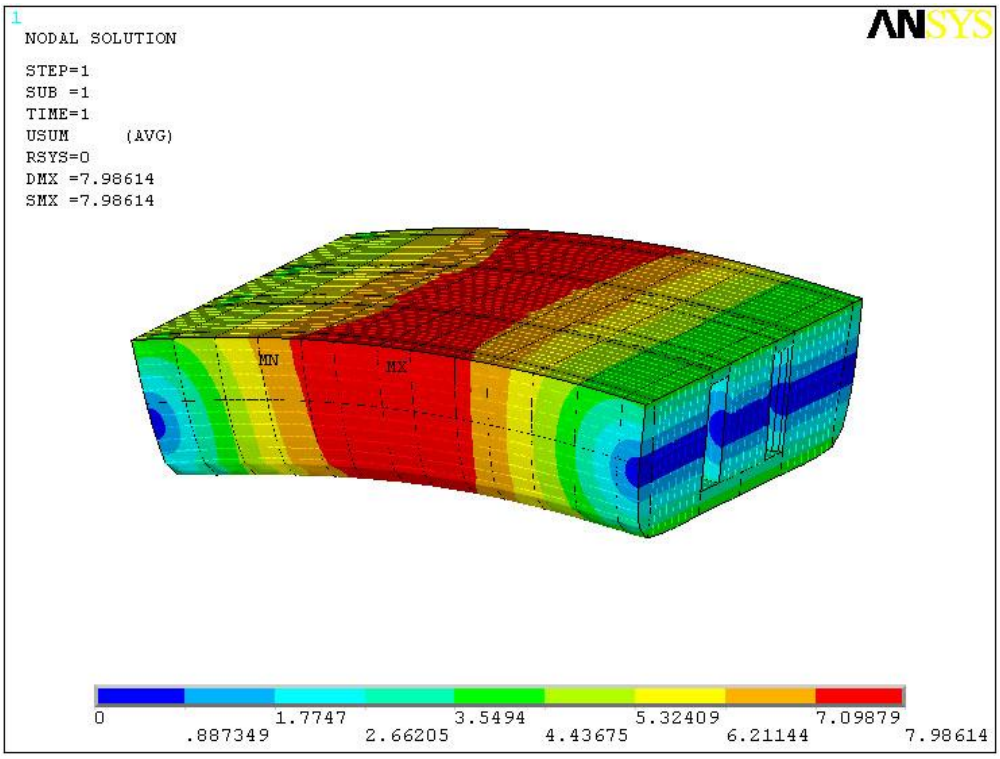

Figure 86: Parabolized Hull Wave Bending Moment Displacement Values, (mm)

7.3.5 Parabolized hull Horizontal Wave Bending Moment

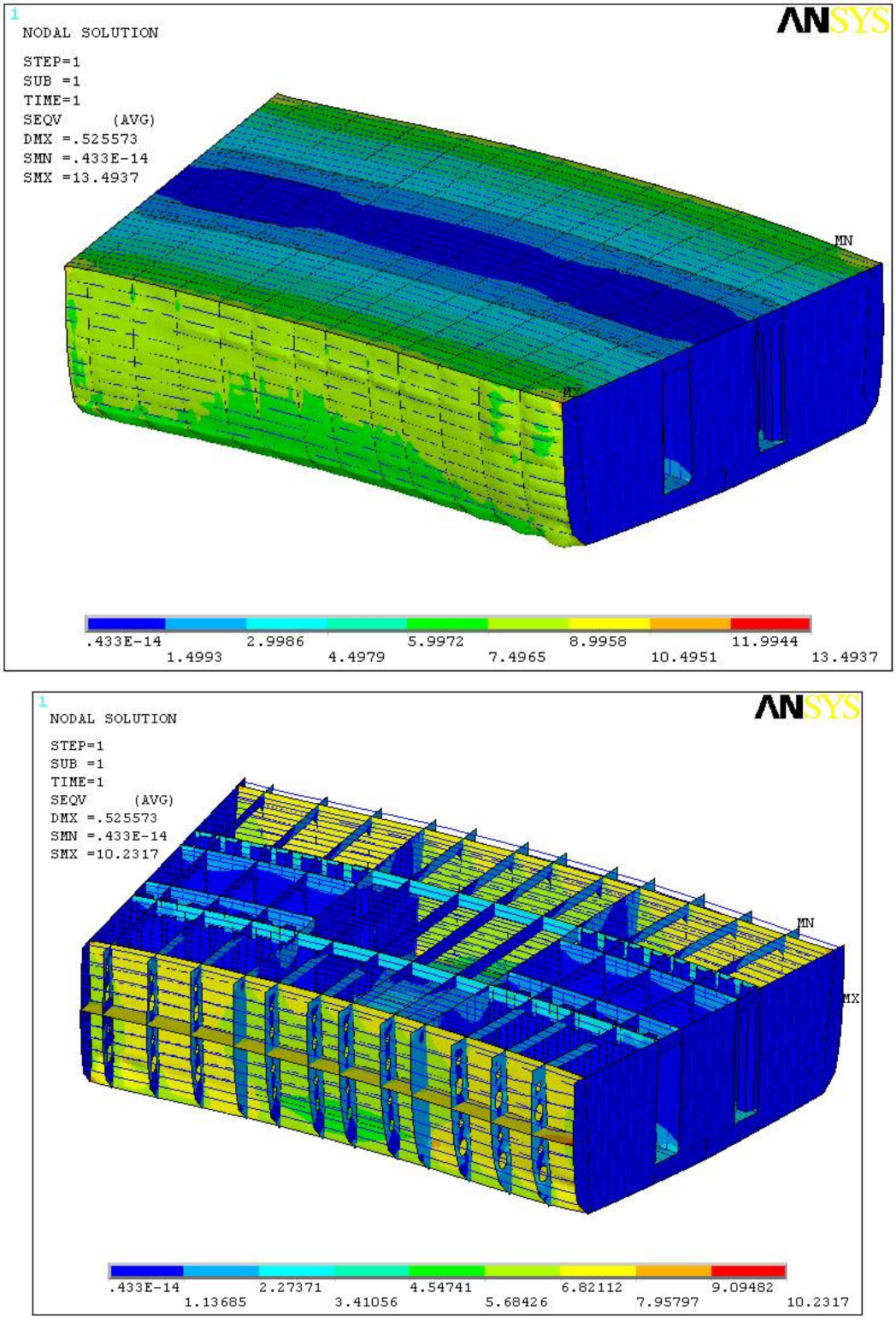

Figure 87: Parabolized Hull Horizontal Wave Bending Moment Von Mises Stress values, (MPa)

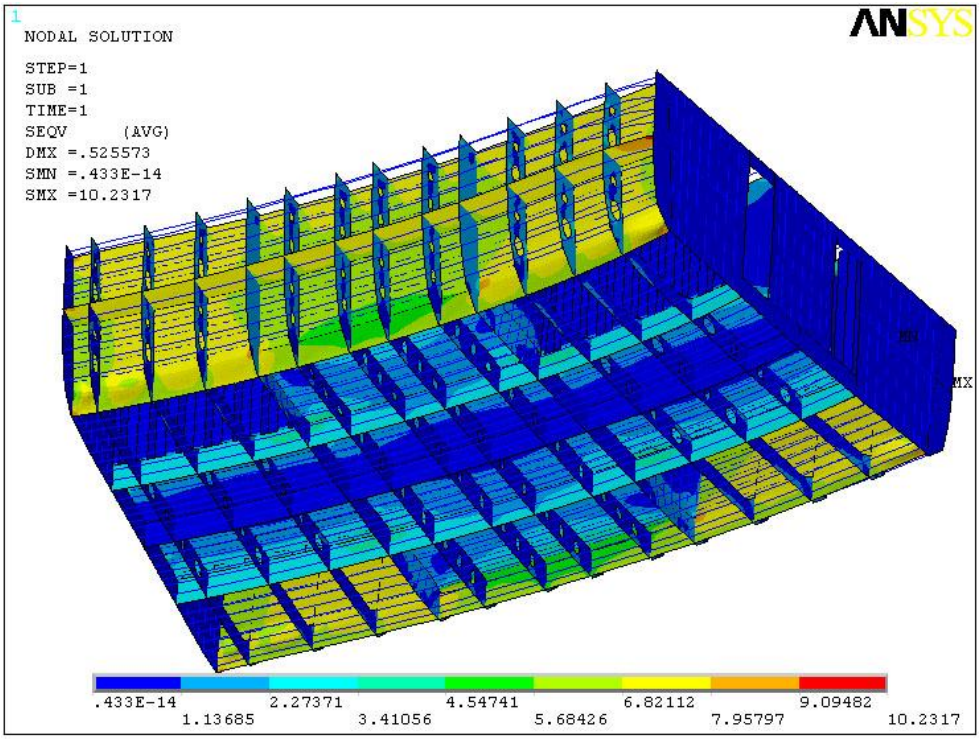

Figure 88: Parabolized Hull Horizontal Wave Bending Moment Von Mises Stress values, (MPa)

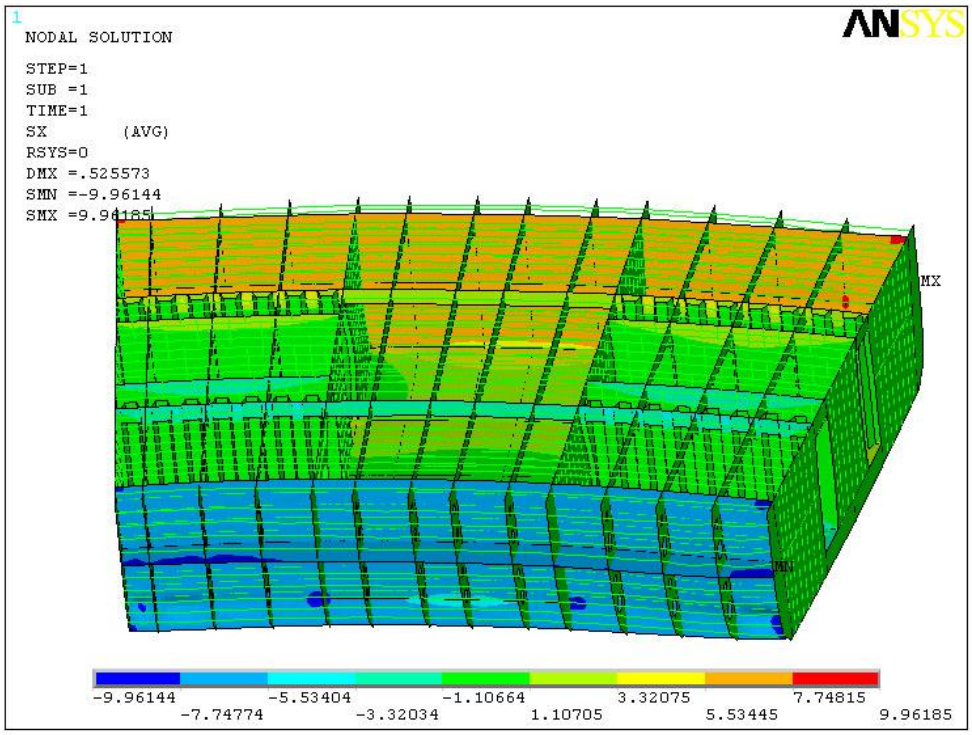

Figure 89: Parabolized Hull Horizontal Wave Bending Moment longitudinal Component Stress, (MPa)

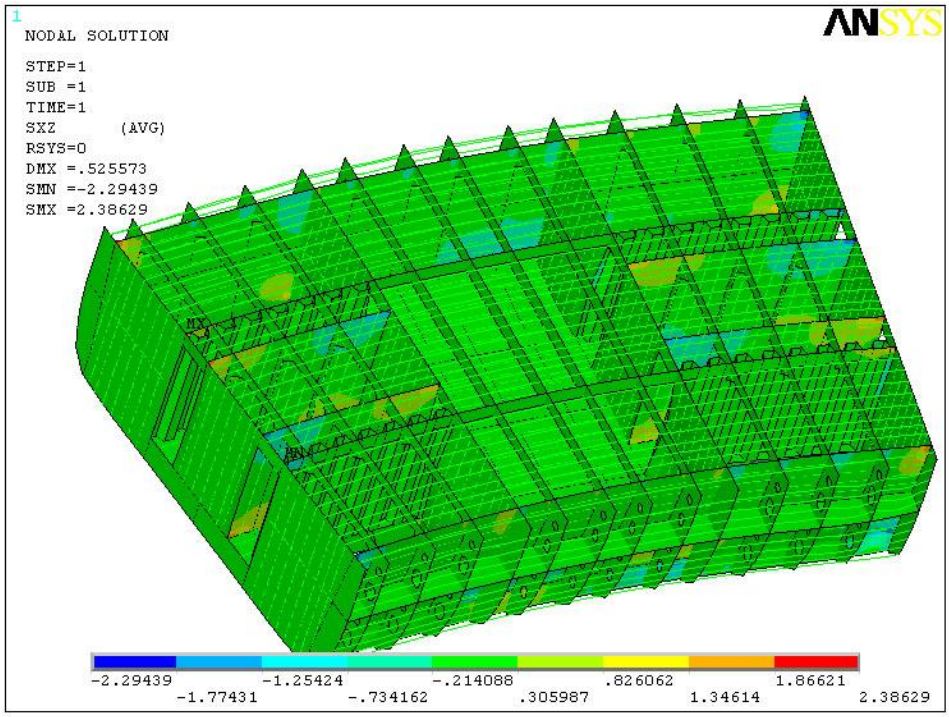

Figure 90: Parabolized Hull Horizontal Wave Bending Moment Longitudinal- Horizontal Shear Stress, (MPa)

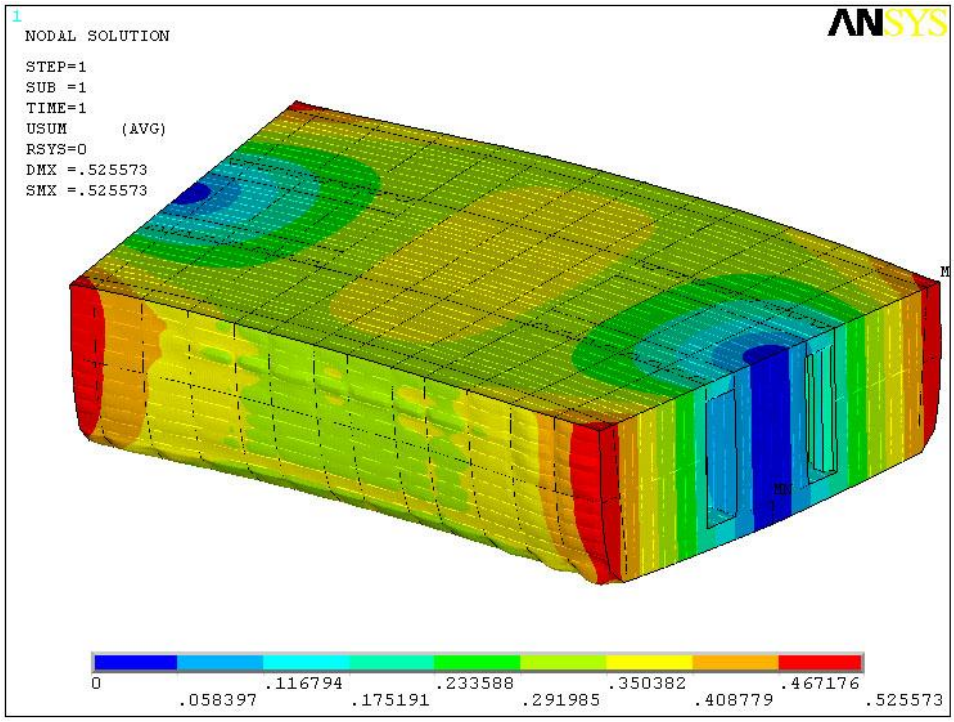

Figure 91: Parabolized Hull Horizontal Wave Bending Moment Displacement Values,(mm)

8. COST ANALYSIS OF PSV SIDEBULB APPLICATION

As the result of this research we parabolized the hull and created retro fit hull with an amidships bulb on PSV parent hull. The results are showing 5,88 % reduction in the total resistance of the vessel. This can be used either to reduce powering requirement or sailing range of the vessel. On the other hand the complex shaped structure of the hull will incease the construction cost of the vessel. In this section the financial analysis of our platform supply vessel with its operation are at Atlantic offshore of Brazil are estimated.

8.1 PSV operations on world sea water

The sample PSV is designed to operate at Atlantic coast of Brazil as mentioned earlier. The vessel has rotation to operate between couple of possible offshore platforms. Here we will examine Campos Basin offshore platform. The information about Compas Basin is like below.

Figure 92: Campos oil field shown on the map of South America.

Oil Field

Name : Campos oil field

Coordiate : 22° 28′ 52″ S, 34° 50′ 0″ W

Distance : 465 Nautical Miles to Rio de Janeiro

8.2 Cost savings for the PSV with a parabolic bulb

The vessel will operate at 13,61 kts as service speed and sails 465 miles to offshore platform. The reduction of resistance will drop down the fuel consumption of vessel. The power and fuel consumption calculations are as in table 4-5. You can see the calculation about time for sailing to oil rig in table 4.

Destination to Campos oil field	
Round trip time port to platform	68 hours 20 min
Trips per year	56 times
Operational hours per year	Round 3827 hours

Table 4: PSV route details

The fuel consumption assumed for parent hull form and also retro fit parabolized hull with an amidship bulb. The main propulsion of vessel is assumed to be powered by caterpillar 4 stroke marine diesel C280-8 series engines. The fuel consumption is scaled linearly regarding to powering requirements calculated

	Parent Hull	Parabolized Hull
Powering	100 %	100%-5,88%=94,12%
Powering	5300 kW	5300x 94,12%=4988,36 kW
Chance in PB (Break Power)	0	311,64 kW
Fuel Consumption	0,235 lt/(kWxhr)	0,235 lt/(kWxhr)
Cost of Fuel	0,85 $ / lt	0,85 $ / lt

Table 5: Powering and cost details of PSV

PB is the installed break horsepower of the engines calculated by the designer. Therefore, the resistance has dropped down 5,88 % by parabolic amidships bulb. The change in PB calculated is a saving of 311,64 kW. For the purposes of this analysis, it is assumed that the engines could be exchanged prior to installation to realize all of the possible cost savings. The operational informations like working hours, fuel consumptions and fuel prices help us to calculate the benefit we gain by retro fit parabolic bulb platform supply vessel.

$$Fuel\ Savings = Fuel\ cons.\frac{lt}{kW\ x\ h} x\ Chance\ in\ PB\ (kW) x Opr\ hours\ (hr)$$

$$Fuel\ Savings = 0{,}235 x 311{,}64 x 3827 = 280\ 271{,}9 \frac{lt}{year}$$

The price of marine grade diesel oil varies from region to region and for Rio de Janeiro is 1000,00 usd/mt and it make 0,840 usd/lt. The prices can be updated daily from relevant web sites on the internet. (www.shipandbunker.com)

$$Fuel\ Cost\ Savings = Fuel\ savings \frac{lt}{year} x\ Cost\ of\ Fuel \frac{\$}{lt}$$

$$Fuel\ Cost\ Savings = 280\ 271,9 x\ 0{,}840 = 235\ 428{,}4\ \frac{\$}{year}$$

8.3 Construction costs of a “retro-fit” parabolic bulb for the PSV

The parabolized hull has cost savings by reduction of hull resistance. The parabolic amidship bulb construction is an extra cost for construction of the vessel. This section provides cost estimation for the construction of amidship bulb structure of PSV. The Product-Oriented Design and Construction (PODAC) cost model (Ennis, Dougherty et al. 1997) is used for cost estimation calculations that are presented at following part of this section.

There are many factors that increase the cost of the amidship bulb construction. Basically the additional bulb shape at retro fit parabolized hull increases the amount of construction steel. The shape of amidship bulb also makes the parallel body or wall structure hull shape more complex full form shape. This new form is also a factor to increase labor costs at the construction site.

8.3.1 Complexity Factors for the PODAC Cost Model

For PODAC (Product Oriented Design and Construction) cost model at the concept level, the price of the total ship is a function of displacement, speed, and a complexity factor. The complexity factor is necessary to normalize the data and achieve better equations because the cost data available to the IPT was for various ship types. For the complexity factor the IPT used is derived from a Size Factor and Ship Type Factor (Ennis, Dougherty et al. 1997).

SHIP TYPE	TYPE FACTOR
Crude Oil Tanker	0.80
Product Tanker	1.13
Chemical Tanker	1.25
Double Hull Tanker	0.90
Bulk Carrier	0.86
Oil/Bulk/Ore Carrier	0.95
Containership	0.96
Roll-On/Roll-Off	0.83
Car Carrier	0.61
Ferry	1.25
Passenger Ship	3.00
Fishing Boat	2.20
Tug	0.80
Combatant - Cruiser (Nuclear)	9.00
Combatant - Destroyer	8.00
Combatant - Frigate	7.00
Amphibious - LHA/LHD	7.00
Amphibious - LSD/LPD	5.00
Auxiliary - Oiler	2.25
Auxiliary - Tender	4.50
Naval Research	1.25
Naval Tug, Oceangoing	1.00
Coast Guard Icebreaker	4.50
Coast Guard Buoytender	2.00

Table 8: Ship type factors for the PODAC Cost Model Parametric Module. (Ennis, Dougherty et al. 1997)

For our platform supply vessel there is no ship type factor has been derived. The oceangoing naval tug is similar concept and hull type vessel. So an oceangoing naval tug ship type factor of 1.00 is selected for our PSV for this project.

The ship size factor needs to be calculated by equation below. The ship size factor is PODAC model and the Δ is full load displacement of the vessel.

$$Ship\ Size\ Factor = 32.47\ x\ \Delta^{-0.3792}$$

$$Ship\ Size\ Factor = 32.47\ x\ 6900^{-0.3792} = 1.137$$

The ship complexity factor is a sum of multiplication of ship size factor and ship type factor. The ship complexity factor is a data to use for prediction of labor for vessel construction. The calculation for PSV is like below.

$$Complexity\ Factor = \ Ship\ size\ factor\ x\ Ship\ type\ factor$$

$$Complexity\ Factor = \ 1.137\ x\ 1.00 = 1.137$$

8.3.2 Weight and labor cost estimate for the "retro-fit" parabolic bulb

There are several different methods of calculating the weight of steel structure of several type of vessels. These methods are mainly empirical formulation that predicted from statistical data from similar ships. Here we made an FEA by using Ansys software and we can get this weight difference between parent hull and retro fit parabolized hull directly from Ansys. The additional weight comes from amidship bulb structure is shown below.

$$Weight_{100} = \ 21{,}7\ tons$$

The man hour labor estimation can be calculated at PODAC system with a given complexity factor and structural weight of the amidship bulb to be built.

$$Man\ hour = CF\ x\ 177\ x\ Weight_{100}^{0,862}\ (hours)$$
$$Man\ hour = 1.137\ x\ 177\ x\ 21{,}7^{0,862} = 2856.03\ (hours)$$

The following formula is used for estimation of added labor that comes from difficulties of constructing complex form structures (SPAR Associates Inc. 2010) Here we assume that 100% of the amidship bulb is considered to have complex curvature.

$$Added\ man\ hour = Weight_{100}\ x\ \%\ Area\ of\ complex\ curvature\ x\ 3.12$$
$$Added\ man\ hour = 21{,}7\ x\ 100\ \%\ x\ 3.12 = 67{,}7\ hours$$

With all calculations above we can add all labor and calculate the total man hour for amidship calculation of PSV.

$$Total\ man\ hour = Man\ hour + Added\ man\ hour\ (hours)$$
$$Total\ man\ hour = \ 2856{,}03 + 67{,}7\ = 2923{,}73\ hours$$

The platform supply vessel can be built in US shipyards at Mexican Gulf region. US ship building industry is capable of building such a vessel. The labor cost can be calculated by manhour cost for shipyard. The manhour labor cost varies region to region but the labor rate in US assumed to be 22$ an hour. The indirect cost of overhead for shipyard is 100% of the labor cost (Ennis, Dougherty et al. 1997).

$$Labor\ Cost = \ 2923{,}73\ x\ 22\ = 64322{,}06\ \$$$
$$Overhead\ on\ Labor = \ 100\%\ x\ labor\ cost\ = 64322{,}06\ \$$$
$$Total\ Labor\ Costs = \ 64322{,}06 + 64322{,}06\ = 128644{,}12\ \$$$

8.3.3 Material cost for the “retro-fit” parabolic bulb

The materials cost in the construction of a hull shell component is small relative to labor costs. The following calculation relates to the price of mild Steel to the weight of the component to be built. Shipyard indirect cost of overhead is 2% of the total material cost (Ennis, Dougherty et al. 1997).

$$Material\ Costs\ (\$) \quad = 800x\ Weight_{100} \quad = 800\ x21{,}7 \quad = 17360\ \$$$$
$$Overhead\ on\ Materials\ = 2\ \%\ x\ Material\ Costs\ = 2\%\ x\ 17360\ = 347{,}2x\ \$$$

8.3.4 Final cost estimates for the “retro-fit” parabolic bulb

For the new building PSV project all the labor, material and overhead costs are calculated. The sum of all these cost will show us the final cost of this retro fit parabolic amidship bulb. The sum value is shown below.

$$Subtotal\ Cost = \ Labor + Material + Overhead$$
$$Subtotal\ Cost = \ 64322{,}06 + 17360 + (64322{,}06 + 347{,}2) = 146351{,}3\ \$$$

The very final indirect cost is the profit for shipyard. The profit is assumed to be 10% of the total cost (Ennis, Dougherty et al. 1997).

$$Shipyard\ Profit\ = 10\ \%\ x\ Subtotal\ Cost\ = 10\%\ x\ 146351{,}3\ = 14635{,}13\ \$$$

$$The\ Final\ Cost\ = Shipyard\ Profit + Subtotal\ Cost$$

$$The\ Final\ Cost\ = 14635{,}13 + 146351{,}3 = 160986{,}43\ \$$$

The final cost roundly 161000 USD for amidship bulb structure for our vessel.

8.4 Financial payback for the “retro-fit” parabolic bulb for the PSV

The preliminary cost and savings estimates done for retro fit parabolized hull of Platform supply vessel. This amidship bulb construction is a type of investment wihich will cover its expenses in some period of time. The investment is the constructional cost of the structure and income represented by the fuel cost savings during operation of the vessel. The initial capital costs of construction which is first investment is 161 000 $. The fuel cost savings of 235 428 $ is considered as annual income.

While we analyse the financial return of amidship bulb application We will consider about the cost of investment present and future value. The interest rate of debt in Brazil is 10 % (http://www.tradingeconomics.com/brazil/interest-rate). This capital is used with interest rate compounded monthly. So the following formula calculates the payback period of investment.

$$Monthly\ interest\ rate = \frac{Annual\ interest\ rate}{12} = \frac{10\%}{12} = 0{,}833\ \%$$

$$PV = Px\left[\frac{1-(1+i)^{-n}}{i}\right]$$

$$161\,000 = 19619x\left[\frac{1-(1+0{,}00833)^{-n}}{0{,}00833}\right]$$

$$n \approx 9\ months$$

Here

r : interest rate

n :Number of periods

PV : Present Value of investment

P : Monthly payment : 235 428 /12 = 19619 $

Figure 93: The savings data for 60 months of time period. (USD - month)

The graph above is show the financial savings of PSV by 60 months of time period. The first investment cost is $16100 and the investment comes into a break-even point just before 9th month of the operation time. The savings are increasing steady and it grows up to 762461 at the end of 60th month. Here we assume that the vessel operates continuously for 60 months at the same route.

8.5 Cost return of amidship bulb with different ship type factors for the PODAC cost model

The cost of amidship bulb construction and its return is effecting directly by the Ship Type Factor for PODAC cost model. The ship type factor varies from different types of ships. The table 8 shows the ship type factors which are already ben calculated and defined for some type of ships. Platform supply vessels are not one of them on the table so we can only assume by similar construction and installations on board. For this reason it may not be accurate for our sample vessel.

Here we will calculate the same cost and financial return for 2 other similar ships to see how much it will chance our calculation at previous study. The other similar ships are like below.

- Naval Research Shiptype factor 1,25
- Coast Guard Buoytender Shiptype factor 2

After the calculation for 2 model the values with the first calculations are like in the table below.

PODAC Calculation	DATA	STF 1	STF 1,25	STF 2
Ship Type Factor		1	1,25	2
Ship Size Factor	1			
CF		1,137	1,42125	2,274
Weight 100 (ton)	21,7			
Man Hour (hours)		2856,03	3570,03	5712,05
Added man hour (hours)		67,70	67,70	67,70
Total Man hour (hours)		2923,73	3637,74	5779,75
Labor Price ($/hour)	22			
Labor Cost ($)		64322,04	80030,18	127154,59
Overhead Labor ($)		64322,04	80030,18	127154,59
Material Price ($/ton)	800			
Material Cost ($)		17360,00	17360,00	17360,00
Overhead on Material ($)		347,20	347,20	347,20
Subtotal Cost ($)		146351,28	177767,56	272016,39
Shipyard Profit ($)	10,0%			
Final Cost ($)		160986,41	195544,31	299218,02

Table 9: Cost calculation results for different Ship Type Factors for the PODAC cost calculation

Figure 94: The savings data for 60 months of time period for three different ship type factors for PSV. (USD - month)

The figure shows that the return of the PODAC ship factor 1,25 for Naval Research Vessel with is about 17 months and PODAC ship factor 2,00 for Coast Guard Buoytender is about 11 months.

9. CONCLUSIONS

In this research a synthesis of parabolization, FEA of ship structure and cost analysis of amidship bulb has done. The start point of the research was the waterline parabolization method to reduce the powering requirements of a platform supply vessel with a displacement hull type. This method is developed to reduce the wave resistance by modifying the wave characteristic of vessel by adding an amidship bulb over the parent hull. The results present a “retro-fit” amidships bulb design that can reduce the wave resistance as well as the total resistance of the vessel. Although the Froude Number of the vessel was below 0,3 we gain 5,88 % that is reasonable reduction at total resistance of the vessel. The sample ship was a platform supply vessel which will operate at Atlantic ocean, waterway between several offshore oil rigs and and shore of Brazil. The vessel has long wall structure hull which was useful for our parabolization work.

The parabolization has done by couple of commercial and research software packages. The Argos software which is based on a potential flow panel method code named Trawson solved the wave resistance problem of the vessel by using Dawson’s algorithm. This software calculates the wave resistance and plots the wave characteristics of the hull form at given speeds. The second software is Argos optimization creates an amidship bulb geometry to reduce wave resistance of the hull. For this process all 3D modeling, meshing and preprocessing of the ship hullforms have been done using the commercial software called Rhinoceros. The 3D model has 1588 mesh elements to run the software.

The beam of the vessel increases as a result of amiship bulb creation on the parallel body. The parent hull has beam 18,3 m and it increase to 20,12m. We achieve 5,88% of total resistance reduction at Froude Number 0,244 for the service speed.

The vessel was classified by American Bureau of Shipping. The new hull form structural scantling has controlled regarding to American Bureau of Shipping (ABS) Rules for building and classing, Offshore Support Vessel 2013, Part 3 Hull construction and

equipment. On this sample ship the increase of the beam was not much and it was helpful not to make a major modification at the structure of the vessel. Small extensions and chances over the frames and beams were enough to create structure for the amidship bulb. While controlling scantling of the hull structure we didn't need to increase the size of most of the members and their material thicknesses. This also help to reduce construction cost of the amidship which analysed at financial part of the research

Hull	Analysis Type	Max Stress (MPa)	Type and Place
Parent Hull	Wave Bending Moment	111.849	Von misses,Under deck structure
Parent Hull	Wave Bending Moment	53,83	Longitudinal Horizontal shear stress, Under deck structure
Parent Hull	Horizontal Wave bending moment	12,86	Von misses,deck shell plate
Parent Hull	Horizontal Wave bending moment	2,69	Longitudinal Horizontal shear stress, Under deck structure
Parabolized hull	Deck Load	220	Von misses, Under deck structure
Parabolized hull	Deck Load	18,93	Shear stress at vertical orientation, under deck structure
Parabolized hull	Wave Bending Moment	118,24	Von misses,Under deck structure
Parabolized hull	Wave Bending Moment	56,62	Longitudinal Horizontal shear stress, Under deck structure
Parabolized hull	Horizontal Wave bending moment	13,49	Von misses, deck shell plate
Parabolized hull	Horizontal Wave bending moment	2,38	Longitudinal Horizontal shear stress, Under deck structure

Table 10: FEA results stress values

Hull	Analysis Type	Displacement (mm)
Parent Hull	Wave Bending Moment	7.46
Parent Hull	Horizontal Wave bending moment	0,59
Parabolized hull	Wave Bending Moment	7,98
Parabolized hull	Horizontal Wave bending moment	0,55

Table 11: FEA results displacement values

The parent hull and parabolized hull structures are examined by FEA software Ansys structurally. The modelling and the mesh elements of the hull structural members have done by the modelling part of Ansys. All shell plates are modelled by using shell element and profiles are modelled by using beam elements. Instead of modelling the whole ship structure, 3 tank method has used. It is the name of the modelling technique of modelling 3 tanks with 2 bulkheads at midship area by creating a rigid region at bow and stern end of the model. For the parent hull FEA model there are 117635 elements and for the parabolized hull there are 123013 mesh elements used to run the software.

Regarding to Analysis on the deck loading there are some local stresses occurred. The frames and longitudinal member joint just below the deck plate has some stress around 200 MPa. This is coming close to tensile stress of St-42 steel plate which is 235 MPa. The stress can be lower down by local reinforcement by brackets at joint area or increasing the beams and longitudinal structure. The maximum stress and displacement values are like in the table 9 and table 10

The final part of the research was the financial analysis of the amidship bulb application. This analysis gave us an idea about how feasible this construction? How much it cost to build this structure? How long it takes to return the investment cost?. The shape and the size of the amidship bulb is unique and comes up with speed and draft of the vessel. The sample PSV has a small sidebulb with a simple smooth curvature shape that make all simple and cheap. Small extensions on the frames help us to create the structure of amidship bulb. So it increase the labor cost 128644,12 $, 17707,2 $ of material and 347,2 of overhead cost. The total cost of the operation is 160986,43$ and we round it into 161000 $. The power reduction, smaller engine selection and powering equipments like flexible couplin, shaft, sleeve, propeller etc are neglected. The fuel savings by 5,88% reduction at total ship resistance gain us 235 428 $ annually. The investment cover itself within shorter than 9 months of operation at given conditions.

The other advantage of parabolization is having low CO_2 emission by less fuel consumption. 1 liter of marine grade fuel produces 2.69 kg/lt of CO_2 (US Environmental

Protection Agency) and 57 g/kg NO_x for medium speed vessels (Kean, Sawyer and Harley, 2000). So the sample vessel will save 753931,7 kg of CO_2 and 13419 kg NO_x by saving 280272 liters of fuel per year. The vessel helps to save environment and helps world to keep green. Around the world the transportation authorities are considering new emission and operational regulations based on the EEDI rating of each vessel. For this reason the Energy Efficient Design Index (EEDI) rating of a ship should be determined by the waterline parabolization. According to the International Marine Organization, the EEDI rating is used to gauge the energy efficiency per capacity mile of a ship and is meant to drive technical advancements in technology to improve fuel efficiency (IMO 2011).

The future work for parabolization should be a work for a new hull both examined by computational and experimental work. The parent and parabolized hull should be tested at towing tank. This will give us more data about how different the computational and experimental results will be. Because the amidship bulb shape is unique for each hull shape, draft and speed of the vessel the results can be much more different than the previous experience. A synthesis of structural integration, new constructional modification and its additional cost, seakeeping behavior, stability improvement and the total financial analysis of work might be the next research about parabolization theory.

Bibliography

ABS (2013). American Bureau of Shipping (ABS) Rules for building and classing, Offshore Support Vessel 2013, Part 3 Hull construction and equipment.

Adams V. and Askenazi A. (1999), Building Better Products with Finite Element Analysis, Santa Fe, Onword Press

Aertssen, G. and Van Sluijs M. F. (1972), "Service Performance and Seakeeping trials on a Large Container Ship" Trans RINA 114

Andrew J. Kean A. J., Sawyer R.F. and Harley R.A. (2000)." A Fuel-Based Assessment of Off-Road Diesel Engine Emissions" Air & Waste Management Association 50: 1929-1939

ANSYS user manual (2013), www.ansys.com

Bertram, V. (1990). "Ship Motions by Rankine Source Method." Ship Technology Research
37(4): 143-152.

Bull D, (2013), "Offshore Support Vessels and Mobile Rig Fleets Set for Major Growth" England, Ocean Shipping Consultants

Çalisal, S. M., B.-Y. J. Tan, et al. (2009). "A Systematic Investigation of Ship Resistance Reduction by Beam Increment on Small Craft." Journal of Ocean Technology 4(3): 57 to 72.

Çalisal, S. M. and D. McGreer (1993). "A Resistance Study on a Systematic Series of Low L/B Vessels." Marine Technology 30(4): 286-296.

Çalisal, S. M., M. şirelli, et al. (2009). "A Direct Measurement of Wave Resistance by the Measurement of Wave Height on a Surface Patch." Journal of Ship Research 53(3): 170-177.

Dawson, C. W. (1977). A practical computer method for solving ship-wave problems. 2nd International Conference on Numerical Ship Hydrodynamics, Berkeley, CA.

Deli O. (2002), Structural Analysis Of Yacht Masts Using Finite Element Modelling. Faculty of Maritime Transport and Engineering, Tasmania, Australia, Australian Maritime College. Graduation Thesis

Ennis, K. J., J. J. Dougherty, et al. (1997). "Product-Oriented Design And Construction Cost Model." Ship Production Symposium Society of Naval Architects and Marine Engineers.

Erdemir Steel Manufacturing Plant (2013). "Steel Sheet and Plate Data,." from http://www.erdemir.com.tr/

Gauld K. (2011). The Influence of Hullform Parabolization on the Powering and Seakeeping Characteristics of the UBC Ferry. Mechanical Engineering. Vancouver, University of British Columbia. Masters of Applied Science:

Giulio Bottazzi (2014). " Short Report on Oil Price History" from **http://cafim.sssup.it/~giulio/other/oil_price/report.html**

Gören, Ö. and M. Atlar (1998). A Computational Study for the Wave Resistance Analysis of Multi Hullforms. Newcastle upon Tyne, Newcastle University School of Marine Science and Technology.

Hally, D. (1995). Tests of the Sensitivity of Dawson's Panel Method to the Free Surface Panels. D. R. D. C. Atlantic. Dartmouth, Deffence Research and Development Canada.

Harvald, S. A. (1992). Resistance and Propulsion of Ships. Malabar FL, Krieger.

Kaydihan, L., Gul, Y. (2001), Structural and Vibration Analyses for 244 passengers and 48 cars capacity Ferry, 6th Figes ANSYS users' Meeting, Bursa, Turkey

Kent, J. L. (1919). "Model Experiments on the Effect of Beam on the Resistance of Mercantile Ship Forms." Institution of Naval Architects Transactions LXI: 311-319.

Klaptocz, V. (2006). Effect of Parabolization on Viscous Resistance of Displacement Vessels. Mechanical Engineering. Vancouver, British Columbia, Canada, University of British Columbia. Masters of Applied Science:

Lamb, T., Ed. (2004). Ship Design and Construction. Jersey City, NJ, Society of Naval Architects and Marine Engineers.

Lewis, E. V., Ed. (1988 a.). Principles of Naval Architecture. Stability and Strength. Jersey City, New Jersey, Society of Naval Architects and Marine Engineers.

Lewis, E. V., Ed. (1988 b.). Principles of Naval Architecture. Resistance, Propulsion and Vibration. Jersey City, New Jersey, Society of Naval Architects and Marine Engineers.

Ozguc O. (2002) Modal And Harmonic Response Analyses Of A 7000 Dwt Chemical Tanker Using Finite Element Method. Faculty Of Naval Architecture and Ocean Engineering, Istanbul, Turkey, Istanbul Technical University, Graduation Thesis

Raven, H. C. (1992). A Practical Nonlinear Method for Calculating Ship Wavemaking and Wave Resistance. 19th Symposium on Naval Hydrodynamics, Seoul, Korea.

Rawson, K. J. and E. C. Tupper (2001). Basic Ship Theory. Woburn MA,

Butterworth-Heinemann.
Sclavounos, P. D., D. C. Kring, et al. (1997). "A Computational Method as an Advanced Tool of Ship Hydrodynamic Design." Society of Naval Architects and Marine Engineers Transactions 105: 375-397.

Schneekluth, H. (1987). Ship Design for Efficiency and Economy. London UK, Butterworths.

Ship & Bunker (2014).”World bunker prices for marine grade diesel oil” http://shipandbunker.com/prices#MGO

Tan, B.-Y. J. (2004). An Experimental Investigation for Resistance Reduction of Displacement-Type Ships By Parabolization of Hull Form at Waterline. Mechanical Engineering. Vancouver, British Columbia, Canada, University of British Columbia. Masters of Applied Science:

Trading Economics (2014). "Interest rates at Brasil” http://www.tradingeconomics.com/brazil/interest-rate

US Environmental Protection Agency (2014). “ CO2 emission values for marine grade diesel ” from http://www.epa.gov/

Uslu Y. and Bal Ş. (2008).”Numerical Prediction of Wave Drag of 2-D and 3-D Bodies under or on a Free Surface.” Turkish J. Eng. Env. Sci. 32: 177 – 188.

Vyselaar, D. P. (2006). Using Parabolic Waterlines to Reduce the Resistance of a Trimaran. Mechanical Engineering. Vancouver, University of British Columbia. Masters of Applied Science:

Yong Bai, 2003. Marine Structural Design. Kidlington, Oxford, UK, Elsevier.

Zienkewicz,O.C. and Taylor, R.L. (2000) The Finite Element Method Volume1 and 2 Fifth edition. Woburn, MA, Butterworth-Heinemann